The tumor suppressor Annexin A6 increases the sensitivity towards anti-cancer drugs targeting the EGFR/Ras/MAPK pathway

THE UNIVERSITY OF SYDNEY

Yasmin Ahmed Mohamed Soliman Elmaghrabi

A thesis submitted in fulfillment of the requirements for the degree of Master of Philosophy

Faculty of Pharmacy **The University of Sydney**

March 2016

Declaration

I hereby declare that this thesis is my own work and that it is not submitted for the award of any other degree or diploma at the University of Sydney or any other institution. All the work was performed under the supervision of Associate Professor Thomas Grewal, Faculty of Pharmacy, University of Sydney.

Yasmin Ahmed Mohamed Soliman Elmaghrabi

2nd March 2016

Table of Contents

Acknowledgement

First, I must thank God for helping, guiding, and supporting me throughout my life, for all the blessings that he showered on me and for giving me the beautiful life that I live.

"Allah is sufficient for me; there is no deity except Him. On Him I have relied, and He is the Lord of the Great Throne (Quran: Surat At-taubah, 129)"

Second, I would like to thank my supervisor Associate Professor Thomas Grewal for giving me this valuable opportunity to be part of his research team. I learnt a lot of things from him, and I must admit that he devoted many hours of his precious time for me. He allowed me to take many independent decisions about the research, followed by high quality feedback to help me becoming a better independent researcher. He always inspired and motivated me.

Also, I would like to express my deep appreciation for the Australian government, the sponsor of my scholarship. I take this opportunity to thank all the "Australia Awards" scholarship team for all the support and care they offered during my studies.

Special thanks to the academic staff in the City of Scientific Research and Technological Applications (SRTA-City), especially the head of my department, Associate Professor Raoufa Ahmed Abdel Rahman, who I consider as my mentor and role model that always provide me with support and guidance.

My sincere gratitude goes to all my mates specially Monira Hoque, Sundeep Joshua Wason, Mohamed Wahba, Jacky Hanh, Jennifer Ong, Helen Gao, Pavan Prabhala, Brijeshkumar Patel, Parth Upadhyay and Shereen Aleidi who all helped me a lot during my master's degree. You are the best company ever!

Finally, I would like to thank my hidden treasure and most important part of my life, my parents and family, who always encourages me with love for more success in life, with thirst for knowledge and adventure. Thank you.

Abbreviations

AnxA6	Annexin A6
ATP	Adenosine triphosphate
CaM	Calmodulin
CaMK-II	Calmodulin-dependant protein kinase II
CCP	Clathrin coated pits
cPLA$_2$	Cytosolic phospholipase A_2
DAG	Diacylglycerol
DPBS	Dulbecco's phosphate-buffered saline
EE	Early endosomes
EGF	Epidermal growth factor
EGFR	Epidermal growth factor receptor
Grb2	Growth factor receptor-binding protein-2
GAP	GTPase activating protein
GDP	Guanosine diphosphate
GTP	Guanosine triphosphate
HNSCC	Head and neck squamous cell carcinoma
IP$_3$	Inositol triphosphate
iPLA$_2$	Ca^{+2}-independent phospholipase A_2
LDL	Low-density lipoprotein
LE	Late endosomes
LPA	Lysophosphatidic acid
mAb	Monoclonal antibody
MAFP	Methyl arachidonyl fluorophosphonate
MAPK	Mitogen-activated protein kinase

MTS	3-(4,5-dimethylthiazol-2-yl)-5-(3-carboxymethoxyphenyl)-2-(4-sulfophenyl)-2H-tetrazolium, inner salt
MVB	Multivesicular bodies
NSCLC	Non-small-cell lung carcinoma
PAF-AH	Platelet-activating factor hydrolases
PI(4,5)P2	Phosphatidylinositol-4,5-bisphosphate
PKC	Protein kinase C
PLA_2	Phospholipase A_2
PLC	Phospholipase C
PMS	Phenazine methosulfate
PS	Phosphatidylserine
SOS	Son of sevenless
$sPLA_2$	Secretory phospholipase A_2
TKI	Tyrosine kinase inhibitor

Abstract

Sustained EGFR/Ras/MAPK signaling is associated with various cancers. Hence, blocking EGFR and its downstream effectors has become an established target in anti-cancer therapeutics. However, targeted agents face several challenges which limit their clinical use such as inter-patient variation, mutation, and resistance. Therefore, the identification of biomarkers that could predict the treatment outcome in cancer patients is crucial. Annexin A6 (AnxA6) is a calcium-dependent membrane binding protein with potential tumor suppressor properties. It was shown to bind and promote the involvement of p120GAP and protein kinase Cα (PKCα), two negative regulators of the EGFR/Ras/MAPK pathway, in the signal termination of this cascade. Increasing evidence points at the involvement of scaffold proteins, like AnxA6, in the sensitivity of cancer cells towards anti-cancer drugs. In this study, we examined the influence of single and combinatorial treatments targeting the EGFR/Ras/MAPK signaling cascade on the oncogenic proliferation of A431 cells in the presence and absence of AnxA6. Using A431wt cells, which lack endogenous AnxA6, and A431-A6 cells, a well characterized cell line which stably overexpress AnxA6, we investigated clonogenic growth in the presence of the EGFR tyrosine kinase inhibitors (TKIs) erlotinib and gefitinib, the EGFR-targeted monoclonal antibody cetuximab, the MEK1/2 inhibitor PD98059, and the PKCα inhibitors BIM-I and Gö 6976 via clonogenic and MTS assays. We found that treating the cells with TKIs, MEK1/2 or PKCα inhibitors was able to effectively reduce colony and cell growth more than the individual drugs, and this inhibition was more pronounced in AnxA6 overexpressing cells. Furthermore, combinatorial treatment of A431 cancer cells with TKIs together with MEK1/2 inhibitors was more effective in cells expressing AnxA6. The data presented here suggest AnxA6 as a possible biomarker that could predict treatment outcome in EGFR-related cancers.

Chapter 1: Introduction

1.1 Overview

Epidermal growth factor receptor (EGFR)/Ras/mitogen-activated protein kinase (MAPK) pathway is one of the targets that are under investigation for the treatment of cancer. Strong evidence points at the significant influence of mutations on the occurrence of tumors with high frequency of reported EGFR, Ras, and Raf mutations (1-10). In fact, the three isoforms of Ras (H-, K-, and N-Ras) were found mutated in different types of cancer and were shown to occupy 20-30 % of human cancers. These mutations lead to failure of Ras inactivation and a sustained cell proliferation (11-15). EGFR mutations were also reported and were associated with a more aggressive disease and a poorer prognosis (1-9). In addition, it was shown that EGFR overexpression could lead to a hyperactive wild type Ras with a subsequent cellular oncogenic transformation (16-19). Moreover, the heterodimerization of EGFR with other deregulated ErbB receptors and its transactivation by heterogeneous signals were also linked to cancer with increased cell growth, angiogenesis, and metastasis (1-9). Therefore, drugs targeting EGFR/Ras/MAPK pathway have developed into several potent anticancer medications (3, 9, 20).

However, different regulatory factors in the EGFR pathway seem to modulate/potentiate drug efficiency in patients. This also includes several scaffold proteins that are involved in the regulation of EGFR signaling such as cortactin, caveolin, and annexin A6 (AnxA6). AnxA6 is a calcium-dependent membrane binding protein that is suggested to have tumor suppressor properties owing to its inhibitory effect on the EGFR/Ras/MAPK pathway. Although AnxA6-KO mice appear normal and do not develop spontaneous tumors (3, 21), several studies correlated the loss of AnxA6 with increased EGFR/Ras/MAPK activity and cell proliferation

(3, 16, 22, 23). For example, human A431 carcinoma cells, which overexpress EGFR and show elevated Ras/MAPK activity, lack endogenous AnxA6 (3, 16, 22, 23). However, upon ectopic expression of AnxA6, Ras/MAPK activity and cell growth were reduced in A431 cells (3, 16, 22-25). Likewise, several estrogen receptor-negative breast cancer cell lines showed reduced AnxA6 levels that upon elevation via AnxA6 overexpression, EGFR/Ras was inhibited (3, 22). In addition, the transformation of prostate cancer and human melanoma from benign to malignant phenotypes showed AnxA6 downregulation correlating with deregulated EGFR and hyperactive Ras (3, 16, 26, 27). Also the metastatic development of B16F10 mouse melanoma showed AnxA6 downregulation (3, 16). This suggests a strong relationship between reduced AnxA6 levels and elevated Ras activity in EGFR overexpressing cancer cells leading to a significant influence on EGFR/Ras/MAPK pathway, a cascade that is highly regulated to control cell proliferation and differentiation.

1.2 The EGFR/Ras/MAPK pathway

EGFR or ErbB-1 is a member of the ErbB family that has three other members, HER2 (ErbB-2), HER3 (ErbB-3), and HER4 (ErbB-4). It is a transmembrane receptor with an extracellular region, which binds ligands such as EGF and EGF-like molecules, and an intracellular domain with a tyrosine kinase activity (17, 28). Its enzymatic activity is kept inactive as long as the receptor is in the monomeric state, but following ligand binding, EGFR dimerization is triggered leading to receptor activation. Consequently, the active tyrosine kinase in one receptor phosphorylates the tyrosine residues present in the other receptor in an autophosphorylation process (2, 8, 29), leading to the formation of phosphotyrosine-containing motifs which act as docking sites for adaptor proteins (Figure 1A). Growth factor receptor-binding protein-2 (Grb2) is an adaptor protein which associates with these motifs and then binds simultaneously to the son of sevenless (SOS) (30). SOS is a guanine nucleotide exchange factor which activates the membrane bound Ras by exchanging the Ras-

bound guanosine diphosphate (GDP) with guanosine triphosphate (GTP) (31). Ras activation leads to the recruitment and activation of the serine/threonine-protein kinase Raf. Activated Raf then phosphorylates and activates MEK1/2 which in turn phosphorylates and activates ERK1/2 (MAPK) (19). Finally, activated ERK1/2 phosphorylates nuclear proteins and modulates the activity of several transcription factors regulating gene expression to induce cell growth and differentiation.

Overactivity of the EGFR pathway is associated with oncogenesis (16, 22, 32, 33). Hence, EGFR downregulation has been recognized as an important step in the cell to prevent oncogenic events.

1.3 EGFR/Ras/MAPK signal termination

The EGFR/Ras/MAPK pathway is a highly regulated process that involves the cooperation of multiple proteins in order to initiate signal termination and prevent sustained cell proliferation and differentiation (1, 3-8). Following receptor activation, the signal is terminated through the internalization of EGFR via endocytosis. Then, the endocytic vesicles traffic through late endosomes (LE) and/or multivesicular bodies (MVB) to lysosomes for degradation and signal termination (Figure 1A). Although the Ras/MAPK pathway proteins can remain associated with EGFR along this route, the majority of Ras is transported back to the plasma membrane via the recycling endosomes (1, 3, 6, 7, 16, 22).

It was revealed that EGFR internalization occurs through clathrin coated pits (CCP) and to a lower extent via caveolae/lipid rafts depending on EGFR concentration. At low EGFR concentration, EGFR internalization occurs through CCP leading to either its lysosomal degradation or recycling (3, 34, 35). However, at high EGFR concentration both CCP and caveolae/lipid rafts are involved in EGFR internalization, with the caveolae/lipid raft pathway leading only to EGFR degradation not recycling (1, 3, 6, 7, 35-37). This two way mechanism

can help the cell to deal with any physiological concentrations of EGF (~ 1-100 ng/ml) and to prevent its overstimulation (1, 3, 5-7, 35-37).

The inhibition of the EGFR/Ras/MAPK cascade involves multiple proteins such as protein kinase Cα (PKCα), p120GAP, and calmodulin. PKCα is a classical isoform of the serine/threonine PKC family that is activated by the second messengers, calcium and diacylglycerol (DAG), at the plasma membrane, endosomes, Golgi or mitochondria (38, 39). Binding of phospholipase Cγ (PLCγ) to activated EGFR leads to the hydrolysis of phosphatidylinositol-4,5-bisphosphate (PI(4,5)P2) into DAG and inositol-1,4,5-triphosphate (IP_3). IP_3 binds IP_3 receptors causing the release of the intracellular calcium stores in the endoplasmic reticulum, hence the intracellular calcium level increases (3, 5). DAG binds to the C1 domain of PKC and elevates the affinity of PKC to phosphatidylserine (PS) in membranes with subsequent conformational changes to allow substrate binding, while calcium association with the C2 domain of PKC leads to increased and stabilized membrane binding (38, 40-44). Then, PKCα phosphorylates EGFR at threonine 654 leading to the inhibition of its tyrosine kinase activity, internalization, and lysosomal degradation. AnxA6 was also found to bind PKCα in a calcium-dependent manner and to potentiate both the transport of PKCα to the membrane and its ability to bind and inhibit EGFR (45-47). Finally, the inactive EGFR is targeted to the recycling endosomes which is responsible for transporting the EGFR back to the plasma membrane in a highly regulated process involving the actin cytoskeleton (19) (Figure 1B).

GTPase activating proteins (GAPs) such as p120GAP are other negative regulators of EGFR and Ras. Although a role for p120GAP in EGFR inhibition has been described, it is not well understood. In contrast, the role of GAPs in Ras inactivation is well documented. When GAPs translocate to the plasma membrane and bind to Ras, Ras GTPases are inactivated and switch from the active (Ras-GTP) to the inactive (Ras-GDP) (13, 14, 48). In EGFR

overexpressing cancer cells, p120GAP was reported to bind to AnxA6. This binding stabilized H-Ras/p120GAP assembly and led to H-Ras inactivation (19, 22, 49-51) (Figure 1C).

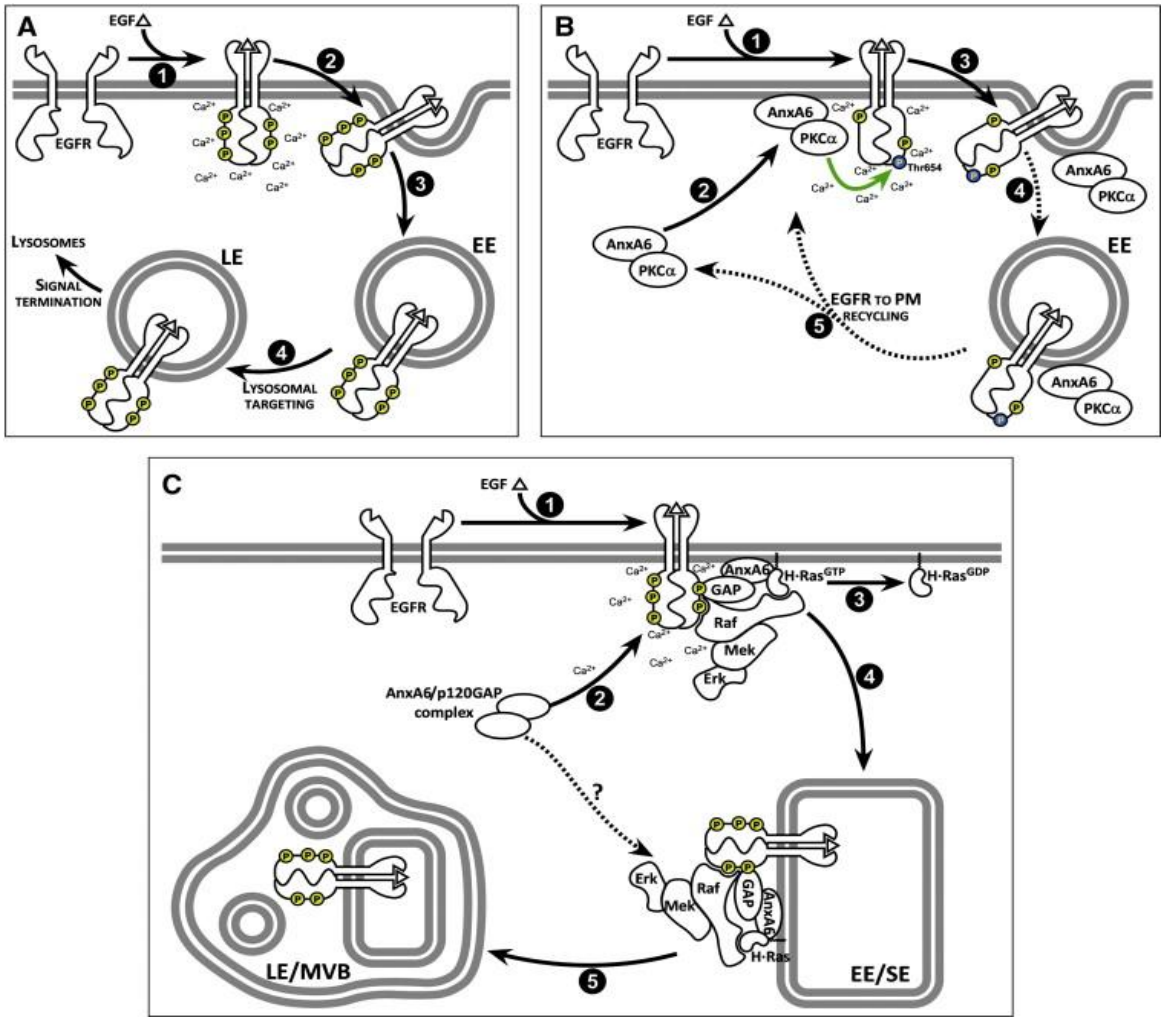

Figure 1. (A) EGFR signal termination. (1) When EGF binds EGFR in cells with low AnxA6 levels, EGFR dimerization and a subsequent tyrosine kinase activation is followed by signal termination via (2,3) endocytosis and (4) lysosomal degradation. (B) The role of AnxA6 and PKCα in EGFR signal termination. (1) EGF binds to EGFR leading to receptor dimerization and activation. (2) AnxA6 and PKCα interact in the cytosol which leads to PKCα membrane binding potentiation. (3) PKCα phosphorylates EGFR at threonine 654 which inhibits its tyrosine kinase activation and reduces its internalization. (4) AnxA6 and PKCα remain attached to EGFR in early endosomes (EE). (5) Finally, AnxA6 and PKCα dissociate from EGFR which is sent to the plasma membrane for recycling for another round of signaling. (C) The role of AnxA6 and p120GAP in EGFR signal termination. (1,2) AnxA6 and p120GAP interact in the cytosol of resting cells with AnxA6 potentiating the targeting of p120GAP to the plasma membrane when EGF binds EGFR and calcium levels increase. (3) A complex of several proteins is formed which includes EGFR, p120GAP, AnxA6, and H-Ras which leads to the inactivation of H-Ras and signal termination. (4) The complex is internalized. (5) AnxA6/p120GAP complex dissociate into the cytosol, H-Ras recycles to the plasma membrane, and EGFR is either targeted to the recycling endosomes or to late endosomes/ multivesicular bodies (LE/MVB). Taken from (19).

Calmodulin (CaM) is another example of a protein that can inhibit EGFR/Ras pathway at multiple levels. CaM is a small protein found abundantly in most eukaryotic cells. It can activate calmodulin-dependent protein kinase II (CaMK-II), which phosphorylates EGFR leading to the inhibition of its tyrosine kinase activity and a subsequent decrease of Ras signaling (3, 14, 52). Out of the three Ras isoforms, CaM can release K-Ras from the plasma membrane inhibiting its activation (3, 53, 54). In addition, CaM can directly bind to EGFR in a calcium-dependent interaction inhibiting its tyrosine kinase activity at the plasma membrane (55), disrupting PKC binding at threonine 654 (56, 57), and preventing EGFR signaling (3, 58). Moreover, CaM regulates the endocytosis and trafficking of EGFR through endosomes (3, 59-61).

In addition to these negative regulators of the EGFR/Ras pathway, AnxA6 also has a significant role in the downregulation and signal termination of the EGFR/Ras/MAPK pathway and, as outlined in more details below, it is considered as a promising target to develop a novel treatment for cancer (3, 10).

1.4 Annexin A6

Annexins are a group of structurally related proteins that have the ability to bind negatively charged phospholipids in a calcium-dependent manner. They are found in different species ranging from protists to humans in most cell types and tissues with the exception of annexin A8 which is only found in lung, skin, liver and kidney (3, 62-65). They are divided into five groups (A-E) with the 12 proteins found in human and vertebrates occupying group A (19).

Annexins consist of two domains; the first one is the variable N-terminal tail, while the other is the conserved C-terminal annexin core that contains calcium and phospholipid binding sites. All annexins have one core with four repeats of a 70 amino acids sequence except AnxA6, which has two cores with eight disk-like repeats connected by a flexible linker

(Figure 2) (66). Hence, AnxA6 may attach to one or two membranes owing to the flexible orientation of these two cores relative to each other.

It was proposed that the duplication and fusion of the genes encoding for annexin A5 and annexin A10 may be the reason for this unique structure of AnxA6 among all other annexins (19, 67-70). Chromosome 5q32-q34 harbors the AnxA6 gene which is ~60.000 bp long with 26 exons (Figure 2).

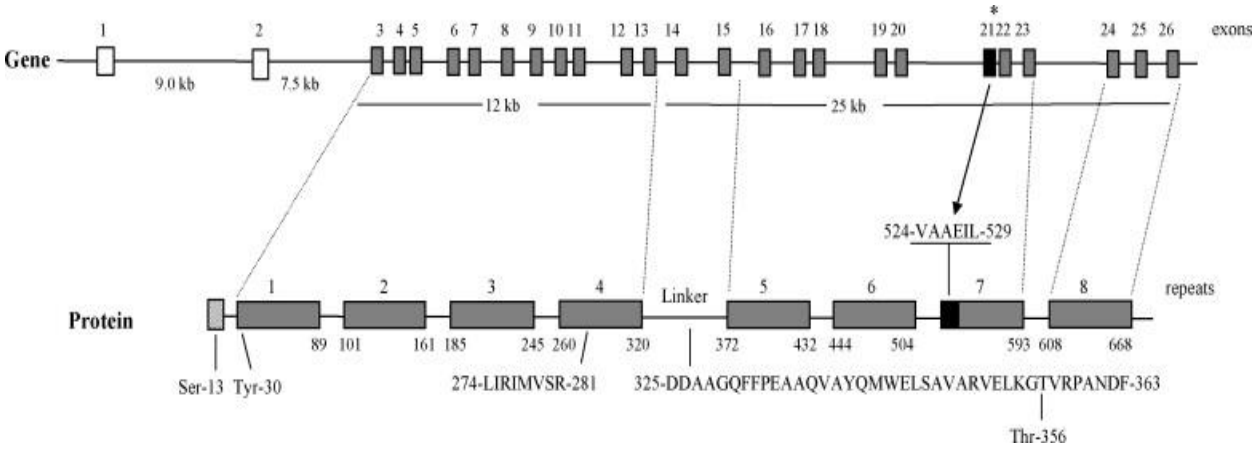

Figure 2. The gene and protein structure of AnxA6. The exon-intron structure of the AnxA6 gene and the eight annexin repeats of AnxA6 protein are illustrated; exons and annexin repeats are numbered and represented as boxes. The amino acid positions of each repeat are indicated. The lengths of regions in kilobases (kb) within the AnxA6 gene are indicated. The asterisk indicates the position of the alternatively spliced exon 21 (black box). The first two exons code for the N-terminus, while exons 3-13 and 16-26 code for repeats 1-4 and 5-8, respectively. The amino acid sequence of a potential F-actin binding site (Pos. 274–281), the p120GAP binding domain within the linker region (Pos. 325–363), and the larger splice variant (Pos. 524–529) are indicated. Phosphorylation sites at serine 13, tyrosine 30 and threonine 356 are given. Taken from (66).

AnxA6 was shown to bind PS, phosphatidylinositol, phosphatidic acid (65), with some affinity for phosphatidylethanolamine, and arachidonic acid (19, 71). It was found at the plasma membrane, early endosomes (EE), LE, and recycling endosomes (3, 16, 65, 72-85) with some studies indicating its presence in mitochondria (86), lipid droplets (87) and the secretory pathway (44, 65, 80, 88-90).

In Chinese hamster ovary cells (CHO), 70-80% of AnxA6 proteins were found attached to membranes in a calcium-dependent manner, while the rest was found linked to endosomal membranes in a calcium-independent manner with a potential influence of cholesterol. It was demonstrated that cholesterol is a potential modulator of AnxA6 membrane binding affinity

as well as its intracellular localization. In one study cholesterol was depleted by methyl-β-cyclodextrin which reduced the calcium-independent membrane binding affinity of AnxA6 to early and late endosomes. On the other hand, the use of Low-density lipoprotein (LDL) or U18666A to load cells with cholesterol in LE stimulated AnxA6 binding to late endosomal membranes (72, 85). In addition to cholesterol, pH was found to affect the membrane binding affinity of AnxA6. Conformational changes of AnxA6 were observed in acidic pH which increased its hydrophobicity, membrane binding affinity and enhanced its binding to monolayers containing cholesterol (19, 91-93).

AnxA6 has two mRNA isoforms, the full-length AnxA6-1 and the shorter isoform AnxA6-2 which lacks 524-VAAEIL-529 from the seventh repeat (Figure 2). AnxA6-1 is found more abundant in normal tissues and cells, while AnxA6-2 is highly expressed in some transformed cell lines (94). AnxA6-2 has lower hydrophobicity, more calcium affinity and lower negative surface charge (95), but AnxA6-1 is the isoform that was found to have an inhibitory effect on EGF-dependent calcium influx in A431 cells (19, 96). However, despite these findings, the overall roles of the two AnxA6 mRNA isoforms have remained elusive.

1.5 The role of annexin A6 in the EGFR/Ras/MAPK pathway

AnxA6 influences the EGFR/Ras/MAPK pathway through its multifunctional properties relevant for signal transduction, endocytosis and lysosomal degradation, actin dynamics, caveolae/lipid raft formation and cholesterol homeostasis (45, 65, 73-80, 97, 98).

The tumor suppressor effect of AnxA6 is suggested to be a consequence of its potential influence on EGFR signaling. AnxA6 potentiates EGFR signal termination via several protein-protein interactions involving multiple Ras regulators/effectors such as PKCα, Raf-1, and p120GAP (29, 99, 100). AnxA6 was found to be a scaffold for PKCα via an interaction possibly involving the C2 domain of PKCα and the threonine 356 residue in the AnxA6 linker region (90, 101). Thus, AnxA6 plays a significant role in the association of PKCα to

membranes by acting as a docking site as well as potentiating its membrane binding, in order to promote PKCα-mediated inhibition of the EGFR signaling (Figure 1B) (3, 19, 29, 44, 102, 103). AnxA6 was also found to be a scaffold for p120GAP, most likely through the association of the AnxA6 linker region with the C2 domain of p120GAP (100, 104), which is important for the inactivation of Ras, and it was proposed that AnxA6 is part of and stabilizes the HRas-GTP/p120GAP complex (23) to ensure Ras inactivation. Here, AnxA6 may act as the calcium sensor of p120GAP which lacks the aspartate residues necessary for the calcium-dependent membrane targeting (Figure 1C) (19, 23, 105, 106). In summary, AnxA6 potentiates the involvement of p120GAP and PKCα in H-Ras and EGFR signal termination.

AnxA6 was also found to play a significant role in the internalization and lysosomal degradation of endocytic vesicles. It was reported that LDL receptor-mediated endocytosis occurs after a sequence of interactions that starts with the association of AnxA6 with spectrin and a subsequent calcium and cysteine-dependent protease (calpain-1) recruitment. Then, calpain-1 cleaves the actin-spectrin cytoskeleton to make remodeling of the spectrin cytoskeleton leading to the release of the endocytic vesicle into the cytosol with AnxA6 attached to it (3, 72-74). Similarly, AnxA6 translocates to LE upon elevation of LDL or cholesterol levels in them (72, 85). This may induce spectrin reorganization, leading to the release of the budding vesicles from LE for degradation in the lysosomes (19, 74, 84). Likewise, AnxA6 was found associated with EGFR targeted for lysosomal degradation (44). Altogether, this suggests the crucial role of AnxA6 in endocytosis and lysosomal degradation. Several cellular functions of AnxA6 are facilitated via its highly dynamic interaction with the actin cytoskeleton which may not only impact on EGFR endocytosis and degradation (3, 107-110), but also on EGFR recycling (59, 60). It was demonstrated that upon calcium elevation AnxA6 binds F-actin (111, 112), and both co-localize at membrane ruffles (112, 113) and circular-dorsal ruffles leading to a membrane-cytoskeleton interaction as well as cortical

cytoskeleton stabilization (114). AnxA6 was also found to bind spectrin which in turn influences the F-actin bundling activity in a PS- and calcium-dependent manner (115). In addition, annexin-actin interaction was demonstrated to be involved in the regulation of store-operated calcium entry (SOCE) as reduced SOCE was observed following the stabilization of the cortical cytoskeleton (19, 114, 116-118).

Moreover, AnxA6 regulates EGFR mobility and distribution at the cell surface through controlling caveolae/lipid rafts formation directly via its interaction with phospholipids, actin, and signaling proteins or indirectly through the regulation of the intracellular distribution of cholesterol. The cholesterol-containing particles known as LDL are internalized from the cell surface via receptor-mediated endocytosis. In this process, AnxA6 interacts with the endocytic machinery including dynamin and AP1 leading to LDL endocytosis. Following internalization, the endocytic vesicle fuses with EE, then later targeted to lysosomes (66, 119). Generally little amounts of cholesterol are found in LE and lysosomes in normal cells. However, increased AnxA6 levels were shown to sequester cholesterol in LE and prevent its transport to the plasma membrane or the Golgi apparatus possibly via the cholesterol transporter Niemann Pick Type C1 (NPC1). Cholesterol depletion in the Golgi prevents the binding of cholesterol-sensitive cytosolic phospholipase A_2 ($cPLA_2$) to the Golgi, which is required to stimulate the transport of caveolin from the Golgi to the plasma membrane. Consequently, caveolin-1 is sequestered in Golgi, and caveolae formation is inhibited (3, 66, 75, 76) (Figure 3). It was reported that cells with increased AnxA6 showed a significant reduction of condensed membrane domains and suggested the ability of AnxA6 to promote changes in membrane architecture (19). These microdomain forming abilities of AnxA6 are likely to affect EGFR signaling and trafficking.

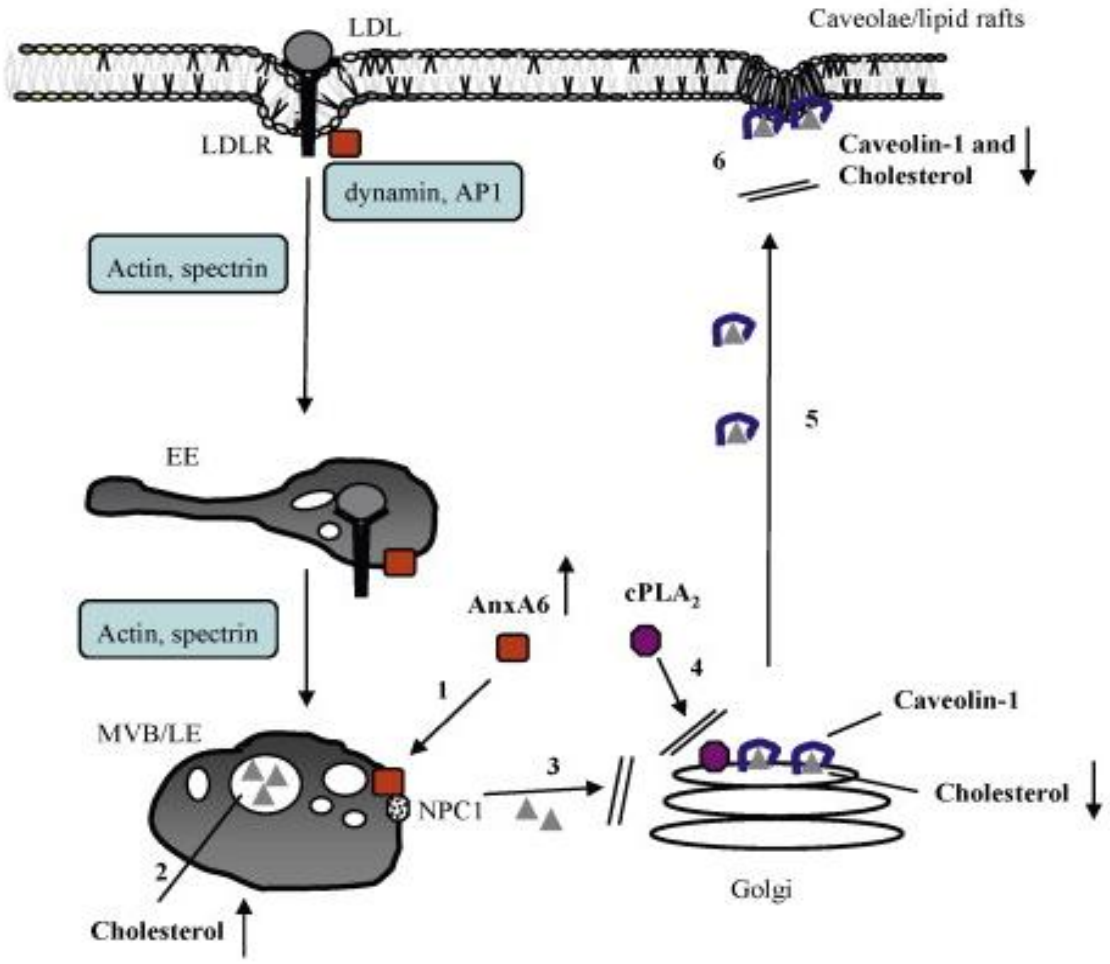

Figure 3. The role of AnxA6 in late endosomal cholesterol transport and caveolae/lipid raft formation. AnxA6 interacts with the endocytic machinery (dynamin, AP1) and induces the remodeling of the actin-spectrin cytoskeleton leading to low-density lipoprotein receptor (LDLR)-mediated endocytosis to early endosomes (EE) and lysosomal targeting of LDL. (1,2) In cells with high AnxA6 levels, AnxA6 translocates to multivesicular bodies/late endosomes (MVB/LE) upon LDL or cholesterol elevation. (3) AnxA6 interferes with Niemann Pick Type C1 (NPC1) protein to inhibit the transport of cholesterol to the Golgi apparatus. (4,5) Cholesterol depletion in the Golgi inhibits the binding of cytosolic phospholipase A_2 ($cPLA_2$) to the Golgi leading to the prevention of caveolin transport from the Golgi to the plasma membrane. (6) Caveolae formation is reduced as a result of decreased amounts of caveolin-1 and cholesterol at the plasma membrane. Taken from (66).

1.6 EGFR/Ras/MAPK pathway inhibitors

The crucial role that the EGFR/Ras/MAPK signaling cascade plays in cancer and other diseases has led to an intense research focusing on developing inhibitors of the pathway. Small molecule inhibitors blocking Raf or MEK1/2 as well as tyrosine kinase inhibitors and monoclonal antibodies targeting EGFR are examples of these inhibitors.

1.6.1 MEK1/2 inhibitors

MEK1 and MEK2 are closely related dual-specificity kinases that are activated by Raf kinases. Following their activation, they phosphorylate ERK1 and ERK2 kinases at serine/threonine and tyrosine residues leading to their activation (120). MEK and ERK were reported to be highly activated in cancer which attracted the interest of researchers to develop MEK inhibitor molecules in order to block the oncogenic signaling in a targeted approach (120, 121). PD98059 is one of the early compounds that were synthesized to block MEK1/2. It is a small molecule that performs its action via binding to the inactive form of MEK1/2 at a site other than the active site. Subsequently, the phosphorylation and activation of MEK1/2 are inhibited in a process that does not involve competing adenosine triphosphate (ATP) at the catalytic site, which may explain the high selectivity of the compound (120, 122). PD98059 is an important experimental tool for exploring the MEK-ERK pathway in studies targeting the role of ERK signaling in cancer (20, 120, 123).

1.6.2 EGFR inhibitors

Several approaches have been developed to inhibit the EGFR in order to treat cancer. The most clinically advanced approaches are monoclonal antibodies (mAbs) and tyrosine kinase inhibitors (TKIs), which perform their actions by two different mechanisms. Monoclonal antibodies bind to the extracellular ligand-binding domain of EGFR followed by internalization of the EGFR-mAb complex and inhibition of the signaling cascade. In contrast, tyrosine kinase inhibitors interact with the intracellular TK domain of the receptor by competing with ATP for the binding site. Thus, the enzymatic activity of the receptor is inhibited as well as its autophosphorylation leading to the inhibition of the EGFR signaling pathway (124, 125). These two mechanisms of action have been utilized to develop anticancer medications. For example, cetuximab (Erbitux®) is a chimeric monoclonal antibody that was approved for the treatment of metastatic colorectal and head and neck

cancers, as well as Panitumumab (Vectibix®), which is an approved fully humanized monoclonal antibody for metastatic colorectal cancer treatment. On the other hand, gefitinib (Iressa®) and erlotinib (Tarceva®) are two examples of approved tyrosine kinase inhibitors that are used to treat non-small-cell lung carcinoma (NSCLC) (126).

Although these medications are very successful in the treatment of cancer patients, their clinical use is still limited. Resistance to EGFR inhibitors, expression levels of EGFR regulatory factors and the not well characterized tumor microenvironment appear to influence drug efficiency.

1.6.3 Resistance to EGFR inhibitors

Cancer cells often have genetic mutations that lead to a sustained cell growth and an intrinsic resistance to some anticancer therapies. They can also develop an acquired resistance to EGFR inhibitors after a prolonged exposure to these medications (127, 128). Multiple mechanisms of action were reported to explain the reason behind this observed resistance; mutations are the most common ones. For example, KRAS gene mutations represent 35-40% of resistant cases and were demonstrated to be responsible for the resistance of lung adenocarcinoma against gefitinib and erlotinib (129, 130). The mutation of the catalytic subunit α of phosphatidylinositol 3-kinase (PI3KCA) and the inactivation of its negative regulator phosphatase and tensin homolog deleted on chromosome 10 (PTEN) were also found abundantly and were shown to cause resistance to mAbs targeting EGFR in colorectal cancer (131, 132). In addition, the expression of the mutated variant EGFRvIII produced cells with ligand-independent EGFR phosphorylation that showed resistance to gefitinib in glioblastoma multiform (133). Another example is the EGFR mutation in position 790 as a result of the substitution of threonine by methionine (T790M), which causes resistance as a consequence of the steric hindrance exhibited by the bulky methionine preventing TKIs from binding EGFR (126, 134, 135).

In addition, other mechanisms have been suggested. For example, NSCLC were reported to develop acquired resistance following the transactivation of HER2 and HER3 (136) and not to respond to cetuximab following hepatocyte growth factor receptor activation (126, 137). Head and neck squamous cell carcinomas (HNSCC) with cyclin D1 gene amplification and/or overexpression showed resistance to gefitinib (138, 139). Altered angiogenesis and the production of proangiogenic growth factors such as vascular endothelial growth factor (VEGF) and basic fibroblast growth factor (bFGF) could also be responsible for resistance to EGFR inhibitors (139). The activation of alternative growth factor receptor systems, such as insulin-like growth factor-I receptor (IGF1R), has also been associated with EGFR TKI resistance (126, 140).

Furthermore, up- or down-regulation of factors that regulate EGFR signaling and trafficking may also contribute (141). This includes scaffold proteins, which organize and stabilize the assembly and disassembly of EGFR signaling complexes at the plasma membrane and during endocytosis. Elevated expression of these scaffold proteins can lead to the increased recruitment of EGFR adaptors or effectors, thereby affecting signaling output. For example, cortactin overexpression led to a sustained EGFR signaling and an increased cell proliferation in HNSCC cells, in addition to a decreased sensitivity towards gefitinib (141, 142). Other scaffold proteins, such as caveolin and kinase suppressor of Ras (KSR), have also been reported to affect TKI sensitivity (143-148). This indicates that expression levels of scaffold proteins may serve as prognostic markers that predict the response towards EGFR-targeted therapies. However, markers with potential role in EGFR-related cancers still need to be identified. This would enable the medical team to provide patients with the proper treatment and to avoid medications, and consequently their undesired side effects.

1.7 PKC enzymes as targets for cancer treatment

PKC plays a critical role in cancer that led research to target this group of enzymes for anti-cancer drug development (41). PKC is a family of enzymes that phosphorylate serine and threonine residues of many proteins. They are encoded by nine genes and consist of 12 isozymes which were divided into three groups depending on their structures and regulation. The classical or conventional PKCs consist of PKCα, PKCβI, PKCβII, and PKCγ isozymes which all require calcium and DAG for activation and bind to negatively charged membrane phospholipids, specially PS. The second group is known as the novel PKCs which consist of PKCε, PKCδ, PKCθ, and PKCη isozymes; these PKC isozymes do not need calcium for activation but require DAG and PS. The atypical PKCs are the last group with PKCζ and PKCλ/ι as its members that do not require either calcium or DAG for activation but can be activated by PS (44, 149, 150).

Many PKC isozymes had been reported to associate with several physiological processes that are important for cancer. PKCα was found to be involved in cell proliferation, differentiation, apoptosis, cell cycle regulation, and cell adhesion (151); while PKCβ was reported to have a critical role in vasculogenesis (152). The level of some PKC isozymes was noted to increase in some cancers. For example, PKCθ is overexpressed in gastrointestinal stromal cancer (153), PKCη in NSCLC (154), and PKCε in colon, stomach, thyroid, lung, and breast cancers (155). Evidence also indicates the relation between the increased level of PKCη and cancer aggressiveness and proliferation (156), and correlates PKCδ activation to increased angiogenesis in prostate cancer (41, 157). As described above (section 1.3), out of the PKC family, PKCα is an important negative regulator of the EGFR and the Ras/MAPK pathway. Hence, the PKC family was considered as a possible anti-cancer therapeutic target, promoting research for the development of isozyme-specific PKC inhibitors.

BIM-I (also known as GF109203X or Gö 6850) is a potent PKC inhibitor. It is a bisindolylmaleimide derivative that inhibits α, β and γ isoforms. It performs its action through targeting the ATP-binding site of the kinase catalytic domain of PKC (158-160). Another example of a more selective PKC inhibitor is the indolocarbazole derivative Gö 6976 which is a selective inhibitor of both α and β1 isozymes. Similar to BIM-I, it functions as a competitive inhibitor at the ATP binding site of PKC (161). Specific PKC inhibitors are important experimental compounds in studies aiming at exploring PKC as a possible anti-cancer therapeutic target.

1.8 Phospholipase A_2

Besides PKC, members of the PLA_2 family have also been associated with EGFR activation in cancer. Hence, PLA_2 was suggested as a possible target for cancer therapy (162, 163). Phospholipase A_2 (PLA_2) is a set of esterase enzymes that catalyze the hydrolysis of glycerophospholipids at the sn-2 ester bond to yield a lysophopholipid and a fatty acid (162, 163). They are divided into five groups; secretory PLA_2 ($sPLA_2$), cytosolic PLA_2 ($cPLA_2$), Ca^{+2}-independent PLA_2 ($iPLA_2$), platelet-activating factor hydrolases (PAF-AH), and lysosomal PLA_2 (162, 164-166). $sPLA_2$ enzymes use histidine residues for the hydrolysis process and require Ca^{+2} for their activity, while $cPLA_2$ and $iPLA_2$ do not utilize histidine, but serine for the ester bond cleavage. $cPLA_2$ does not require Ca^{+2} for activation, rather Ca^{+2} is needed for their translocation to membranes. In contrast, $iPLA_2$ does not require Ca^{+2} for either activity or translocation (163, 165). Also, PAF-AH and lysosomal PLA_2 utilize serine residues in the hydrolysis process but on two different substrates; PAF-AH hydrolyzes the acetyl groups of PAF, while lysosomal PLA_2 catalyzes the hydrolysis of ceramide at its C-1 position (162, 166). The different isozymes of PLA_2 were found to correlate with cancer.

1.9 Phospholipase A_2 and cancer

PLA_2 enzymes were found to have a wide range of functions in different physiological processes. Evidence supports their role in cell growth (163, 167-171), cell signaling (163, 172-175), cell death (163, 164, 176, 177), inflammation (163, 172, 178, 179), and maintenance of membrane phospholipids (163, 180-182). It was reported that PLA_2 levels increase in several human cancers such as breast, colorectal, lung and prostate cancers (163, 183-191).

Several mechanisms were suggested to explain the role of PLA_2 in cancer formation. It was reported that PLA_2 cleaves glycerophospholipids into arachidonic acid and lysophospholipids; both of them are further metabolized into other molecules that were found to induce cell growth (163, 192-194). One important molecule is lysophosphatidic acid (LPA), which is released following the metabolism of lysophospholipid. It activates G-protein coupled receptors leading to the elevation of secondary messengers, cytosolic calcium and cAMP, and the subsequent activation of certain enzymes that can contribute to cancer formation such as PKC and Ras/MAPK (163, 194). It was also reported that $iPLA_2$ leads to the transactivation of EGFR in prostate and ovarian cancers (162, 195, 196) and that it regulates MAPK activity (162, 197-199).

Given that PLA_2 enzymes are considered as possible targets for anti-cancer agents and that AnxA6 inhibits caveolae formation via $cPLA_2$ (3, 66, 75, 76), PLA_2 inhibitors were considered in the studies presented here. Methyl arachidonyl fluorophosphonate (MAFP) is an example of a PLA_2 inhibitor which irreversibly inhibits $cPLA_2$, and to some extent $iPLA_2$. It is a phosphonate analogue of arachidonic acid that prevents the catalytic function of $cPLA_2$ via its direct interaction with the serine residues at the active site of $cPLA_2$ (200, 201). Grewal and coworkers had previously shown the potency of MAFP to mimic AnxA6 activity and inhibit the export of caveolin from the Golgi (75).

1.10 Combinatorial targeted therapy

The increased knowledge of cancer pathogenesis revealed its complex multigenic nature. Usually cancer therapy depends on killing rapidly dividing cells; an approach that has several limitations such as the narrow therapeutic index, acquired resistance, and overlapping toxicities (202-204). This justified the replacement of single-targeted drugs by combinatorial therapies (202-204). Combinatorial targeted treatments can be described as either vertical, which targets the same oncogenic signal transduction pathway at several steps, or horizontal, which targets several parallel pathways (202). Such approaches can overcome resistance and lead to increased efficacy and decreased toxicity.

An example of a combinatorial therapy is the mAb trastuzumab combined with the antimitotic chemotherapeutic agent docetaxel for the treatment of patients with human epidermal growth factor receptor 2 (HER2)-positive metastatic breast cancer. The addition of trastuzumab to the treatment, as compared to chemotherapy alone, increased the overall survival in these patients (205, 206). However, HER2 dimerization with other members of the HER family such as HER3 and EGFR led to trastuzumab resistance and a subsequent continued signaling transduction (207). This resistance was successfully targeted in the CLEOPATRA study via the triple therapy of trastuzumab, pertuzumab, and docetaxel; a combination that is now FDA approved. Pertuzumab is a humanized mAb which targets a HER2 epitope other than that of trastuzumab (202, 208-210).

Other successful approved combinations include the use of lapatinib, an EGFR and HER2 tyrosine kinase inhibitor, in combination with the antimetabolite chemotherapeutic agent capecitabine in the treatment of HER2-overexpressing metastatic breast cancer (202, 211, 212). Similarly, the monoclonal antibody cetuximab combined with the topoisomerase I inhibitor cytotoxic agent irinotecan are used for the treatment of patients with metastatic colorectal cancer (202, 213, 214).

1.11 Hypothesis and Aims

Over the years, several small molecules and monoclonal antibodies targeting EGFR-related pathways have been developed. In spite of the success of many TKIs and antibodies as anti-cancer EGFR agents, their clinical use is still very limited not only due to patient variability, but also the development of drug resistance, phenomena that are not well understood (125, 126, 130, 133-135). As outlined above (Section 1.10), one approach to overcome these issues is the replacement of single-targeted drug treatments by combinatorial therapies aiming to inhibit additional targets in the EGFR/Ras/MAPK pathway (202-204). This includes the combination of EGFR-TKIs and anti-EGFR antibodies (215, 216). In addition, the use of anti-EGFR drugs together with (vertical) Raf-1 or Mek1/2 inhibitors, that act downstream of EGFR, appears very promising (for review see (217-219)). Furthermore, the combination of EGFR and PKC inhibitors has also been considered, as PKC inhibition promotes not only apoptosis through other regulatory circuits, but also downregulates EGFR/Ras/MAPK signalling (220, 221).

Despite these promising approaches, there is still little knowledge how to identify patients that will respond well to single or combinatorial anti-cancer treatments aiming to block oncogenic EGFR. Hence, there is a great demand for biomarkers to predict the treatment outcomes and the potential development of drug resistance. As outlined above, scaffold proteins are essential for the formation and disassembly of signalling complexes. Thus, high and low expression levels of a particular scaffold protein can promote or inhibit the formation of multifactorial protein complexes. In the previous sections, the role of AnxA6 as a scaffold protein to recruit negative regulators of the EGFR/Ras/MAPK pathway has been described (Sections 1.4 and 1.5). High levels of AnxA6 increase the recruitment of PKCα and p120GAP to the plasma membrane, thereby increasing EGFR/PKCα and Ras/p120GAP complex formation, leading to inhibition of EGFR and Ras, respectively (22, 23, 29, 44, 100,

102, 104, 105). Based on these observations, it is tempting to speculate that reduced numbers of active EGFR- and Ras/MAPK containing protein complexes in cells with high AnxA6 levels would lessen the amount of drug required to inhibit the remaining pool of active EGFR and Ras/MAPK in every cancer cell.

Hence, we hypothesize that high AnxA6 level will improve the efficacy of single or combinatorial treatments targeting EGFR-related cancer cell growth. To address the hypothesis, we will focus on the following aims:

Aim 1: To compare the efficacy of EGFR-TKIs (erlotinib, gefitinib, AG1478) in EGFR overexpressing cancer cells with high and low AnxA6 levels.

Aim 2: To compare the efficacy of monoclonal anti-EGFR antibodies (cetuximab) in EGFR overexpressing cancer cells with high and low AnxA6 levels.

Aim 3: To compare the efficacy of EGFR-TKIs (erlotinib, gefitinib) in combination with anti-EGFR antibodies in EGFR overexpressing cancer cells with high and low AnxA6 levels.

Aim 4: To compare the efficacy of EGFR-TKIs (erlotinib, gefitinib) in combination with MEK1/2 or PKC inhibitors in EGFR overexpressing cancer cells with high and low AnxA6 levels.

To address these aims, we will determine clonogenic growth and measure cell proliferation (MTS) ± drugs in EGFR-overexpressing A431 cells that lack AnxA6 (A431wt) or overexpress AnxA6 (A431-A6). The identification of AnxA6 upregulation improving drug sensitivity could develop the determination of Anx6 expression as a prognostic tool to predict drug efficacy in patients with EGFR-related cancers.

1.11.1 Cell model and study design

To address the aims listed above, human epidermoid A431 carcinoma cells were utilized. This cell line, with approximately 1-3 x 10^6 EGFR per cell, represents the classical model to study oncogenic EGFR activity due to EGFR overexpression (222). A431 wild type cells (A431wt) lack endogenous AnxA6. On the other hand, Grewal and coworkers established a stably transfected A431 cell line that overexpresses AnxA6. This cell line is well characterized (22, 72, 114), with AnxA6 expression levels comparable to endogenous AnxA6 levels found in many cells and tissues (3, 66, 223, 224). Moreover, A431-A6 cells display reduced EGFR and Ras/MAPK activity compared to A431wt cells (29). Hence, the comparison of growth inhibition upon exposure to EGFR/Ras/MAPK inhibitors in A431wt versus A431-A6 cells is ideal to identify if elevated AnxA6 levels provide an opportunity for improved drug efficacy. We employed the colony formation assay in our investigations which is well documented to reflect the oncogenic potential of a cancer cell (Figure 4). It is a commonly used test to investigate the effectiveness of anti-cancer therapeutics.

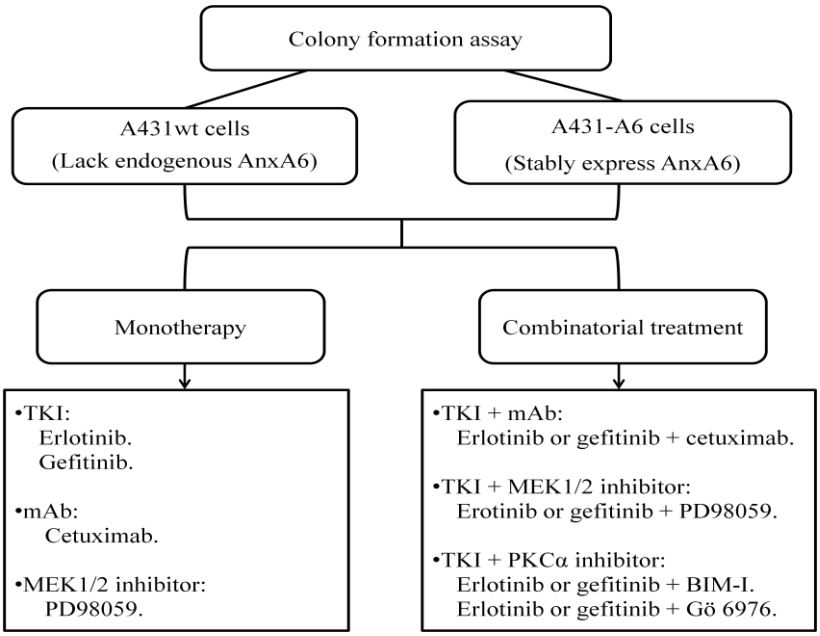

Figure 4. Scheme illustrating study design. The colony formation assay was adopted to determine if elevated AnxA6 levels increase drug efficacy in A431 cells. A431wt (lack endogenous AnxA6) and A431-A6 (stably express AnxA6) cells were treated with TKIs (erlotinib or gefitinib), mAb (cetuximab), MEK1/2 inhibitor (PD98059) and PKCα inhibitors (BIM-I, Gö6976) alone (monotherapies) or in combination (combinatorial treatment) as indicated.

1.11.2 Drug selection

The focus of this study was to determine if the presence of AnxA6 improves anticancer drug performance. Hence, rather than analyzing novel EGFR-TKIs or anti-EGFR antibodies, that are being developed currently, we reasoned that commercially available anti-EGFR drugs would provide the opportunity to deliver proof-of-principle. Hence, drugs were selected based on their mechanisms of action in relation to the EGFR/Ras/MAPK pathway and AnxA6 (Figure 5). TKIs and mAbs are the two major classes of EGFR inhibitors, which function by two different mechanisms to block EGFR signaling (124, 125). We selected three FDA approved drugs that are commercially available in our investigations, erlotinib and gefitinib as examples of TKIs, and cetuximab as an example of mAb (126). In addition, in one set of experiments, to further validate erlotinib- and gefitinib-based data, we tested AG1478, which is considered more potent than erlotinib and gefitinib (225-228).

MEK1/2 acts downstream of EGFR and is critical to propagate the growth-promoting signal from EGFR. As combinatorial drug treatments of EGFR and MAPK inhibitors have provided potential to improve treatment efficacy (229-231), we included the combination of EGFR-TKIs with MEK1/2 inhibitors. MEK1/2 is highly activated in EGFR-related cancers (120, 121) and can be blocked effectively with PD98059, a small molecule that is highly selective for MEK1/2 within the MAPK protein family (120, 122). It is considered a useful experimental tool in exploring the MEK-ERK pathway in cancer studies (20, 120, 123).

PKCα was also targeted in this study. Blocking PKC activity has long been considered an option to reduce oncogenic cell behavior. As described in the introduction (section 1.3), AnxA6 facilitates the membrane recruitment and association of PKCα with EGFR, leading to EGFR Threonine 654 phosphorylation and consequently EGFR inactivation. As PKCα knockdown restores EGFR activity in A431-A6 cells (29), we reasoned that blocking PKCα activity via small molecules might interfere with the ability of AnxA6 to negatively regulate

EGFR signaling (45-47). As outlined in the results and discussion, we chose Gö6976 and BIM-I in our investigations, which are commonly used in the field and represent two potent PKC inhibitors (158-161).

In addition, some experiments were performed with $cPLA_2$ inhibitors (MAFP). These studies are based on the ability of AnxA6 to inhibit $cPLA_2$-dependent membrane trafficking events (3, 19, 66, 75, 76) that might interfere with the cell surface expression of EGFR.

As the combinatorial treatment of EGFR inhibitors with anti-EGFR antibodies as well as MAPK and PKC inhibitors has provided promising results previously (215, 229-234), we decided to test the efficacy of all of the above drugs alone and in combination. To reduce the complexity, the number of control samples required, and to reduce the risk of undesired drug-drug interactions, we limited the project to analyzing drugs alone or in pairs.

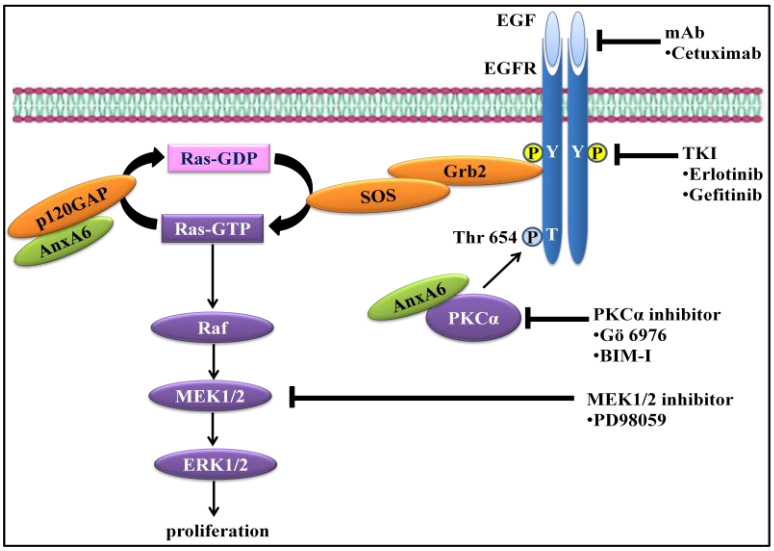

Figure 5. EGFR/Ras/MAPK pathway highlighting the different inhibitors used in this study. The association of EGF to EGFR induces receptor dimerization and TK activation, followed by autophosphorylation of the receptor. Grb2 is an adaptor protein which binds phosphorylated EGFR and other TK residues. Consequently, SOS binds Grb2 and activates Ras by exchanging the inactive Ras-GDP with active Ras-GTP. This leads to the recruitment and activation of the serine/threonine-protein kinase Raf. Activated Raf then phosphorylates and activates MEK1/2, which in turn phosphorylates and activates ERK1/2. Then, activated ERK phosphorylates nuclear proteins and modulates the activity of several transcription factors regulating gene expression to induce cell growth and differentiation. Annexin A6 is a scaffold protein for p120GAP and PKCα, both are negative regulators of the EGFR signaling pathway. p120GAP inactivates Ras, while PKCα phosphorylates EGFR at threonine 654 leading to the inhibition of its TK activity. The selection of inhibitors used in this study was based on their mechanisms of action. Cetuximab is a monoclonal antibody which binds the extracellular ligand-binging domain of EGFR, thereby blocking EGF ligand binding. In contrast, erlotinib and gefitinib represent TKIs which compete with ATP for the intracellular binding site in the EGFR tyrosine kinase domain. Finally, Gö 6976 and BIM-I are two potent PKC inhibitors, while PD98059 is a selective MEK1/2 inhibitor.

Chapter 2: Materials and Methods

2.1 Study drugs

To investigate the impact of inhibiting EGFR, MAPK, PKCα and cPLA2 (alone or in combination) on cancer cell growth, commercially available EGFR-TKIs (erlotinib, gefitinib, AG1478), MAPK (MEK1/2 inhibitor PD98059), PKCα (BIM-I, Gö6976) and $cPLA_2$ (MAFP) inhibitors, as well as a clinically used monoclonal EGFR antibody available through collaborators (cetuximab) were analyzed. Erlotinib, gefitinib, MAFP, and BIM-I were purchased from Cayman Chemical Company (Ann Arbor, Michigan, USA). Gö6976 and AG1478 were obtained from Sigma-Aldrich (Castle Hill, NSW, Australia), while PD98059 was from Sigma-Aldrich (St. Louis, Missouri, USA). Cetuximab was kindly provided by Dr. Fiona Simpson (The University of Queensland Diamantina Institute, Brisbane, Queensland, Australia).

2.2 Cell culture

The human epidermoid carcinoma A431 cell line was chosen as this cell line represents the classical model to investigate oncogenic EGFR activity due to EGFR overexpression (29, 222). This cell line expresses approximately 1-3 x 10^6 EGFR per cell, and has been utilized in numerous studies to investigate the efficacy and mode of action of EGFR-TKIs as well as monoclonal antibodies targeting EGFR. A431wt cells lack endogenous AnxA6, and A431-A6 stably express AnxA6 at levels that are commonly observed in many cells and tissues (3, 22, 66, 72, 114, 223, 224), making the two cell lines ideal to compare anticancer drug efficacy in the absence or presence of AnxA6.

2.2.1 Culture media

Cells were cultured in Dulbecco's Modified Eagle's medium (DMEM, Gibco, USA) formulated with low glucose (1 g/L), sodium pyruvate (110 mg/L), and GlutaMAX™-I (500ml DMEM (1X) + GlutaMAX™-I). The media were supplemented with 10% fetal bovine serum (FBS, Gibco, USA) and 1% penicillin/streptomycin (Gibco, USA).

2.2.2 Culture of A431wt and A431-A6 cells

A431wt cells were purchased from the American Type Culture Collection (ATCC; Manassas, VA, USA), while the stable A431-A6 cell line was generated in the Grewal laboratory (23).

Cells grown in tissue cultures lose their characteristic features when cultured for an extensive long period. This is associated with changes in cell morphology and growth behavior, which can affect the experimental outcome. To ensure reproducibility of results, cells growing no longer than 15 passages were used. This required the freezing of cells very early in this project to ensure a reliable source of cells throughout the 1-year project. The protocol to preserve A431 cells was as follows: Preservation in liquid nitrogen was adapted for long term storage of the cells using freezing media with DMEM (1X) + GlutaMAX™-I, 20% FBS, and 10% DMSO. Frozen cells were thawed as follows: The cells were quickly thawed in a 37°C water bath, added to 6ml culture media, and centrifuged at 1400 rpm for 5 minutes. The supernatant was removed by suction, and 5ml of Dulbecco's phosphate-buffered saline (DPBS calcium, magnesium, and Phenol Red free, Gibco, USA) was added in which the cells were resuspended, and then centrifuged for 5 minutes at 1400 rpm. The supernatant was removed, and cells were resuspended in 6ml media and transferred to a T25 cell culture flask (Corning Incorporated Life Sciences, USA) which was then placed in a humidified incubator at 37°C and 5% CO_2. When 60-70% confluency was reached, the cells were transferred to a T75 cell culture flask and passaged twice a week thereafter.

2.2.3 Passaging of A431wt and A431-A6 cells

To avoid cell overgrowth and consequently apoptosis, passaging of the cell line ensures cell viability under standard culture conditions. Cancer cell lines such as A431 replicate approximately every 22-24 h, and when cultured in a 75 cm^2 flask, they have to be passaged every 3-5 days to avoid overgrowth. In this technique, the culture medium was removed by suction using a Pasteur pipette, followed by washing cells with 2ml DPBS in order to remove dead cells debris and the remaining growth medium which contains FBS that can inhibit trypsin. Then, 2ml of the proteolytic enzyme trypsin (1X) (0.5% Trypsin-EDTA (10X); Gibco, USA) was added to detach the cells by disrupting the cell-substratum and cell-cell interactions. Cells were incubated with trypsin for 8 minutes in a humidified incubator at 37°C and 5% CO_2. The detachment was evaluated microscopically, using a Nikon Eclipse TS100 microscope, and enhanced by strongly tapping the flask to ensure the removal of all the cells from the surface. Then, 8ml of the culture media was added to deactivate trypsin. Finally, 1ml of cells was added to 9ml of fresh media to obtain a 1:10 split ratio. Cells were passaged twice per week and kept in a humidified incubator at 37°C and 5% CO_2.

2.3 Colony formation assay

The growth inhibitory effect of drugs was evaluated using the colony formation assay (also known as the clonogenic assay). It is a commonly used assay to investigate the effect of anti-cancer agents on the proliferative ability of transformed cell lines (235). It depends on the capacity of a single cell to retain its reproductive ability and to grow into a colony (236). Here, the test was used to compare the growth inhibitory effect of anticancer drugs targeting the EGFR/Ras/MAPK pathway in the presence or absence of AnxA6 in A431 cells. Therefore, A431wt and A431-A6 cells were passaged by trypsinization, counted using a haemocytometer, and plated in a six-well culture plates at a density of 7000 cells per well to

a total volume of 2ml culture medium. The plates were incubated overnight in a humidified incubator at 37°C and 5% CO_2.

On the following day, drugs were added at the appropriate concentrations to the cells. DMSO (less than 0.1%) was used as the negative control in all of the experiments except when cetuximab was tested for which only the culture medium was the control. Cells were incubated for further four to five days, depending on the growth rate, with and without drugs in a humidified incubator at 37°C and 5% CO_2.

Then, the cells were washed twice with DPBS, fixed with Diff Quik Fixative, and stained with Diff Quik stain (Lab Aids Pty Ltd, North Narrabeen, NSW 2101, Australia). Finally, cells were rinsed twice with deionized water and left for air dry. Photos for each well were taken by the camera of the cell phone Samsung Galaxy S6 Edge plus (16MP/ F1.9) to illustrate the density of colony formation in the wells. Ten images per well were randomly taken using the P.A.L.M. DuoFlex Combi System (Carl Zeiss) via 5X magnification; these ten images occupy an area of 3.34% of the total area of one well. The number of colonies in the images were counted and plotted against drug concentrations. The percentage of inhibition was calculated according to the equation (% inhibition= [(total number of colonies in the control well- total number of colonies in the sample well)/ total number of colonies in the control well] x 100). Each experiment was independently repeated three times unless otherwise indicated.

2.4 Cell proliferation assay (MTS assay)

To validate data sets obtained from clonogenic assays (see Section 2.3) on A431wt and A431-A6 cell growth ± anticancer drugs, cell proliferation was additionally determined using the MTS assay. This assay determines the metabolic activity of cells and is a convenient methodology to assess cell proliferation and the cytotoxic potential of compounds through

colorimetric determination of metabolic activity. The concept of the assay is the bioreduction of the tetrazolium compound by the dehydrogenase enzymes of the metabolically active cells into formazan. Formazan is an aqueous compound that is soluble in the tissue culture medium. Its absorbance can be measured directly from the 96-well plate at 490 nm, and it is directly proportional to the number of metabolically active (living) cells.

In our experiments CellTiter 96® Aqueous Non-Radioactive Cell Proliferation Assay Kit (Progema) was used which is composed of an electron coupling reagent (phenazine methosulfate; PMS) and a tetrazolium compound (3-(4,5-dimethylthiazol-2-yl)-5-(3-carboxymethoxyphenyl)-2-(4-sulfophenyl)-2H-tetrazolium, inner salt; MTS). The preparation of the reagents included thawing both the 100ml PMS and the 5ml MTS, combining both solutions together, and then storing the final solution in 5ml tubes at -20°C for later use.

The following protocol was adapted in our experiments. A431wt and A431-A6 cells were seeded in 96-well plates at a density of 4000 and/or 8000 cells per well in growth medium (90µl cell suspension/well) and left overnight in a humidified incubator at 37°C and 5% CO_2. On the following day, drugs were added to the wells at the appropriate concentrations. Then, the plates were put back in the humidified incubator at 37°C and 5% CO_2 for additional three days without changing the medium. Quadruple repeats were made for each drug treatment. Then, 20µl of the prepared MTS solution was added to each well, and the plates were incubated for 30-60 minutes in a humidified incubator at 37°C and 5% CO_2. The absorbance was detected at 490 nm using Bio-Rad Model 680 microplate reader. Mean absorbance, percentage of viability, and percentage of growth inhibition for each drug dose were calculated. Then, percentage of viability or growth inhibition was plotted versus drug concentrations.

- Percentage of viability = [(mean absorbance from sample well – mean absorbance from medium (blank)/ (mean absorbance from solvent treated cells (control) – mean absorbance from medium (blank)] x 100
- Percentage of growth inhibition = 100 – cell survival

2.5 Statistical analysis

Statistical analysis is critical when aiming at determining the significance of experimental data. Therefore, in order to obtain the statistical significance that AnxA6 expression impacts on drug performance, each experiment, unless stated otherwise in the figure legend, was performed at least 3 times. The results were expressed as the mean ± SEM except the results of representative experiments which were expressed as mean ± SD. The data was analyzed using GraphPad Prism version 6.07 software. The statistical analysis of all data was done by student's unpaired t-test, in which we compared the results obtained from A431-A6 cells with that of A431wt control unless otherwise indicated. The P value < 0.05 was considered statistically significant (***$P < 0.001$; **$P < 0.01$; *$P < 0.05$).

Chapter 3: Results

3.1 Increased anti-cancer potency of erlotinib in A431-A6 cells

AnxA6 overexpression reduces the growth of A431 cells via its role in the downregulation of the EGFR/Ras/MAPK pathway (22, 23, 29, 99). We wanted to explore if this effect of AnxA6 could lead to increased potency of TKIs in A431 cells. Therefore, the inhibitory effect of erlotinib on the oncogenic growth of A431-A6 cells, which are well characterized and stably overexpress AnxA6 (22, 72, 114), and A431wt cells was compared by employing clonogenic assays. To completely abrogate EGFR signaling, EGFR TKIs are generally used at a concentration of 10µM in cell culture studies (234, 237). A431wt and A431-A6 cells were plated at low density and incubated with different erlotinib concentrations (1µM, 10µM, 25µM) for five days to allow colony formation. Then, the cells were washed twice with DPBS, fixed and stained. Colonies of twenty or more cells were counted and plotted against erlotinib concentrations (Figure 6). The results revealed that the number of colonies decreased by 14.8% in A431-A6 control compared to A431wt control, which confirm the previous findings of our laboratory (22). The dose of 1µM erlotinib decreased the number of colonies in A431wt cells by 39.1% from 227 ± 37.7 to 138.3 ± 19.3, while in A431-A6 cells it was significantly decreased by 61.5% to 87.3 ± 24.4 ($P = 0.036$), which illustrates the potentiating effect of AnxA6 on cell growth inhibition with a small dose of erlotinib. The dose of 10µM erlotinib significantly decreased the number of colonies by 97.5% (5.7 ± 1.8) in A431wt cells ($P = 0.004$), and by 99.6% (1 ± 1) in A431-A6 cells ($P = 0.004$). Lastly, the dose of 25µM caused 99.4% significant inhibition in A431wt colony formation ($P = 0.004$), and 100% inhibition in A431-A6 cells ($P = 0.004$) (Figure 7). The experiment was repeated three times with A431-A6 cells showing less colony formation than A431wt cells, and A431-

A6 cells being more sensitive to erlotinib treatment than A431wt cells, suggesting that AnxA6 has an inhibitory effect on cell growth that is augmented by erlotinib treatment.

3.2 MTS assay identifies increased growth inhibition in AnxA6 expressing cells treated with erlotinib

Erlotinib effectively inhibited A431 colony formation upon AnxA6 overexpression (Figure 6 and 7). Previously Grewal and coworkers showed the increased potency of TKIs in the presence of AnxA6 using MTS assays (unpublished). To confirm these findings, A431wt and A431-A6 cells were seeded at a density of 4000 cells per well and incubated with different erlotinib concentrations (0.5µM, 1µM, 5µM, 10µM, and 50µM) for three days. Quadruple repeats were made for each treatment. Then, MTS reagent was added and the plates were incubated for 30 minutes. The absorbance was detected at 490 nm, and the percentage of viability was calculated and plotted against erlotinib concentrations. The results showed reduced viability of A431wt cells (93.8%, 83.7%, 59%, 44.9%, 37.7%) with increased amounts of erlotinib (0.5µM, 1µM, 5µM, 10µM, 50µM), respectively. Similarly, reduced viability of A431-A6 cells was observed (73.4%, 53.8%, 53.3%, 37.6%, 30.6%) with the above mentioned drug treatments, respectively (Figure 8). In support of the results observed in the clonogenic assays (Figure 6 and 7), the MTS data showed that A431-A6 cells are more sensitive to erlotinib treatment than A431wt cells, supporting our hypothesis that elevated AnxA6 expression can potentiate the growth inhibitory effect of erlotinib.

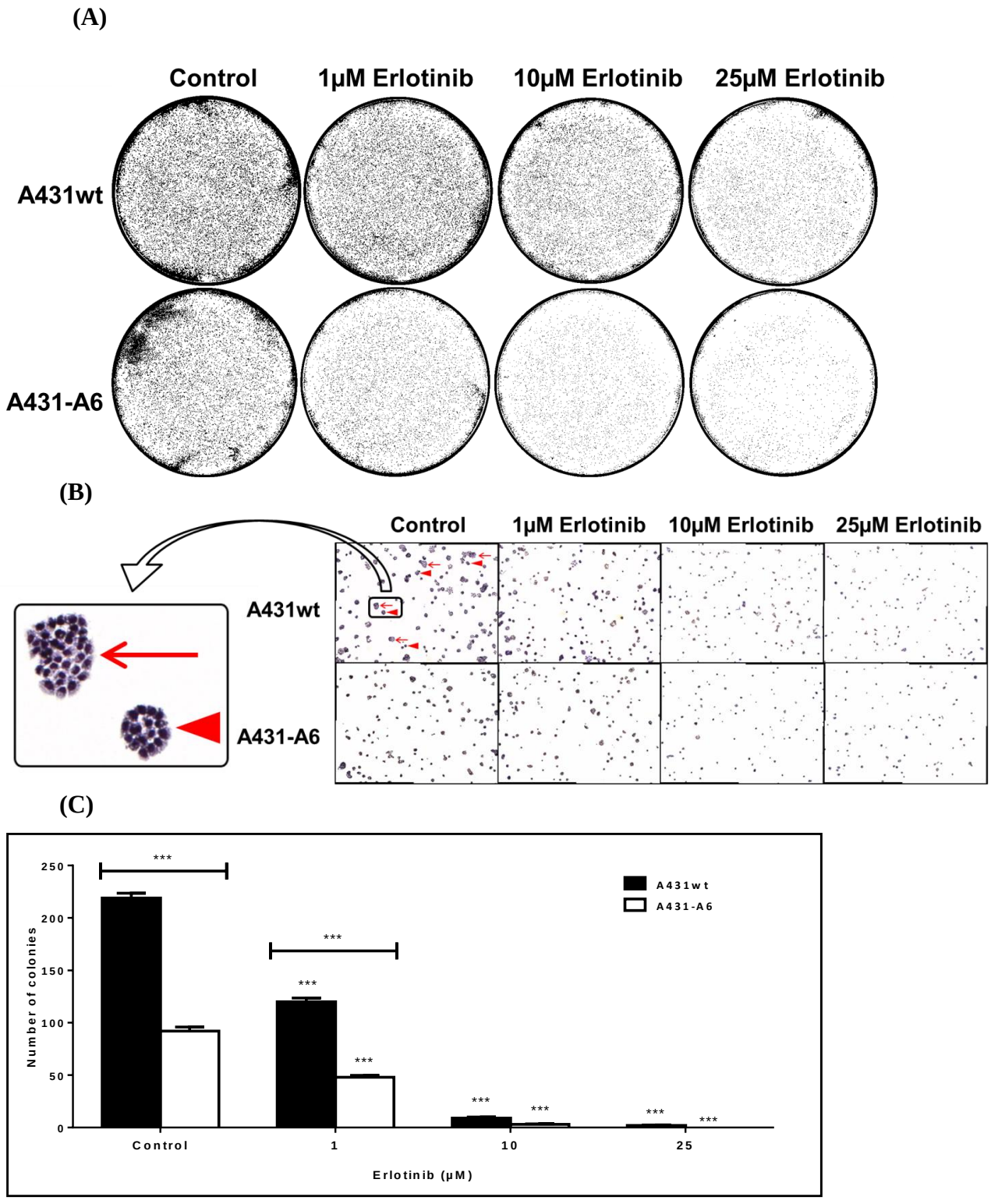

Figure 6. Clonogenic assay of A431wt and A431-A6 cells treated with 0-25µM erlotinib. (A) A431wt and A431-A6 cells were plated in six-well culture plates at a density of 7000 cells per well and treated with 1µM, 10µM, and 25µM erlotinib for five days as indicated. Then cells were fixed and stained. One photo/well was taken to document the density of colony formation in the wells. (B) 10 images/well were randomly taken using the P.A.L.M. DuoFlex Combi System (Carl Zeiss). The arrows indicate colonies composed of 20 cells or more, while arrowheads point at colonies of less than 20 cells (see enlarged section). (C) Colonies of 20 cells or more were counted in 10 images/condition and plotted against erlotinib concentrations. The error bars represent the SD. Statistical analysis was performed using student's unpaired t-test and based on the analysis of 10 images/well that were randomly taken of the same experiment. * represent a significant decrease of colony formation compared to A431wt control; *** $P < 0.001$.

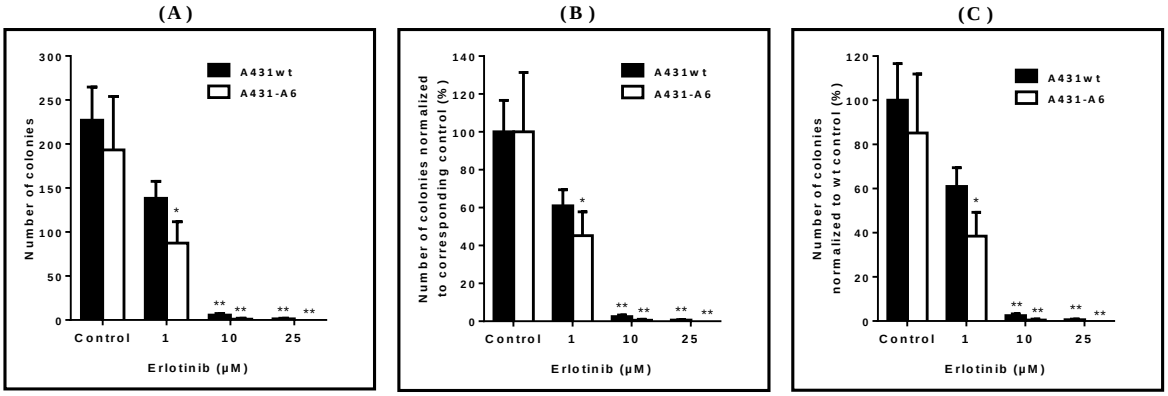

Figure 7. AnxA6 overexpression potentiates erlotinib-mediated growth inhibition in A431 cells. A431wt and A431-A6 cells were incubated with 1μM, 10μM, and 25μM erlotinib for five days. Colonies of 20 cells or more were counted. Data represents the mean ± SEM of three independent experiments. (A) The number of colonies of A431wt and A431-A6 were plotted against erlotinib concentrations. (B) The number of colonies of A431wt and A431-A6 were normalized to A431wt control and A431-A6 control, respectively, and plotted against erlotinib concentrations. (C) The number of colonies of A431wt and A431-A6 were normalized to A431wt control and plotted against erlotinib concentrations. Statistical analysis was performed using student's unpaired t-test where * represents a significant decrease of colony formation compared to A431wt control; * $P < 0.05$; ** $P < 0.01$

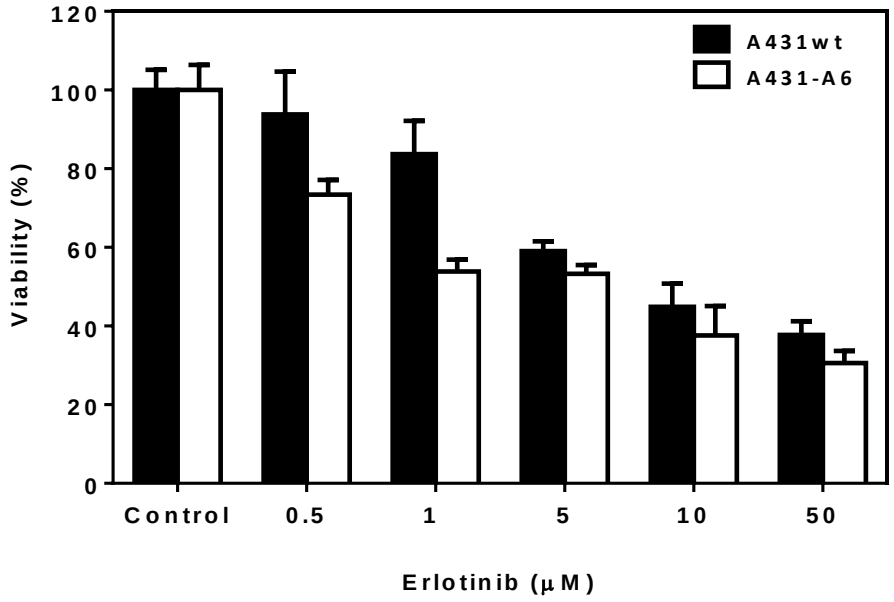

Figure 8. MTS assay showing the effect of erlotinib on A431wt and A431-A6 cell growth. A431wt and A431-A6 cells were seeded at a density of 4000 cells per well, and incubated with 0.5μM, 1μM, 5μM, 10μM, and 50μM erlotinib for three days. Quadruple repeats were made for each treatment. Then, MTS reagent was added and the plates were incubated for 30 minutes. The absorbance was detected at 490 nm, and the percentage of growth inhibition was calculated and plotted against erlotinib concentrations. The error bars represent the SD (n = 1).

3.3 AnxA6 overexpression potentiates the growth inhibition mediated by gefitinib

To extend our findings of the increased sensitivity of A431-A6 cells towards erlotinib (Figure 6 and 8), we next compared colony formation in A431wt and A431-A6 cells after gefitinib treatment. A431wt and A431-A6 cells were plated as described above (section 3.1) and incubated with different gefitinib concentrations (1µM, 10µM, 25µM) for five days to allow colony formation. Then, the cells were washed twice with DPBS, fixed and stained. Colonies of twenty or more cells were counted and plotted against gefitinib concentrations (Figure 9). In agreement with published data and the results shown in Figure 6 and Figure 8, the number of colonies in A431wt control was 254.7 ± 55.3 compared to 205.7 ± 30 in A431-A6 control which represents 19% less colony formation. The number of colonies in A431wt cells treated with 1µM, 10µM, and 25µM gefitinib was 164 ± 16.7, 35.3 ± 8.4, and 1.3 ± 0.9, which represents 35.7%, 86.1%, and 99.5% reduction of colony formation, respectively, that was found to be statistically significant for 10µM and 25µM gefitinib ($P<0.05$). On the other hand, the number of colonies in A431-A6 cells treated with 1µM, 10µM, and 25µM gefitinib was 125 ± 27, 19.7 ± 11.5, and 0.7 ± 0.7, respectively. These results revealed 51% reduction of colony formation in A431-A6 cells treated with 1µM gefitinib, and 92.3 % and 99.7% reduction of colony formation in A431-A6 cells treated with 10µM and 25µM gefitinib, respectively ($P<0.05$). Similar to the data obtained with erlotinib (Figure 6-8), an enhanced inhibition of growth after 1µM gefitinib treatment of A431-A6 cells compared to A431wt cells was observed, while an almost similar inhibition with 10µM and 25µM of the drug was apparent (Figure 10). The experiment was repeated three times which showed less colony formation in A431-A6 cells compared to A431wt cells and an increased potency of the drug at low concentrations in A431-A6 cells.

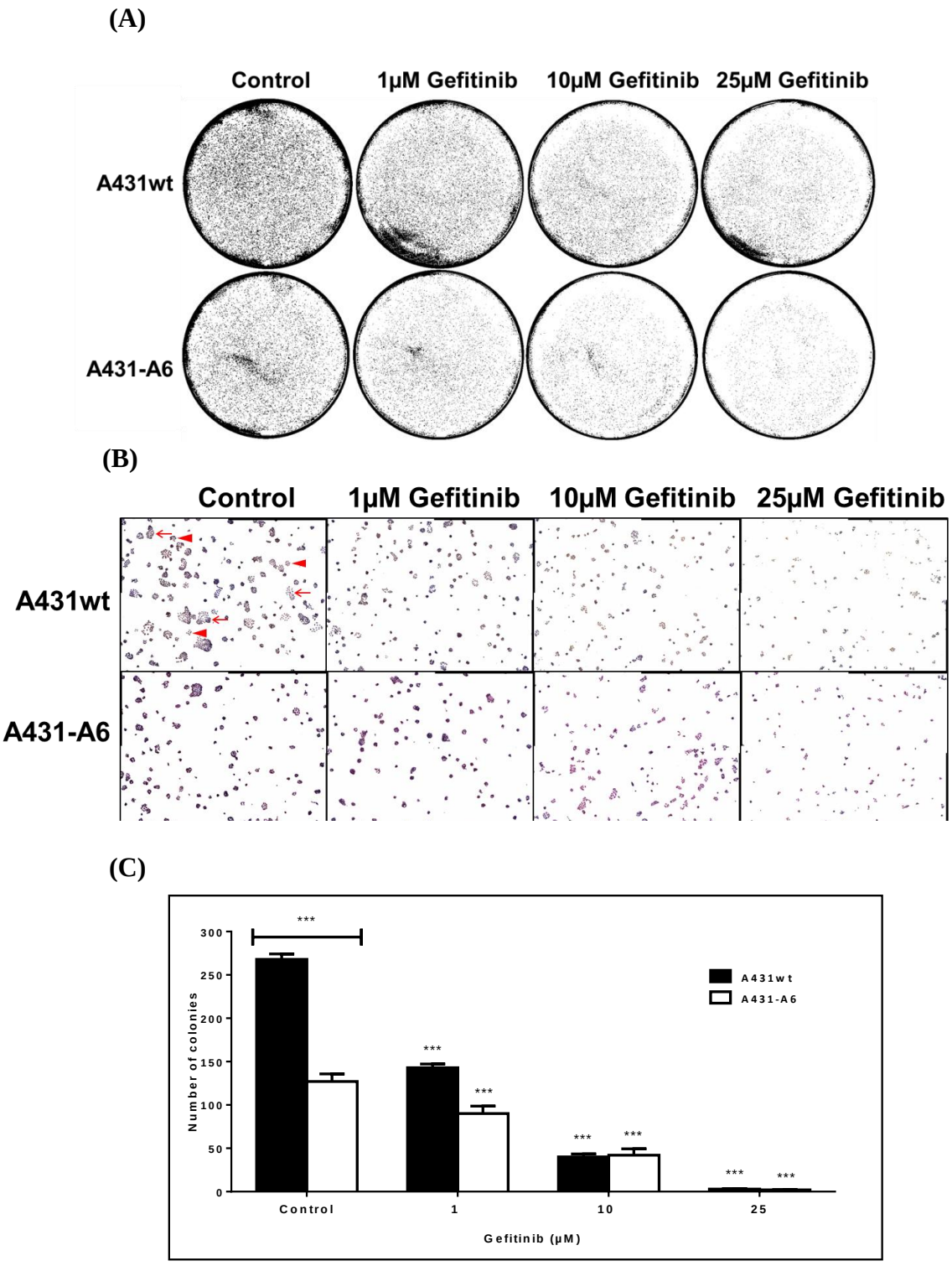

Figure 9. Clonogenic assay of A431wt and A431-A6 cells treated with 0-25μM gefitinib. (A) A431wt and A431-A6 cells were plated in six-well culture plates at a density of 7000 cells per well and treated with 1μM, 10μM, and 25μM gefitinib for five days as indicated. Then cells were fixed and stained. One photo/well was taken to document the density of colony formation in the wells. (B) 10 images/well were randomly taken using the P.A.L.M. DuoFlex Combi System (Carl Zeiss). The arrows indicate colonies composed of 20 cells or more, while arrowheads point at colonies of less than 20 cells. (C) Colonies of 20 cells or more were counted in 10 images/condition and plotted against gefitinib concentrations. The error bars represent the SD. Statistical analysis was performed using student's unpaired t-test and based on the analysis of 10 images/well that were randomly taken of the same experiment. * represent a significant decrease of colony formation compared to A431wt control; *** $P < 0.001$.

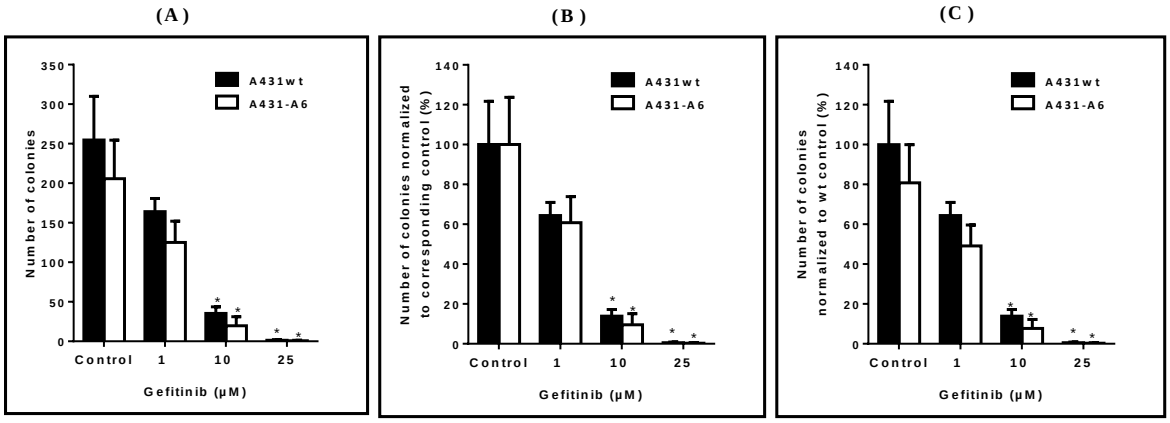

Figure 10. AnxA6 overexpression potentiates gefitinib-mediated growth inhibition in A431 cells. A431wt and A431-A6 cells were incubated with 1μM, 10μM, and 25μM gefitinib for five days. Colonies of 20 cells or more were counted. Data represents the mean ± SEM of three independent experiments. (A) The number of colonies of A431wt and A431-A6 were plotted against gefitinib concentrations. (B) The number of colonies of A431wt and A431-A6 were normalized to A431wt control and A431-A6 control, respectively, and plotted against gefitinib concentrations. (C) The number of colonies of A431wt and A431-A6 were normalized to A431wt control and plotted against gefitinib concentrations. Statistical analysis was performed using student's unpaired t-test where * represents a significant decrease of colony formation compared to A431wt control; * $P < 0.05$.

3.4 Gefitinib treatment effectively inhibits cell growth of AnxA6 expressing cells

Colony formation was effectively inhibited in A431-A6 cells treated with gefitinib (Figure 9 and 10). Using MTS, Grewal and coworkers were recently able to show the increased potency of TKIs in AnxA6 overexpressing cells (unpublished). To confirm these findings, A431wt and A431-A6 cells were seeded at a density of 4000 cells per well and incubated with 10μM and 50μM gefitinib concentrations for three days. Quadruple repeats were made for each treatment. Then, MTS reagent was added and the plates were incubated for 30-60 minutes. The absorbance was detected at 490 nm, and the percentage of growth inhibition was calculated and plotted against gefitinib concentrations. The results showed that the percentage of growth inhibition was 32.8% in A431wt cells compared to 63.8% in A431-A6 cells after the treatment with 10μM gefitinib. When the drug dose was increased to 50μM, the percentage of growth inhibition became 81.5% in A431wt cells and 105.3% in A431-A6 cells (Figure 11). The experiment was repeated three times, and the data shows that A431-A6

cells were more sensitive to gefitinib treatment than A431wt cells, suggesting that elevated AnxA6 levels potentiate the efficacy of TKIs.

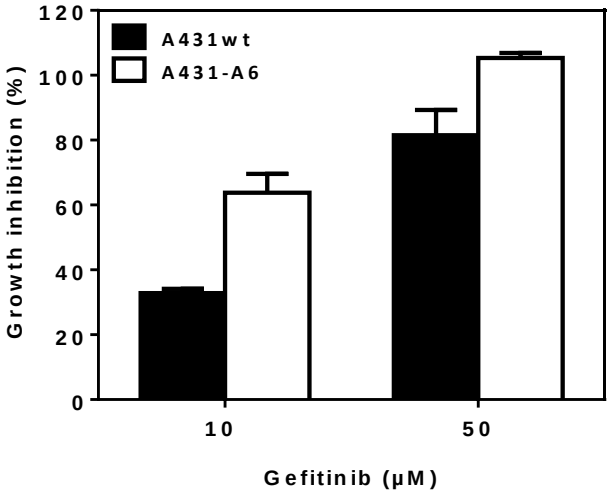

Figure 11. MTS assay showing the effect of gefitinib on the growth of A431wt and A431-A6 cells. A431wt and A431-A6 cells were seeded at a density of 4000 cells per well and incubated with 10µM and 50µM gefitinib for three days. Quadruple repeats were made for each treatment. Then, MTS reagent was added and the plates were incubated for 30-60 minutes. The absorbance was detected at 490 nm, and the percentage of growth inhibition was calculated and plotted against gefitinib concentrations. Data represents the mean ± SEM of three independent experiments.

3.5 AG1478 potently inhibits A431 cell growth

To further validate our findings from MTS and clonogenic assays in which we used erlotinib or gefitinib (Figure 6 and 11), we next analyzed the inhibitory effect of another potent small molecule TKI inhibitor of EGFR, AG1478, on the oncogenic growth of A431 cells by employing the MTS assay. A431wt and A431-A6 cells were plated in 96 well plates at a density of 8000 cells per well, and incubated with 12.5µM and 15µM AG1478 for three days. Quadruple repeats were made for each treatment. Then, MTS reagent was added and the plates were incubated for 30 minutes. The absorbance was detected at 490 nm, and the percentage of growth inhibition was calculated and plotted against AG1478 concentrations. The results showed that the percentage of growth inhibition was 62.2% in A431wt cells compared to 84.2% in A431-A6 cells with 12.5µM AG1478 treatment. When the drug dose was increased to 15µM, the percentage of growth inhibition became 91.3% in A431wt cells

and 101.1% in A431-A6 cells (Figure 12). Compared to the results obtained with gefitinib (Figure 11), AG1478 required much lower dose to cause 100% growth inhibition in A431-A6 cells, indicating a higher potency of AG1478 over gefitinib. In addition, the experiment further supports a model of A431-A6 cells being more sensitive to EGFR TKIs treatment than A431wt cells.

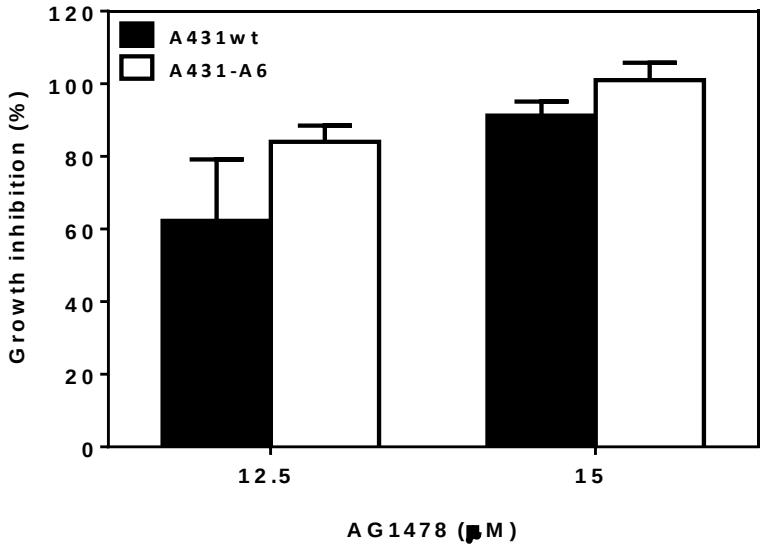

Figure 12. MTS assay showing the effect of AG1478 on A431wt and A431-A6 cell growth. A431wt and A431-A6 cells were seeded at a density of 8000 cells per well, and incubated with 12.5µM and 15µM AG1478 for three days. Quadruple repeats were made for each treatment. Then, MTS reagent was added and the plates were incubated for 30 minutes. The absorbance was detected at 490 nm, and the percentage of growth inhibition was calculated and plotted against AG1478 concentrations. The error bars represent the SD (n = 1).

3.6 Cetuximab reduces colony formation in A431-A6 cells

As discussed previously, EGFR inhibitors include TKIs and mAbs, which interfere with EGFR signaling via two different mechanisms. TKIs are small molecules that compete with ATP for the intracellular TK domain of the receptor; while mAbs such as cetuximab bind to the extracellular ligand binding domain followed by internalization of the EGFR-mAb complex (124, 125). Given that AnxA6 reduces the growth of EGFR overexpressing cells, we next wanted to explore if this could lead to increased potency of mAbs targeting EGFR. Therefore, the inhibitory effect of cetuximab on the oncogenic growth of A431 cells was studied by employing the clonogenic assay. A431wt and A431-A6 cells were incubated with

different cetuximab concentrations (50µg/ml and 100µg/ml) for four days to allow colony formation. Then, cells were washed twice with DPBS, fixed and stained. In these set of experiments, to avoid overlooking the growth-inhibitory effects of AnxA6 occurring at later stages of cell growth and/or proliferation, colonies of thirty, forty and fifty cells or more were counted and plotted against cetuximab concentrations (Figure 13). Taking into consideration colonies of fifty cells or more, A431-A6 control showed 36.8% less colony formation than A431wt control. Upon 50µg/ml cetuximab treatment, colony formation was inhibited by 7.9% (70 ± 4.1) in A431wt cells compared to 59.2% (31 ± 2.1) in A431-A6 cells, and with 100µg/ml cetuximab the inhibition was -11.8% (85 ± 4.9) in A431wt cells compared to 56.6% (33 ± 4.8) in A431-A6 cells. Similar trends were observed when we quantified the counts from colonies with 30, 40 cells or more (Figure 13). Surprisingly, the inhibition of colony formation was most prominent with 50µg/ml cetuximab treatment which may indicate the saturation of the receptor with the mAbs under these conditions (Figure 13C). These findings need to be validated and will require more investigation in the future. However, the preliminary results shown here suggest that A431-A6 cells are more sensitive than A431wt cells to cetuximab, further implicating AnxA6 as a marker in predicting improved outcomes for anti-EGFR cancer therapies.

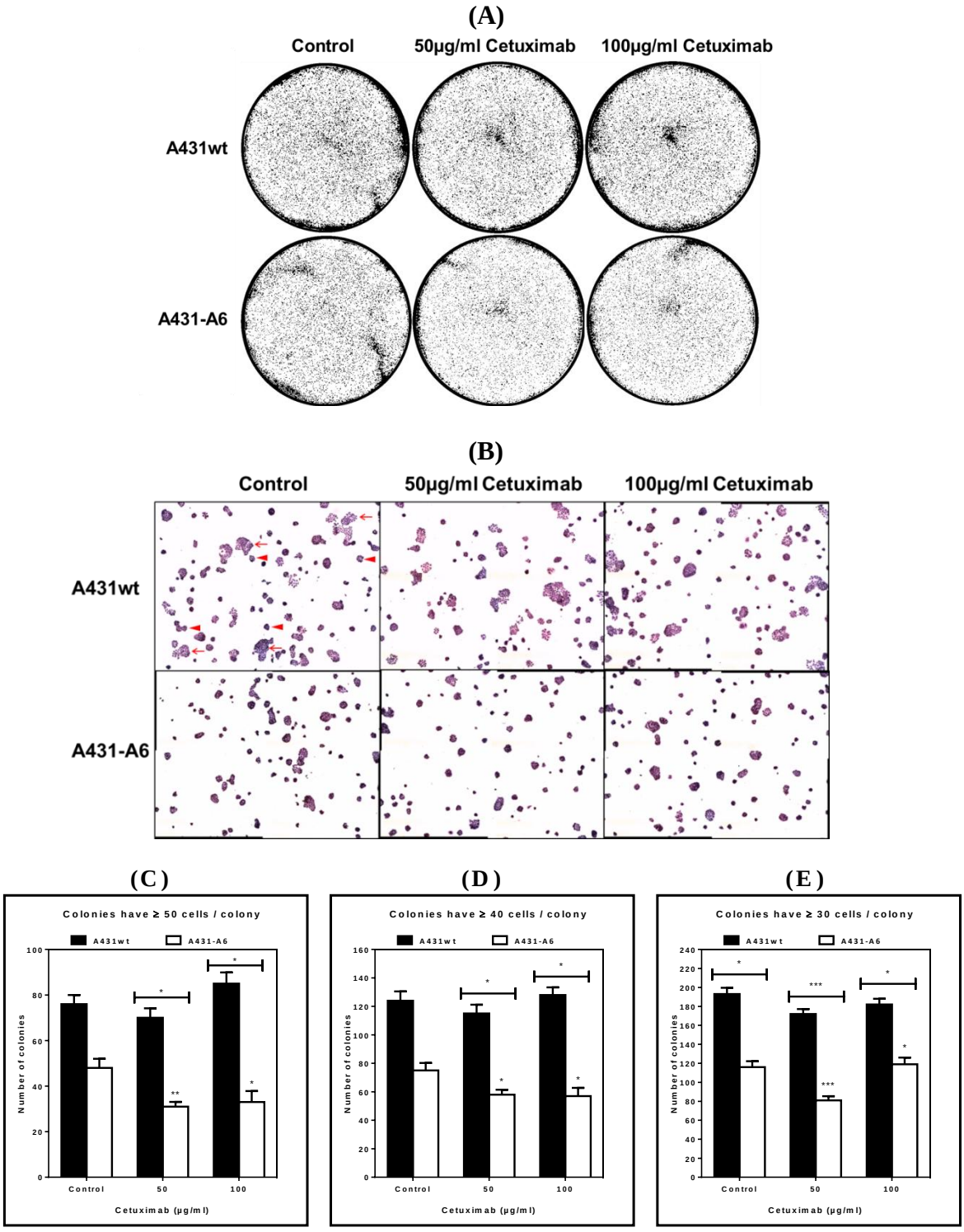

Figure 13. Clonogenic assay of A431wt and A431-A6 cells treated with 0-100µg/ml cetuximab. (A) A431wt and A431-A6 cells were plated in six-well culture plates at a density of 7000 cells per well and treated with 50µg/ml and 100µg/ml cetuximab for four days as indicated. Then cells were fixed and stained. One photo/well was taken to document the density of colony formation in the wells. (B) 10 images/well were randomly taken using the P.A.L.M. DuoFlex Combi System (Carl Zeiss). The arrows indicate colonies composed of 50 cells or more, while arrowheads point at colonies of less than 50 cells. (C-E) Colonies of 50, 40, and 30 cells or more were counted in 10 images/condition and plotted against cetuximab concentrations. The error bars represent the SD. Statistical analysis was performed using student's unpaired t-test and based on the analysis of 10 images/well that were randomly taken of the same experiment. * represent a significant decrease of colony formation compared to A431wt control; * $P < 0.05$, ** $P < 0.01$, *** $P < 0.001$. (n = 1).

3.7 Cell growth inhibition of AnxA6 expressing cells treated with cetuximab

The results presented in section 3.6 indicated the increased efficacy of cetuximab in A431-A6 cells. To substantiate these findings, MTS assays were performed in which A431wt and A431-A6 cells were seeded at a density of 4000 cells per well, and incubated with different cetuximab concentrations (2.5µM, 10µM, and 20µM) for three days. Quadruple repeats were made for each treatment. Then, MTS reagent was added and the plates were incubated for 30 minutes. The absorbance was detected at 490 nm, and the percentage of growth inhibition was calculated and plotted against cetuximab concentrations. The results showed 0.4% growth inhibition in A431wt cells compared to 4.6% in A431-A6 cells with 2.5µM cetuximab. 10µM of the drug caused 2.5% and 5.5% growth inhibition in A431wt and A431-A6 cells, respectively. Finally, 20µM cetuximab led to 10.8% and 18% growth inhibition in A431wt and A431-A6 cells, respectively (Figure 14). These results, in support of the data obtained from clonogenic assays (Figure 13), show a trend that A431-A6 cells are more sensitive to cetuximab than A431wt cells.

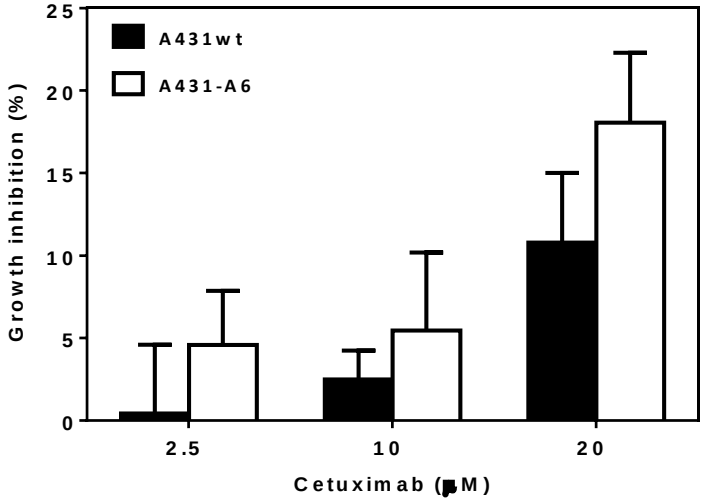

Figure 14. MTS assay showing the effect of cetuximab on A431wt and A431-A6 cell growth. A431wt and A431-A6 cells were seeded at a density of 4000 cells per well and incubated with 2.5µM, 10µM, and 20µM cetuximab for three days. Quadruple repeats were made for each treatment. Then, MTS reagent was added and the plates were incubated for 30 minutes. The absorbance was detected at 490 nm, and the percentage of growth inhibition was calculated and plotted against cetuximab concentrations. The error bars represent the SD (n = 1).

3.8 PD98059 increases growth inhibition of A431-A6 cells

Aberrant EGFR signaling leads to enhanced oncogenic activity of the Ras/MAPK pathway. Small molecules inhibiting MEK1/2 are potent anti-cancer drugs blocking the subsequent ERK activation and inhibiting the growth-promoting signaling cascade (120). AnxA6 was found to inhibit not only EGFR, but also Ras activation (22). We wanted to explore if this potential tumor suppressor activity of AnxA6 could increase the potency of MEK1/2 inhibitors. Therefore, the clonogenic assay was employed to study the inhibitory effect of the MEK1/2 inhibitor PD98059 on the oncogenic growth of A431wt and A431-A6 cells. A431wt and A431-A6 cells were incubated with 1µM and 25µM PD98059 for five days to allow colony formation. PD98059 is commonly used at 10-25µM concentrations in cell culture assays to ensure MEK1/2 inactivation (238). Then, the cells were washed twice with DPBS, fixed and stained. To avoid overlooking growth-inhibitory effects of AnxA6 occurring at later stages of colony growth, colonies of twenty, thirty, forty and fifty cells or more were counted and plotted against PD98059 concentrations (Figure 15). Taking into consideration colonies of fifty cells or more, A431-A6 control had 7.1% less colony formation than A431wt control which is a decrease from 42 ± 1.9 to 39 ± 3.5. When cells were treated with 1µM PD98059, colony formation was unexpectedly increased by 21% in A431wt cells (51 ± 2.0), while decreased by 45.2% in A431-A6 cells (23 ± 2.5). 25µM PD98059 treatment inhibited colony formation in A431wt cells by 33.3% (28 ± 1.5), and by 76.2% (10 ± 1.2) in A431-A6 cells (Figure 15C). Similar trends were observed when we quantified the counts from colonies with 20, 30, 40 cells or more (Figure 15). Hence, similar to the data obtained with EGFR inhibitors, blocking oncogenic MAPK signaling was also substantially more effective upon AnxA6 overexpression.

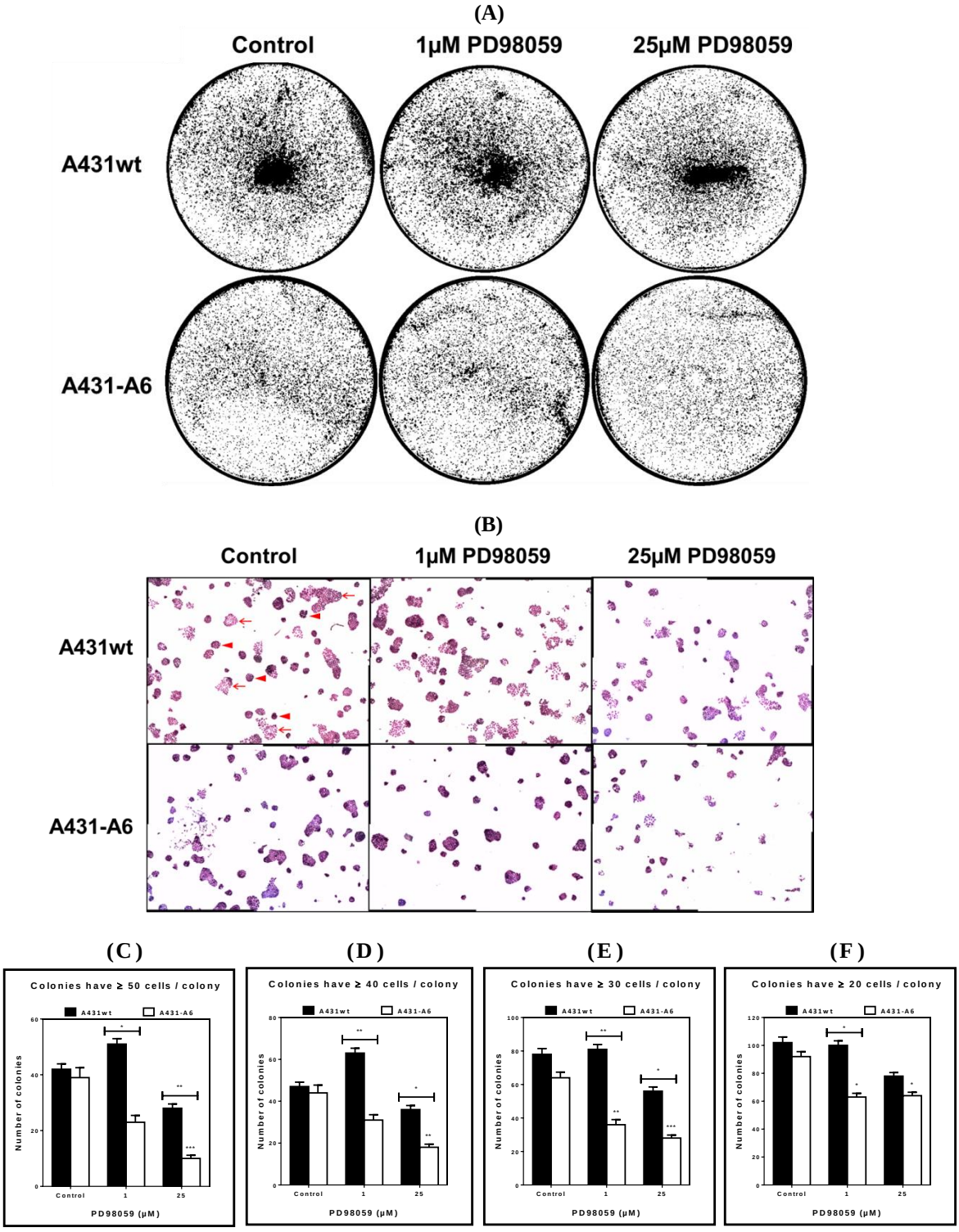

Figure 15. Clonogenic assay of A431wt and A431-A6 cells treated with 0-25µM PD98059. (A) A431wt and A431-A6 cells were plated in six-well culture plates at a density of 7000 cells per well and treated with 1µM and 25µM PD98059 for five days as indicated. Then cells were fixed and stained. One photo/well was taken to document the density of colony formation in the wells. (B) 10 images/well were randomly taken using the P.A.L.M. DuoFlex Combi System (Carl Zeiss). The arrows indicate colonies composed of 50 cells or more, while arrowheads point at colonies of less than 50 cells. (C-F) Colonies of 50, 40, 30, and 20 cells or more were counted in 10 images/condition and plotted against PD98059 concentrations. The error bars represent the SD. Statistical analysis was performed using student's unpaired t-test and based on the analysis of 10 images/well that were randomly taken of the same experiment. * represent a significant decrease of colony formation compared to A431wt control; * $P < 0.05$, ** $P < 0.01$, *** $P < 0.001$.

3.9 Combinatorial treatment with erlotinib and PD98059 potently inhibits oncogenic growth of A431 cells

Elevated expression of AnxA6 was associated with increased sensitivity towards drugs targeting EGFR and MAPK (sections 3.1-3.8). Given that combinatorial treatment is now widely considered as a more effective approach to treat cancers (202-204), we wanted to investigate if AnxA6 could lead to an increased potency upon treating A431 cells with both TKI and MEK1/2 inhibitor simultaneously. Therefore, clonogenic assays were performed to study the inhibitory effect of erlotinib, PD98059, and their combination on the oncogenic growth of A431wt and A431-A6 cells. Both cell lines were incubated with 1µM erlotinib, 25µM PD98059, and a combination of both drugs for five days to allow colony formation. Then, the cells were washed twice with DPBS, fixed and stained. To avoid overlooking growth-inhibitory effects of AnxA6 occurring at later stages of colony growth, colonies of twenty, thirty, forty and fifty cells or more were counted and plotted against the drug treatments (Figure 16 and 17).

The identification of colonies of fifty cells or more revealed that A431-A6 control had 22.9% less colony formation than A431wt control. When 1µM erlotinib was applied, the number of colonies significantly decreased in A431wt and A431-A6 cells (27.5 ± 1.2 and 8.5 ± 3.7) which reflects 65% and 89.1% inhibition, respectively ($P < 0.05$). The use of 25µM PD98059 was able to decrease the number of colonies to 66.5 ± 8.6 and 45 ± 9 in A431wt and A431-A6 cells which is 15.3% and 42.7% inhibition, respectively. These results confirm our previous findings discussed earlier (sections 4.1-4.5, 4.8). In addition, when 1µM erlotinib and 25µM PD98059 were used together as a combinatorial treatment, the number of colonies was significantly decreased to 14 ± 6.5 and 3.5 ± 2 in A431wt and A431-A6 cells, which represents 82.2% ($P < 0.05$) and 95.5% ($P < 0.01$) growth inhibition, respectively (Figure 17 A-C). Similar trends were observed when we quantified the counts from colonies with 20, 30,

40 cells or more (Figure 17). Hence, the combinatorial drug treatment was able to effectively reduce colony formation in A431 cells compared to single drug treatments. Moreover, the results indicated that the combination of both TKI and MEK1/2 inhibitor potently inhibited growth more effectively in the presence of AnxA6.

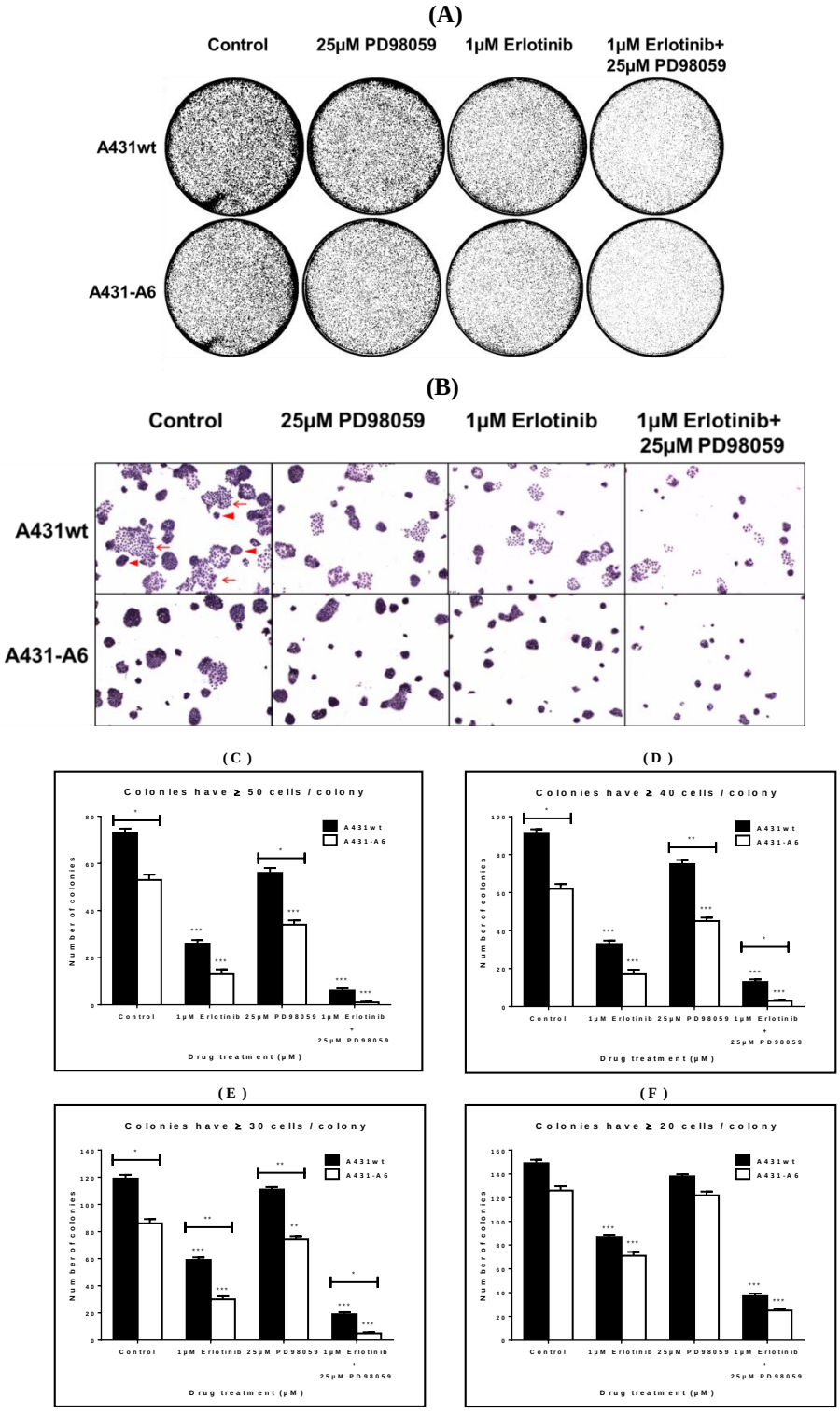

Figure 16. Clonogenic assay of A431 cells treated with 1μM erlotinib and 25μM PD98059 alone or in combination. (A) A431wt and A431-A6 cells were plated in six-well culture plates at a density of 7000 cells per well and incubated with 1μM erlotinib, 25μM PD98059, and a combination of both drugs for five days as indicated. Then cells were fixed and stained. One photo/well was taken to document the density of colony formation in the wells. (B) 10 images/well were randomly taken using the P.A.L.M. DuoFlex Combi System (Carl Zeiss). The arrows indicate colonies composed of 50 cells or more, while arrowheads point at colonies of less than 50 cells. (C-F) Colonies of 50, 40, 30, and 20 cells or more were counted in 10 images/condition and plotted against drug treatments. The error bars represent the SD. Statistical analysis was performed using student's unpaired t-test and based on the analysis of 10 images/well that were randomly taken of the same experiment. * represents a significant decrease of colony formation compared to A431wt control; * $P < 0.05$, ** $P < 0.01$, *** $P < 0.001$.

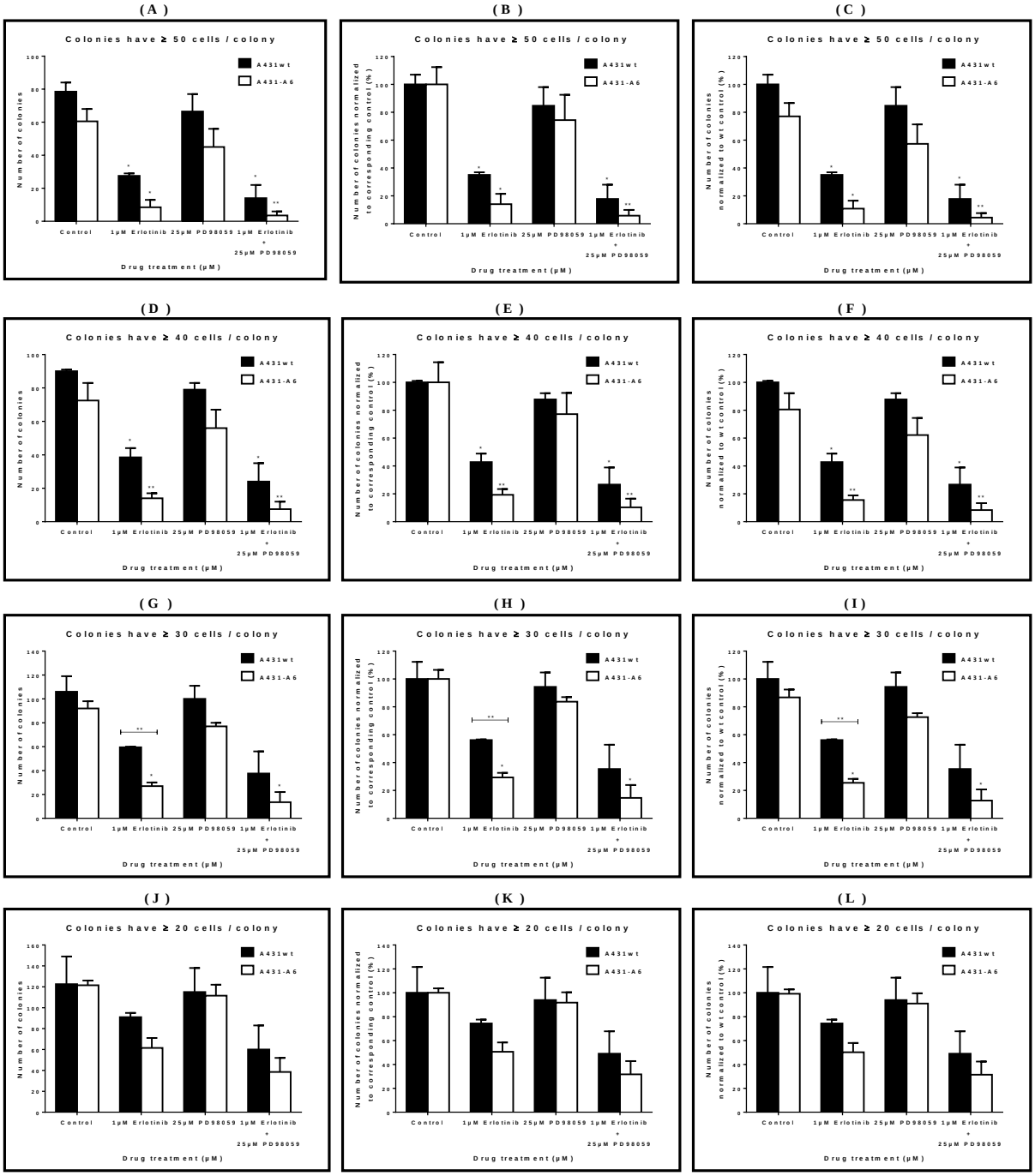

Figure 17. The inhibitory effect of erlotinib, PD98059, and their combination on A431wt and A431-A6 colony growth. A431wt and A431-A6 cells were incubated with 1μM erlotinib, 25μM PD98059, and a combination of both drugs for five days. Colonies of 20, 30, 40, and 50 cells or more were counted. Data represents the mean ± SEM of two independent experiments. (A, D, G, J) The number of colonies of A431wt and A431-A6 were plotted against drug treatments where each colony is 50, 40, 30, 20 cells or more, respectively. (B, E, H, K) The number of colonies of A431wt and A431-A6 were normalized to A431wt control and A431-A6 control, respectively, and plotted against drug treatments where each colony is 50, 40, 30, 20 cells or more, respectively. (C, F, I, L) The number of colonies of A431wt and A431-A6 were normalized to A431wt control and plotted against drug treatments where each colony is 50, 40, 30, 20 cells or more, respectively. Statistical analysis was performed using student's unpaired t-test where * represents a significant decrease of colony formation compared to A431wt control; * $P < 0.05$, ** $P < 0.01$.

3.10 Potent growth inhibition in A431 cells treated with gefitinib together with PD98059

To extend our previous finding (section 3.9) that A431-A6 cells displayed an increased sensitivity towards the combinatorial treatment with TKI and MEK1/2 inhibitors, we next compared colony formation in A431wt and A431-A6 cells treated with gefitinib and PD98059 alone or in combination. A431wt and A431-A6 cells were incubated with 1µM gefitinib, 25µM PD98059, and a combination of both drugs for five days to allow colony formation. Then, the cells were washed twice with DPBS, fixed and stained. To avoid overlooking growth-inhibitory effects of AnxA6 occurring at later stages of colony growth, colonies of twenty, thirty, forty and fifty cells or more were counted and plotted against drug treatments (Figure 18 and 19).

Taking into consideration colonies of fifty cells or more, A431-A6 control had 22.9% less colonies than A431wt control. When 1µM gefitinib was applied, the number of colonies significantly decreased in A431wt and A431-A6 cells (36 ± 4.9 and 10.5 ± 5.3), which reflects an inhibition of 54.1% and 86.6%, respectively ($P < 0.05$). The use of 25µM PD98059 decreased the number of colonies in A431wt and A431-A6 cells (66.5 ± 8.6 and 45 ± 9) by 15.3% and 42.7%, respectively. In line with data shown in section 3.9, when 1µM gefitinib and 25µM PD98059 were used together, the number of colonies decreased in A431wt cells by 72.6%, and significantly decreased in A431-A6 by 97.5% ($P < 0.01$) (Figure 19A-C). Similar trends were observed when we quantified the counts from colonies with 20, 30, 40 cells or more (Figure 19). Hence, the combinatorial treatment with TKI and MEK1/2 inhibitors was more effective in A431-A6 cells compared to A431wt cells.

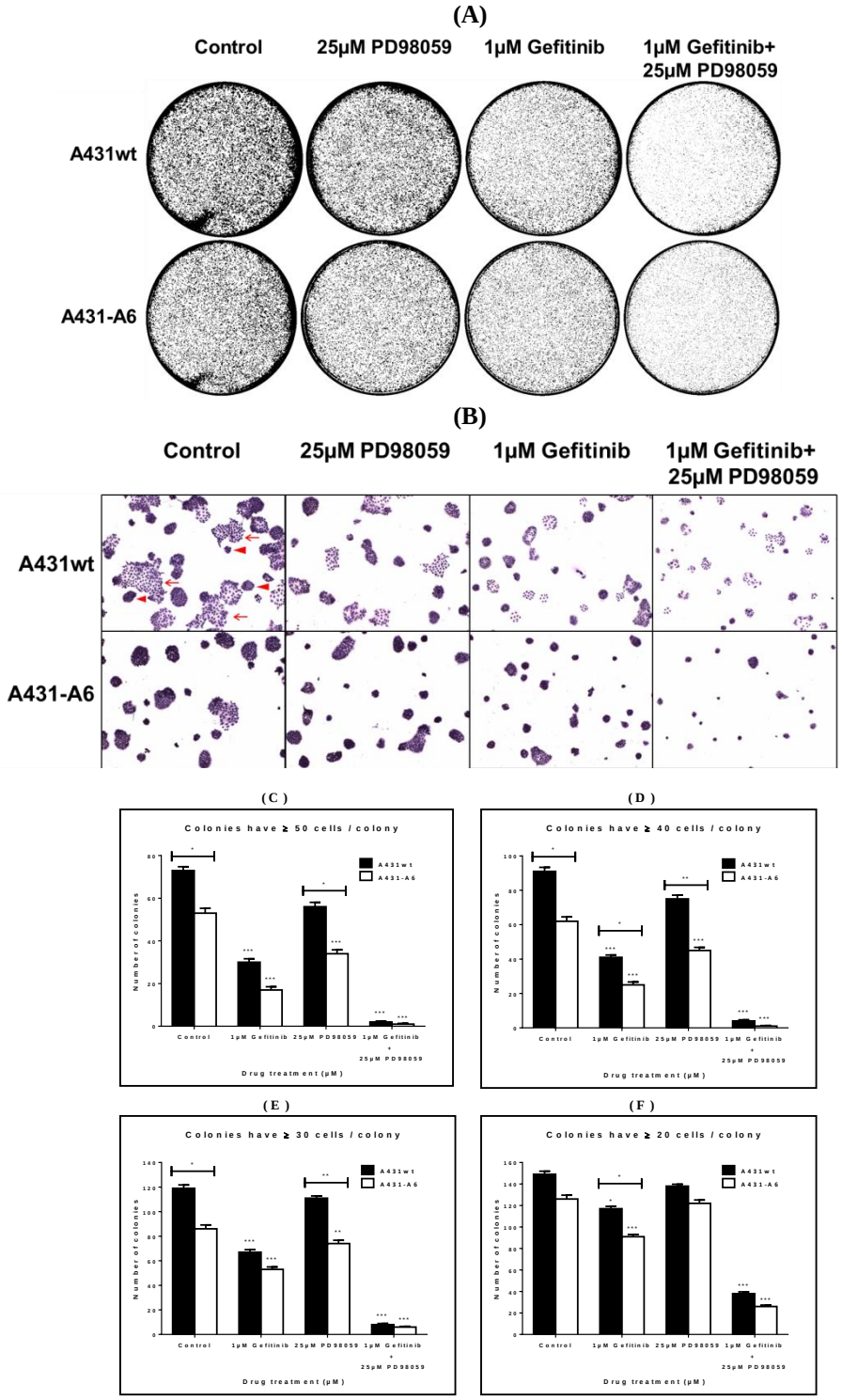

Figure 18. Clonogenic assay of A431 cells treated with 1µM gefitinib and 25µM PD98059 alone or in combination. (A) A431wt and A431-A6 cells were plated in six-well culture plates at a density of 7000 cells per well and incubated with 1µM erlotinib, 25µM PD98059, and a combination of both drugs for five days as indicated. Then cells were fixed and stained. One photo/well was taken to document the density of colony formation in the wells. (B) 10 images/well were randomly taken using the P.A.L.M. DuoFlex Combi System (Carl Zeiss). The arrows indicate colonies composed of 50 cells or more, while arrowheads point at colonies of less than 50 cells. (C-F) Colonies of 50, 40, 30, and 20 cells or more were counted in 10 images/condition and plotted against drug treatments. The error bars represent the SD. Statistical analysis was performed using student's unpaired t-test and based on the analysis of 10 images/well that were randomly taken of the same experiment. * represents a significant decrease of colony formation compared to A431wt control; * $P < 0.05$, ** $P < 0.01$, *** $P < 0.001$.

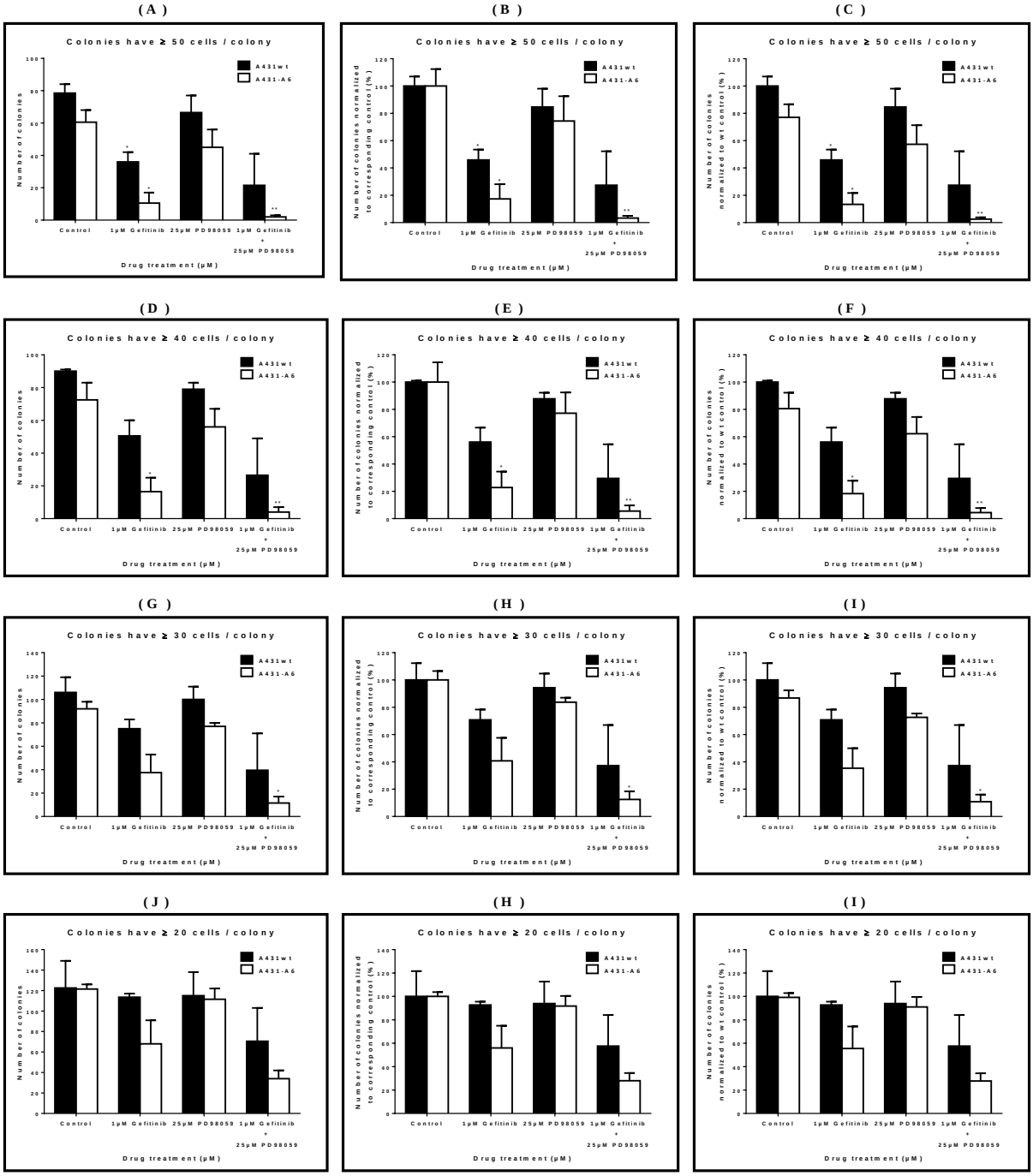

Figure 19. The inhibitory effect of gefitinib, PD98059, and their combination on A431wt and A431-A6 colony growth. A431wt and A431-A6 cells were incubated with 1μM gefitinib, 25μM PD98059, and a combination of both drugs for five days. Colonies of 20, 30, 40, and 50 cells or more were counted. Data represents the mean ± SEM of two independent experiments. (A, D, G, J) The number of colonies of A431wt and A431-A6 were plotted against drug treatments where each colony is 50, 40, 30, 20 cells or more, respectively. (B, E, H, K) The number of colonies of A431wt and A431-A6 were normalized to A431wt control and A431-A6 control, respectively, and plotted against drug treatments where each colony is 50, 40, 30, 20 cells or more, respectively. (C, F, I, L) The number of colonies of A431wt and A431-A6 were normalized to A431wt control and plotted against drug treatments where each colony is 50, 40, 30, 20 cells or more, respectively. Statistical analysis was performed using student's unpaired t-test where * represents a significant decrease of colony formation compared to A431wt control; * $P < 0.05$, ** $P < 0.01$.

3.11 The anti-cancer effects in AnxA6 expressing cells treated with the combination of erlotinib and cetuximab

As discussed in section 1.6.2, cetuximab and erlotinib are two EGFR inhibitors that perform their actions via two different mechanisms. We studied the effect of each drug alone on the oncogenic proliferation of A431 cells and found more effective inhibition upon AnxA6 overexpression (sections 3, 3.2, 3.6, 3.7). Some strategies suggested that combining small molecules such as TKIs with mAbs targeting EGFR could be more effective (237). Hence, we wanted to test the effect of combining the two drugs together and identify if an increased growth inhibition could be observed upon AnxA6 overexpression in A431 cells. Clonogenic assays were performed in which A431wt and A431-A6 cells were incubated with 1µM erlotinib, 50µg/ml cetuximab, and a combination of both drugs for five days. Then, the cells were washed twice with DPBS, fixed and stained. To avoid overlooking growth-inhibitory effects of AnxA6 occurring at later stages of colony growth, colonies of twenty, thirty, forty and fifty cells or more were counted and plotted against drug treatments (Figure 20).

When colonies of fifty cells or more were counted, A431-A6 control had 54.3% less colony formation than A431wt control. When 1µM erlotinib was applied, the number of colonies decreased in A431wt and A431-A6 cells to 9 ± 0.7 and 7 ± 0.7, which reflects 74.3% and 80% inhibition, respectively. When 50µg/ml cetuximab was applied alone as a single drug, the number of colonies became 36 ± 2 and 28 ± 1.8 in A431wt and A431-A6 cells, respectively, which represents an increase of colony formation by 2.9% in A431wt cells and a decrease of colony formation by 20% in A431-A6 cells.

However, treating the cells with the combination of 1µM erlotinib and 50µg/ml cetuximab led to a decrease of the number of colonies to 19 ± 1.4 and 13 ± 1.3 in A431wt and A431-A6 cells, that is 45.7% and 62.9% growth inhibition, respectively (Figure 20C). Similar trends were observed when we quantified the counts from colonies with 20, 30, 40 cells or more

(Figure 20). The results showed that the inhibition of colony formation was always more pronounced in A431-A6 cells as compared to A431wt cells in all settings. Although published data reports cetuximab to inhibit A431wt cell growth (233, 234), cetuximab did not strongly affect A431wt colony formation in our experiment (Figure 20). Moreover, the presence of cetuximab reduced the efficacy of erlotinib in both A431wt and A431-A6 cells. This observation could be due to competition of anti-EGFR agents, or possibly reflects the possibility that our batch of A431 cells had developed resistance to cetuximab, a phenomena also observed by others (239, 240).

3.12 The combination of gefitinib and cetuximab potentiates the inhibition of colony formation in A431 cells

The results obtained using a combination of erlotinib and cetuximab in section 3.11 directed us to try using another TKI, together with the monoclonal antibody cetuximab, in order to compare the cellular oncogenic growth in cells with and without AnxA6 overexpression. Clonogenic assays were adopted using A431wt and A431-A6 cells that were incubated with 1µM gefitinib, 50µg/ml cetuximab, and a combination of both drugs for five days. Then, the cells were washed twice with DPBS, fixed and stained. To avoid overlooking growth-inhibitory effects of AnxA6 occurring at later stages of colony growth, colonies of twenty, thirty, forty and fifty cells or more were counted and plotted against drug treatments (Figure 21).

When colonies of fifty cells or more were identified, the results showed 54.3% less colony formation in A431-A6 cells compared to A431wt cells. 1µM gefitinib reduced the number of colonies in A431wt and A431-A6 cells by 82.9% and 88.6%, respectively. The number of colonies became 36 ± 2 and 28 ± 1.8 in A431wt and A431-A6 cells, respectively, when 50µg/ml cetuximab was used alone as a single drug which represents an increase of colony

formation by 2.9% in A431wt cells and a decrease of colony formation in A431-A6 cells by 20%. Nevertheless, when 1µM gefitinib and 50µg/ml cetuximab were combined together, the number of colonies became 10 ± 1.1 and 6 ± 0.7 in A431wt and A431-A6 cells which represents 71.4% and 82.9% growth inhibition, respectively (Figure 21C). Similar trends were observed when we quantified the counts from colonies with 20, 30, 40 cells or more (Figure 21). These results showed that effective growth inhibition was noted with the combinatorial treatment of cetuximab and gefitinib compared to cetuximab alone. However, these numbers were similar to those obtained from the incubation of gefitinib alone; supporting our previous findings (Figure 20) that cetuximab did not potentiate the growth inhibitory action of TKIs under our experimental conditions.

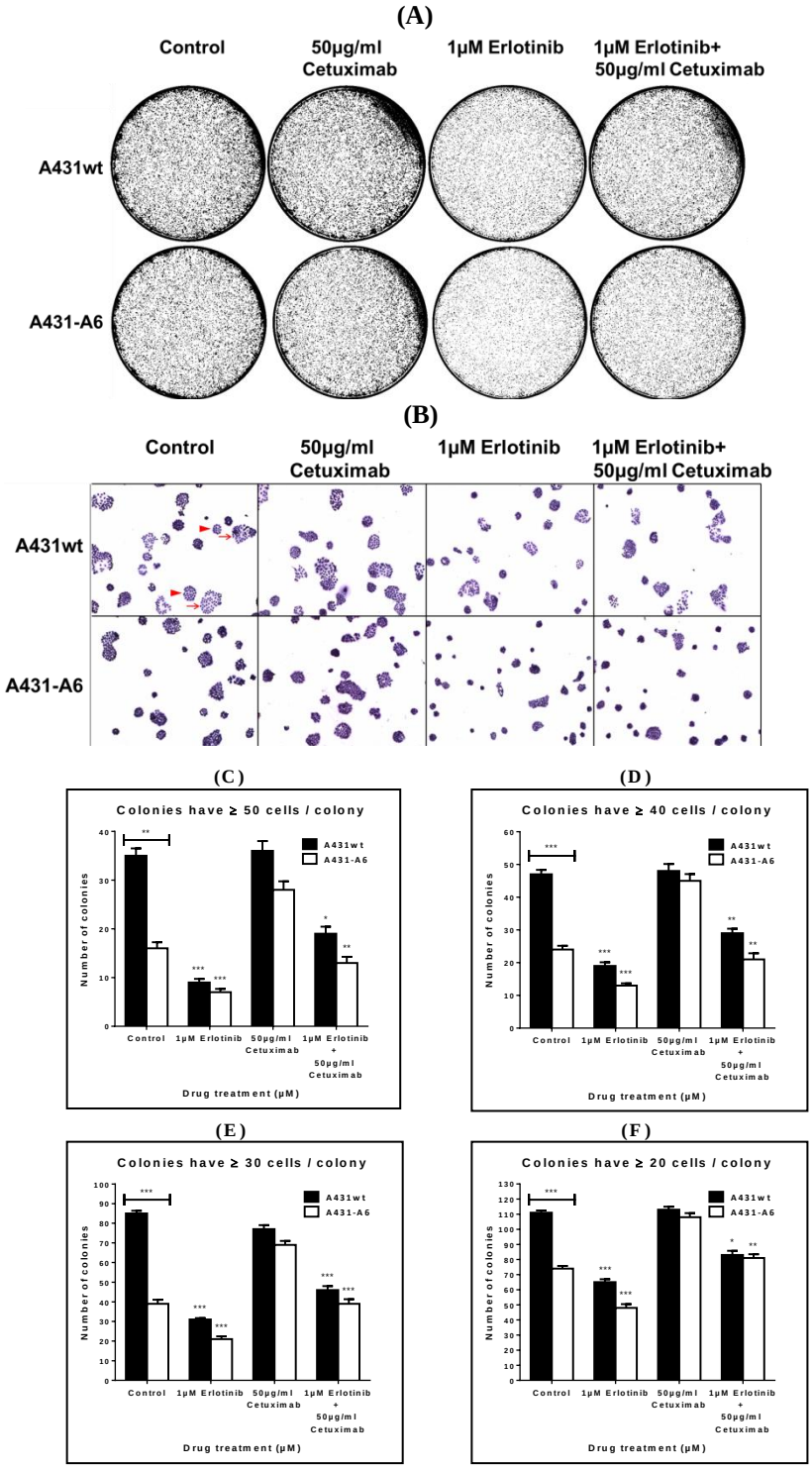

Figure 20. Clonogenic assay of A431 cells treated with 1µM erlotinib and 50µg/ml cetuximab alone or in combination. (A) A431wt and A431-A6 cells were plated in six-well culture plates at a density of 7000 cells per well and incubated with 1µM erlotinib, 50µg/ml cetuximab, and a combination of both drugs for five days as indicated. Then cells were fixed and stained. One photo/well was taken to document the density of colony formation in the wells. (B) 10 images/well were randomly taken using the P.A.L.M. DuoFlex Combi System (Carl Zeiss). The arrows indicate colonies composed of 50 cells or more, while arrowheads point at colonies of less than 50 cells. (C-F) Colonies of 50, 40, 30, and 20 cells or more were counted in 10 images/condition and plotted against drug treatments. The error bars represent the SD. Statistical analysis was performed using student's unpaired t-test and based on the analysis of 10 images/well that were randomly taken of the same experiment. * represents a significant decrease of colony formation compared to A431wt control; * $P < 0.05$, ** $P < 0.01$, *** $P < 0.001$.

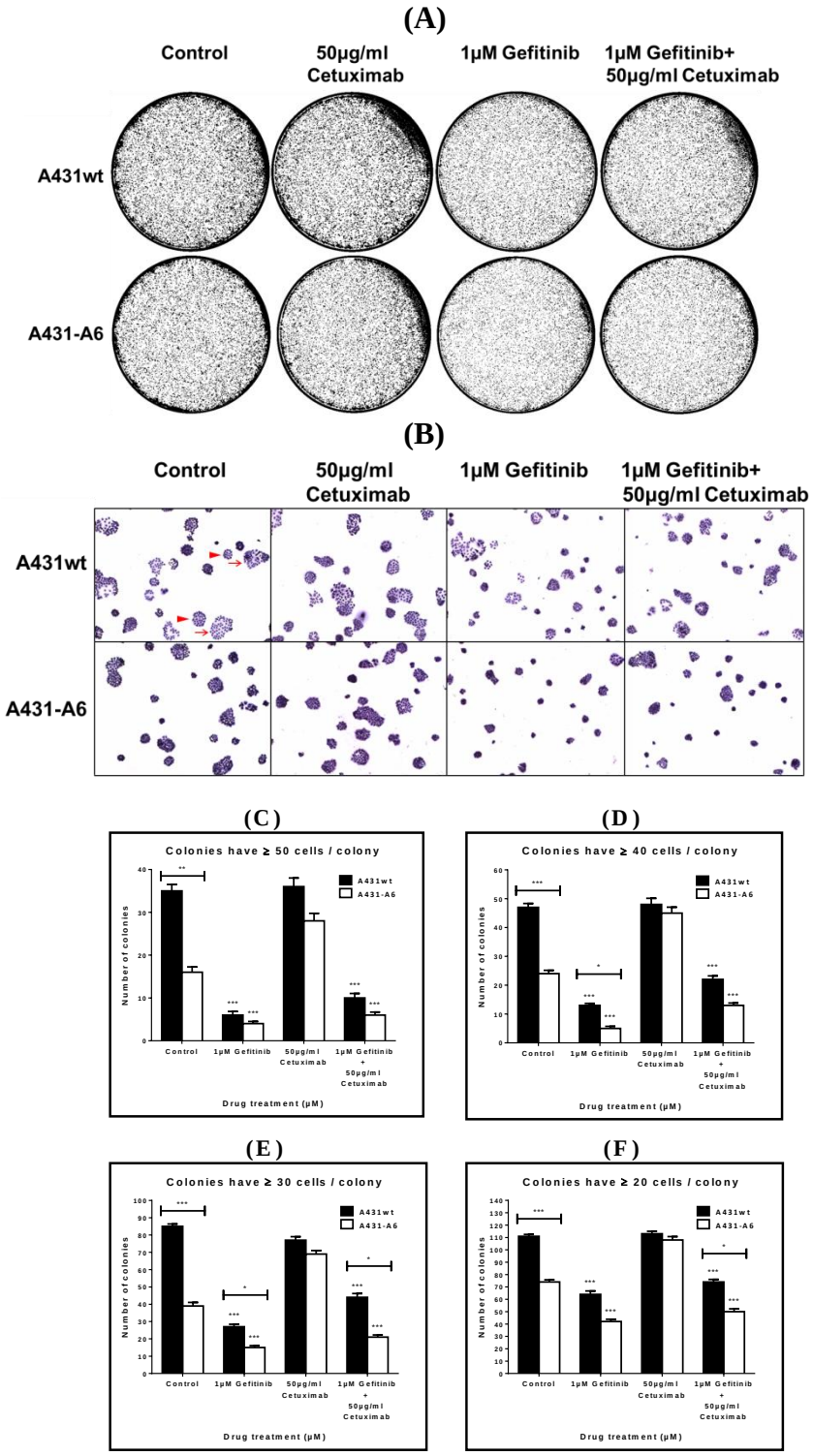

Figure 21. Clonogenic assay of A431 cells treated with 1µM gefitinib and 50µg/ml cetuximab alone or in combination. (A) A431wt and A431-A6 cells were plated in six-well culture plates at a density of 7000 cells per well and incubated with 1µM gefitinib, 50µg/ml cetuximab, and a combination of both drugs for five days as indicated. Then cells were fixed and stained. One photo/well was taken to document the density of colony formation in the wells. (B) 10 images/well were randomly taken using the P.A.L.M. DuoFlex Combi System (Carl Zeiss). The arrows indicate colonies composed of 50 cells or more, while arrowheads point at colonies of less than 50 cells. (C-F) Colonies of 50, 40, 30, and 20 cells or more were counted in 10 images/condition and plotted against drug treatments. The error bars represent the SD. Statistical analysis was performed using student's unpaired t-test and based on the analysis of 10 images/well that were randomly taken of the same experiment. * represents a significant decrease of colony formation compared to A431wt control; * $P < 0.05$, ** $P < 0.01$, *** $P < 0.001$, (n = 1).

3.13 Potent inhibition of colony formation in AnxA6 expressing cells treated with the combination of erlotinib and Gö 6976

The benefits of combinatorial therapies in treating complex diseases like cancer are now evident (202-204). We tested the targeted approach of combining TKIs with not only MEK1/2 inhibitor, but also mAb in cells overexpressing AnxA6 (sections 3.9- 3.12). Grewal and coworkers showed that AnxA6 inhibited EGFR signaling via PKCα-dependent pathways (29). Therefore, we next aimed at identifying the effect of combining a TKI with a PKCα inhibitor on the oncogenic cell proliferation of A431 cells. Clonogenic assays were adapted in this regards and Gö 6976, a selective inhibitor of PKCα, was used. In these assays, A431wt and A431-A6 cells were incubated with 1µM erlotinib, 1µM Gö 6976, and a combination of both drugs for five days to allow colony formation. Then, the cells were washed twice with DPBS, fixed and stained. To avoid overlooking growth-inhibitory effects of AnxA6 occurring at later stages of colony growth, colonies of twenty, thirty, forty and fifty cells or more were counted and plotted against drug treatments (Figure 22 and 23).

Taking into account colonies of fifty cells or more, A431-A6 control had 45.3% less colony formation than A431wt control. When a single drug treatment was applied to the A431wt cells, the number of colonies significantly decreased with 1µM erlotinib to 12 ± 0.6, and with 1µM Gö 6976 to 26.7 ± 10, which represents 71.9% and 37.5% growth inhibition, respectively. In A431-A6 cells, the number of colonies were reduced to 3 ± 1 with 1µM erlotinib and to 12 ± 2.6 with 1µM Gö 6976, which reflects 93% and 71.9% growth inhibition, respectively ($P<0.05$).

Furthermore, the combinatorial treatment of 1µM erlotinib and 1µM Gö 6976 significantly reduced the number of colonies to 5.3 ± 2 and 0.7 ± 0.3 in A431wt and A431-A6 cells which represents 87.5% and 98.4% growth inhibition, respectively ($P<0.05$) (Figure 23A-C). Similar trends were observed when we quantified the counts from colonies with 20, 30, 40

cells or more (Figure 23). The experiment was repeated three times and displayed a weak inhibition of growth when Gö 6976 was used alone as a single agent. This may reflect the controversial results obtained in other studies regarding the use of PKC inhibitors in cancer (41). Although PKCα knockdown restored EGFR activity in A431-A6 cells in another study (29), we observed that the combinatorial targeted therapy of erlotinib and Gö 6976 together displayed a potent inhibition of cell growth especially in A431-A6 cells. We speculate that Gö 6976 might act through an inhibition of other key regulators in cell proliferation, which will be discussed further below (chapter 4).

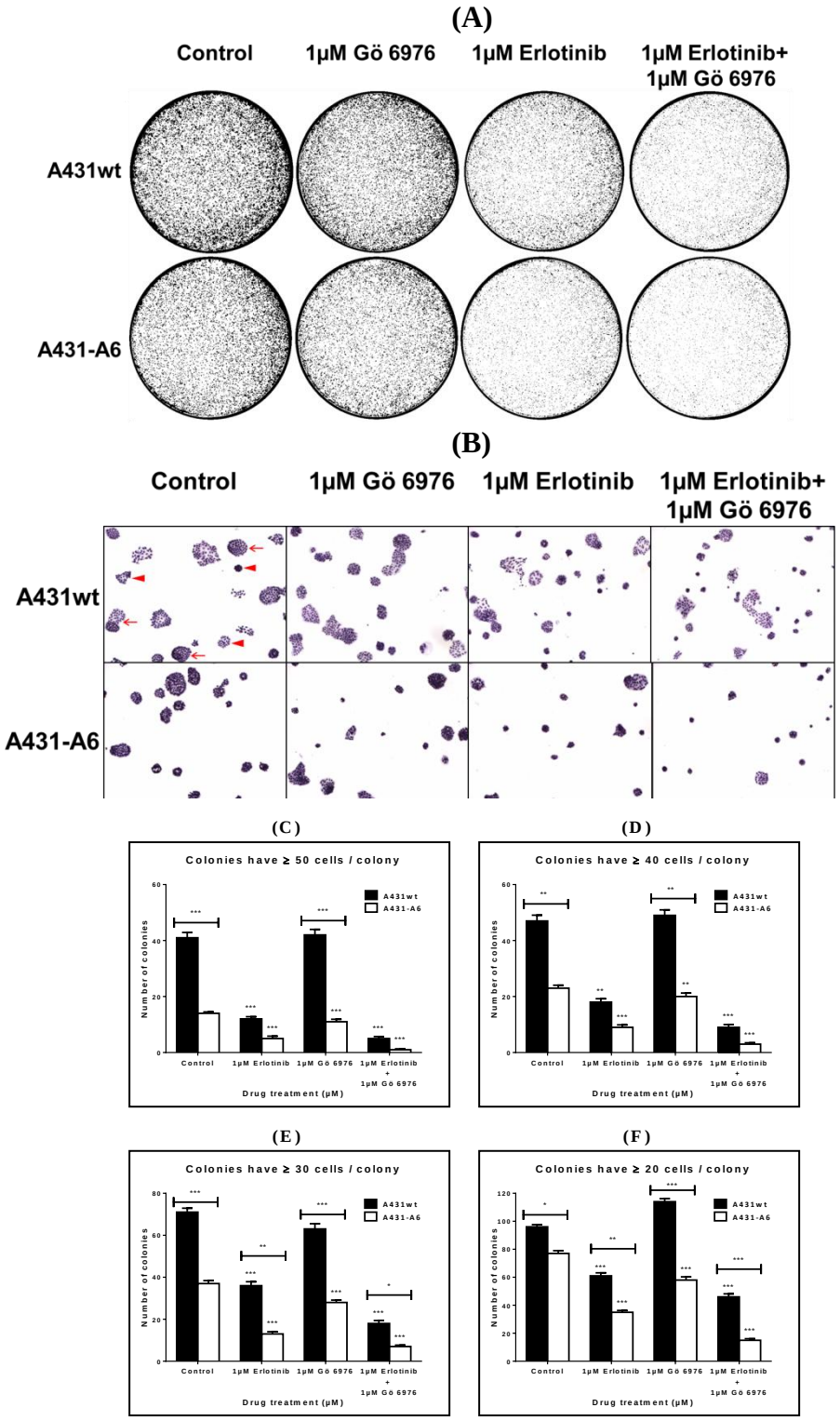

Figure 22. Clonogenic assay of A431 cells treated with 1μM erlotinib and 1μM Gö 6976 alone or in combination. (A) A431wt and A431-A6 cells were plated in six-well culture plates at a density of 7000 cells per well and incubated with 1μM erlotinib, 1μM Gö 6976, and their combination for five days as indicated. Then cells were fixed and stained. One photo/well was taken to document the density of colony formation in the wells. (B) 10 images/well were randomly taken using the P.A.L.M. DuoFlex Combi System (Carl Zeiss). The arrows indicate colonies composed of 50 cells or more, while arrowheads point at colonies of less than 50 cells. (C-F) Colonies of 50, 40, 30, and 20 cells or more were counted in 10 images/condition and plotted against drug treatments. The error bars represent the SD. Statistical analysis was performed using student's unpaired t-test and based on the analysis of 10 images/well that were randomly taken of the same experiment. * represents a significant decrease of colony formation compared to A431wt control; * $P < 0.05$, ** $P < 0.01$, *** $P < 0.001$.

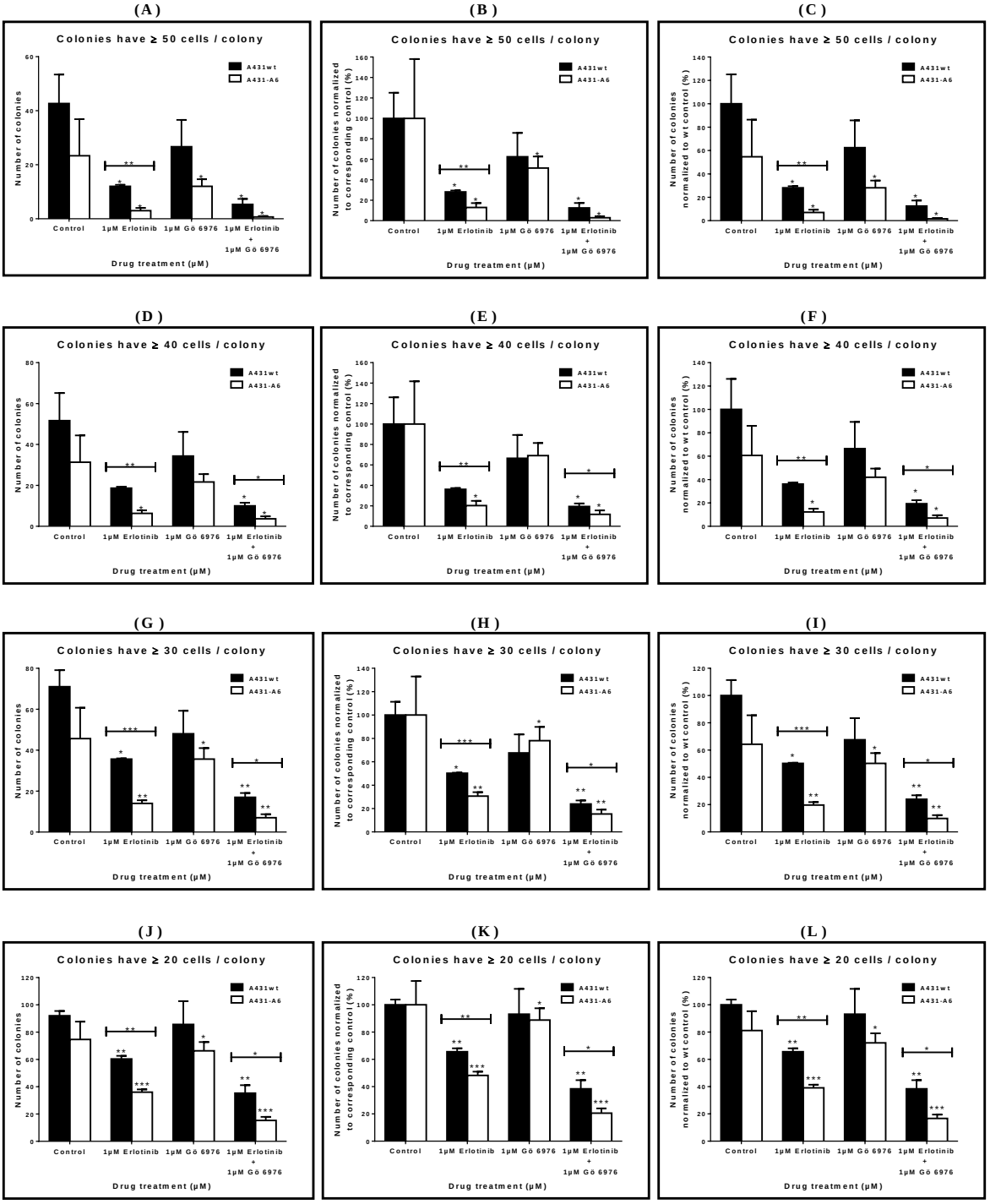

Figure 23. The inhibitory effect of erlotinib, Gö 6976, and their combination on A431wt and A431-A6 colony formation. A431wt and A431-A6 cells were incubated with 1μM erlotinib, 1μM Gö 6976, and a combination of both drugs for five days. Colonies of 20, 30, 40, and 50 cells or more were counted. Data represents the mean ± SEM of three independent experiments. (A, D, G, J) The number of colonies of A431wt and A431-A6 were plotted against drug treatments where each colony is 50, 40, 30, 20 cells or more, respectively. (B, E, H, K) The number of colonies of A431wt and A431-A6 were normalized to A431wt control and A431-A6 control, respectively, and plotted against drug treatments where each colony is 50, 40, 30, 20 cells or more, respectively. (C, F, I, L) The number of colonies of A431wt and A431-A6 were normalized to A431wt control and plotted against drug treatments where each colony is 50, 40, 30, 20 cells or more, respectively. Statistical analysis was performed using student's unpaired t-test where * represents a significant decrease of colony formation compared to A431wt control; * $P < 0.05$, ** $P < 0.01$, *** $P < 0.001$.

3.14 Enhanced anti-cancer properties of the combinatorial use of gefitinib and Gö 6976 in A431-A6 cells

As we found that AnxA6 increases the sensitivity of A431 cells towards the combinatorial treatment of erlotinib and Gö 6976 (section 3.13), we followed this finding by another experiment in which we examined a combination of gefitinib and Gö 6976 in clonogenic assays. Therefore, A431wt and A431-A6 cells were incubated with 1µM gefitinib, 1µM Gö 6976, and a combination of both drugs for five days to allow colony formation. Then, the cells were washed twice with DPBS, fixed and stained. To avoid overlooking growth-inhibitory effects of AnxA6 occurring at later stages of colony growth, colonies of twenty, thirty, forty and fifty cells or more were counted and plotted against drug treatments (Figure 24 and 25).

Counting colonies of fifty cells or more showed that A431-A6 control had 45.3% less colony formation than A431wt control. When a single drug treatment of 1µM gefitinib and 1µM Gö 6976 was applied to the A431wt cells, the number of colonies decreased to 16 ± 2.3, and 26.7 ± 10 that is 61% and 37.5% growth inhibition, respectively. In A431-A6 cells, 95.3% (2 ± 0.6) and 71.9% (12 ± 2.6) growth inhibition ($P<0.05$) was identified when the cells were treated with 1µM gefitinib and 1µM Gö 6976, respectively. Finally, using the combinatorial treatment of 1µM gefitinib and 1µM Gö 6976 lead to 97.7% (1 ± 0.6) growth and colony inhibition in both cell lines ($P<0.05$) (Figure 25A-C). Similar trends were observed when we quantified the counts from colonies with 20, 30, 40 cells or more (Figure 25). The experiment was repeated three times, and the results supported our previous finding that the combination of TKI and PKC inhibitor was more effective in reducing oncogenic cell growth in A431 cells than using the individual drugs. Furthermore, when counting colonies with 20 or 30 cells or more, the combinatorial use of gefitinib and Gö 6976 were more effective in inhibiting colony formation in A431-A6 cells as compared to A431wt cells (Figure 25 G-L).

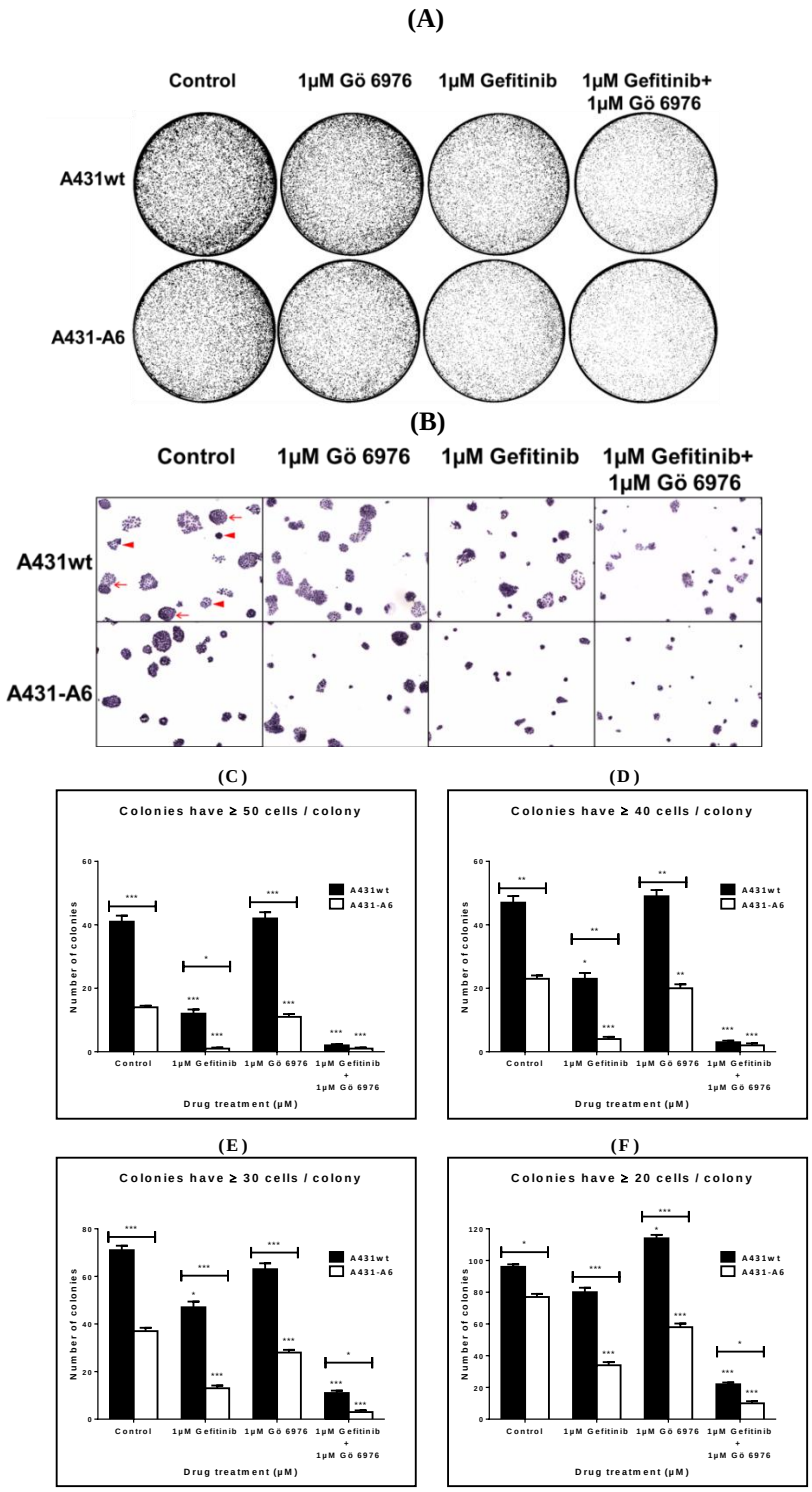

Figure 24. Clonogenic assay of A431 cells treated with 1µM gefitinib and 1µM Gö 6976 alone or in combination. (A) A431wt and A431-A6 cells were plated in six-well culture plates at a density of 7000 cells per well and incubated with 1µM gefitinib, 1µM Gö 6976, and a combination of both drugs for five days as indicated. Then cells were fixed and stained. One photo/well was taken to document the density of colony formation in the wells. (B) 10 images/well were randomly taken using the P.A.L.M. DuoFlex Combi System (Carl Zeiss). The arrows indicate colonies composed of 50 cells or more, while arrowheads point at colonies of less than 50 cells. (C-F) Colonies of 50, 40, 30, and 20 cells or more were counted in 10 images/condition and plotted against drug treatments. The error bars represent the SD. Statistical analysis was performed using student's unpaired t-test and based on the analysis of 10 images/well that were randomly taken of the same experiment. * represents a significant decrease of colony formation compared to A431wt control; * $P < 0.05$, ** $P < 0.01$, *** $P < 0.001$.

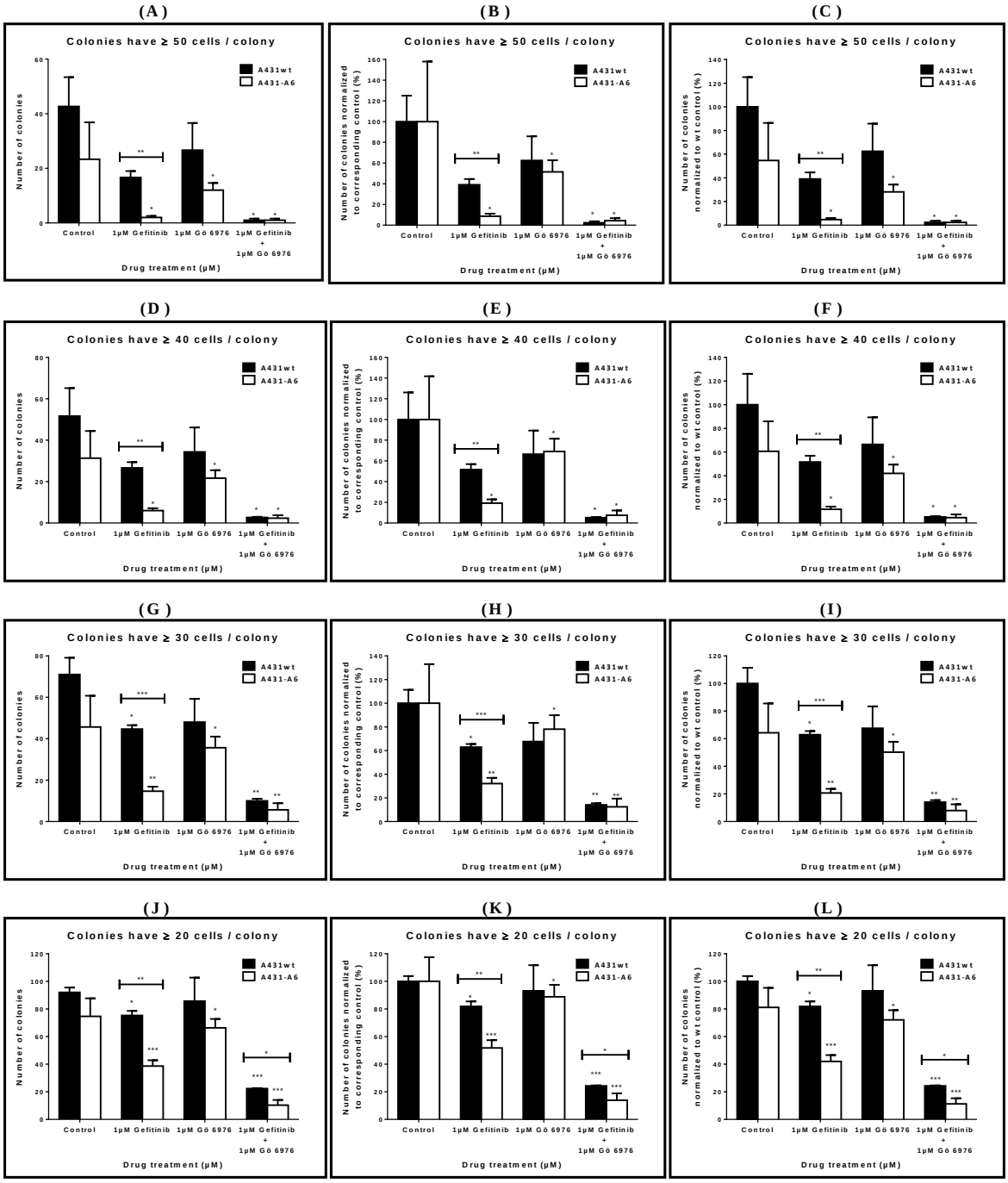

Figure 25. The inhibitory effect of gefitinib, Gö 6976, and their combination on A431wt and A431-A6 cell growth. A431wt and A431-A6 cells were incubated with 1µM gefitinib, 1µM Gö 6976, and a combination of both drugs for five days. Colonies of 20, 30, 40, and 50 cells or more were counted. Data represents the mean ± SEM of three independent experiments. (A, D, G, J) The number of colonies of A431wt and A431-A6 were plotted against drug treatments where each colony is 50, 40, 30, 20 cells or more, respectively. (B, E, H, K) The number of colonies of A431wt and A431-A6 were normalized to A431wt control and A431-A6 control, respectively, and plotted against drug treatments where each colony is 50, 40, 30, 20 cells or more, respectively. (C, F, I, L) The number of colonies of A431wt and A431-A6 were normalized to A431wt control and plotted against drug treatments where each colony is 50, 40, 30, 20 cells or more, respectively. Statistical analysis was performed using student's unpaired t-test where * represents a significant decrease of colony formation compared to A431wt control; * $P < 0.05$, ** $P < 0.01$, *** $P < 0.001$.

3.15 The effect of BIM-I on A431 cell growth in MTS assays.

Besides Gö 6976, BIM-I is a potent inhibitor commonly used to block the conventional PKC enzymes via targeting the ATP-binding site of the kinase catalytic domain. We employed BIM-I in our MTS assay to investigate the effect of AnxA6 upregulation on A431 cell growth. A431wt and A431-A6 cells were seeded at a density of 4000 cells per well, and incubated with different concentrations of the drug (0.1µM, 0.5µM, 1µM) for three days. Quadruple repeats were made for each treatment. Then MTS reagent was added and the plates were incubated for 30 minutes. The absorbance was detected at 490 nm, and the percentage of viability was calculated and plotted against BIM-I concentrations. The results showed a percentage of viability of 101.4%, 105.4%, and 100.2% in A431wt cells treated with 0.1µM, 0.5µM, and 1µM BIM-I, respectively. In A431-A6 cells, the percentage of viability was 98%, 165.6%, and 148.4% with 0.1µM, 0.5µM, and 1µM BIM-I treatments, respectively (Figure 26). Hence, the oncogenic growth in A431-A6 and A431wt cells was not negatively affected by employing an inhibitor of conventional PKC enzymes.

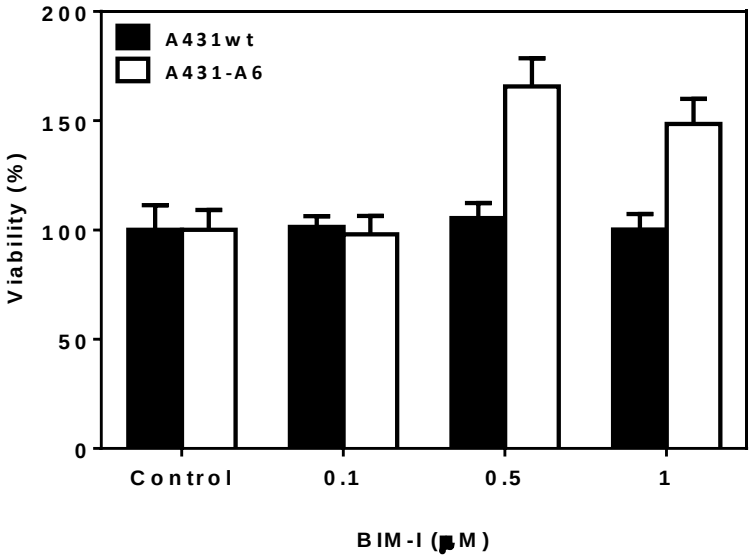

Figure 26. MTS assay showing the effect of BIM-I on A431wt and A431-A6 cell growth. A431wt and A431-A6 cells were seeded at a density of 4000 cells per well, and incubated with 0.1µM, 0.5µM and 1µM BIM-I for three days. Quadruple repeats were made for each treatment. Then MTS reagent was added and the plates were incubated for 30 minutes. The absorbance was detected at 490 nm, and the percentage of viability was calculated and plotted against BIM-I concentrations. The error bars represent the SD (n = 1).

3.16 Combinatorial use of erlotinib and BIM-I potentiates growth inhibition in A431 cells

The combinatorial treatment of TKIs with Gö 6976 potentiated growth inhibition in A431 cells that was more in A431-A6 cells compared to A431wt cells (sections 3.13 and 3.14). To extend these findings, we tested the ability of BIM-I, a potent inhibitor of the conventional PKC isozymes, in combination with erlotinib in clonogenic assays. The cells were incubated with 1µM erlotinib, 1µM BIM-I, and a combination of both drugs for five days to allow colony formation. Then, cells were washed twice with DPBS, fixed and stained. To avoid overlooking growth-inhibitory effects of AnxA6 occurring at later stages of colony growth, colonies of twenty, thirty, forty and fifty cells or more were counted and plotted against drug treatments (Figure 27 and 28).

After the quantification of colonies of fifty cells or more, we found that A431-A6 control had 71% less colony formation than A431wt control. Treating A431wt and A431-A6 cells with 1µM erlotinib reduced the number of colonies to 13.5 ± 1.5 and 5.5 ± 1.5, which is 70.3% and 87.9% inhibition, respectively. In contrast, the application of 1µM BIM-I did not significantly affect the colony growth in either A431wt cells or A431-A6 cells. The combinatorial treatment of 1µM erlotinib and 1µM BIM-I decreased the number of colonies to 11.5 ± 3.5 and 1.5 ± 0.5 in A431wt and A431-A6 cells, which represents 74.7% and 96.7% growth inhibition, respectively (Figure 28A-C). Similar trends were observed when we quantified the counts from colonies with 20, 30, 40 cells or more (Figure 28). The experiment was repeated twice and the results supported our MTS data (Figure 26) in that BIM-I, as a single agent, did not significantly modulate the cell growth of any of the two cell lines. However, when BIM-I was combined with erlotinib, the cell growth was effectively inhibited, particularly in A431-A6 cells. As mentioned above (section 3.15), these findings were unexpected and did not correlate well with the data obtained from PKC knockdown

studies performed by Grewal and coworkers previously (29). This will be discussed in more details in the discussion chapter.

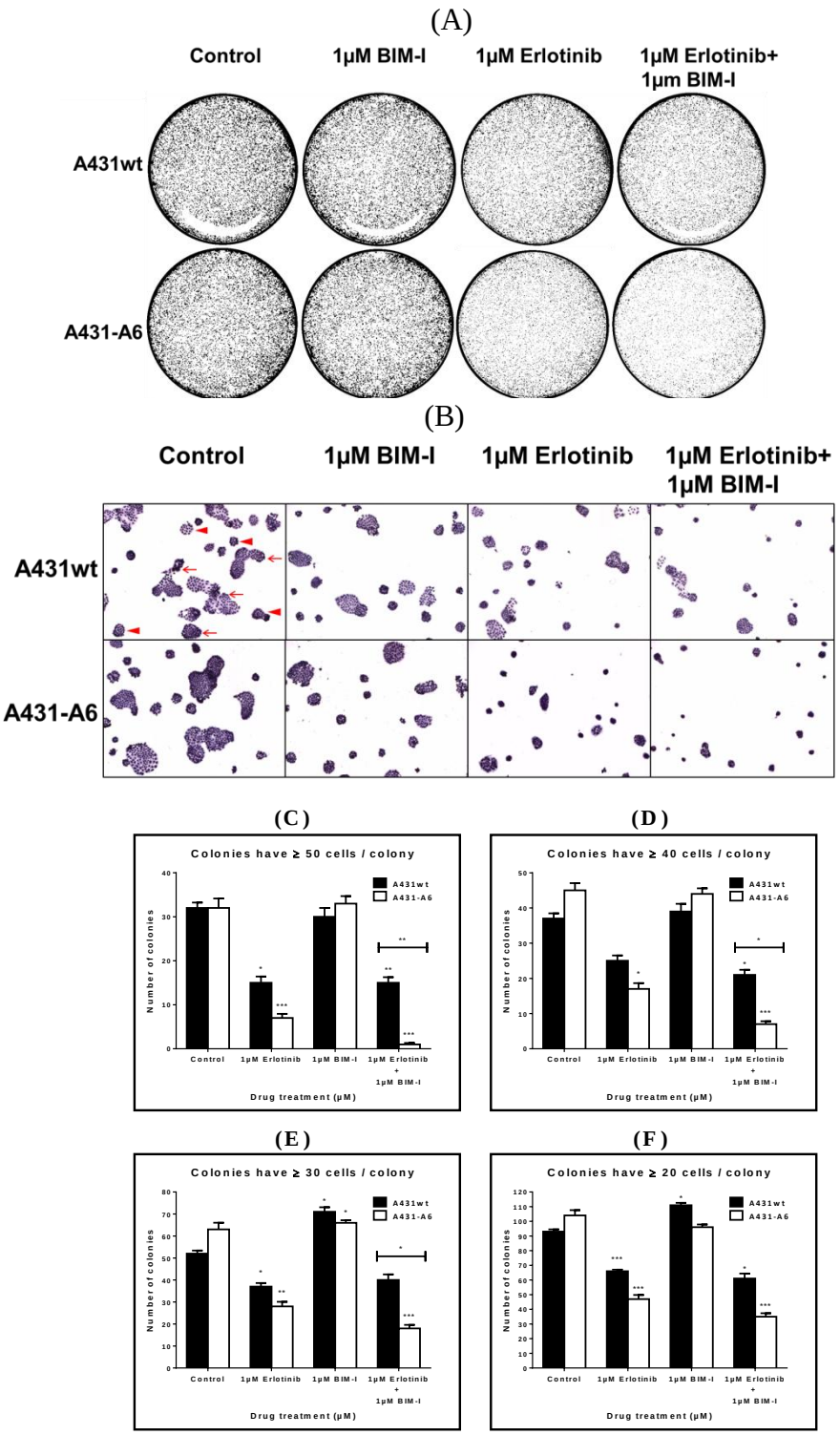

Figure 27. Clonogenic assay of A431 cells treated with 1µM erlotinib and 1µM BIM-I as single or combinatorial treatments. (A) A431wt and A431-A6 cells were plated in six-well culture plates at a density of 7000 cells per well and incubated with 1µM erlotinib, 1µM BIM-I, and a combination of both drugs for five days as indicated. Then cells were fixed and stained. One photo/well was taken to document the density of colony formation in the wells. (B) 10 images/well were randomly taken using the P.A.L.M. DuoFlex Combi System (Carl Zeiss). The arrows indicate colonies composed of 50 cells or more, while arrowheads point at colonies of less than 50 cells. (C-F) Colonies of 50, 40, 30, and 20 cells or more were counted in 10 images/condition and plotted against drug treatments. The error bars represent the SD. Statistical analysis was performed using student's unpaired t-test and based on the analysis of 10 images/well that were randomly taken of the same experiment. * represents a significant decrease of colony formation compared to A431wt control; * $P < 0.05$, ** $P < 0.01$, *** $P < 0.001$.

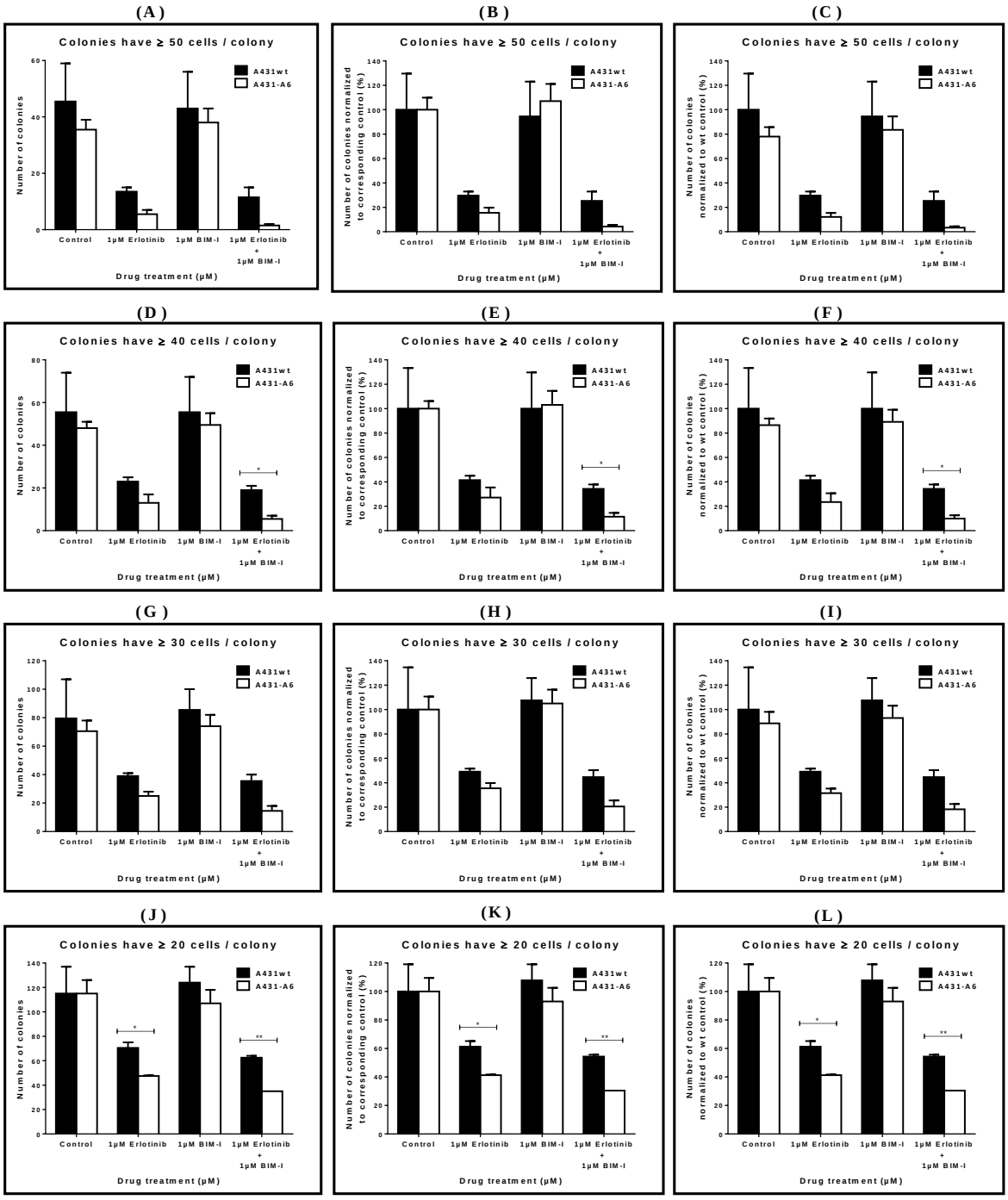

Figure 28. The inhibitory effect of erlotinib, BIM-I, and their combination on A431wt and A431-A6 cell proliferation. A431wt and A431-A6 cells were incubated with 1μM erlotinib, 1μM BIM-I, and a combination of both drugs for five days. Colonies of 20, 30, 40, and 50 cells or more were counted. Data represents the mean ± SEM of two independent experiments. (A, D, G, J) The number of colonies of A431wt and A431-A6 were plotted against drug treatments where each colony is 50, 40, 30, 20 cells or more, respectively. (B, E, H, K) The number of colonies of A431wt and A431-A6 were normalized to A431wt control and A431-A6 control, respectively, and plotted against drug treatments where each colony is 50, 40, 30, 20 cells or more, respectively. (C, F, I, L) The number of colonies of A431wt and A431-A6 were normalized to A431wt control and plotted against drug treatments where each colony is 50, 40, 30, 20 cells or more, respectively. Statistical analysis was performed using student's unpaired t-test where * represents a significant decrease of colony formation when comparing the number of colonies formed by A431wt and A431-A6 cells that were treated with the same drug treatments; * $P < 0.05$, ** $P < 0.01$.

3.17 Combinatorial treatment of gefitinib and BIM-I enhanced growth inhibition in AnxA6 expressing cells

After observing the inhibition of A431wt and A431-A6 growth upon exposure to a combination of erlotinib and BIM-I, we next moved to test another TKI combined with BIM-I via clonogenic assays. 1μM gefitinib, 1μM BIM-I, and a combination of both drugs were applied to A431wt and A431-A6 cells followed by five days incubation to allow colony formation. Then the cells were washed twice with DPBS, fixed and stained. To avoid overlooking growth-inhibitory effects of AnxA6 occurring at later stages of colony growth, colonies of twenty, thirty, forty and fifty cells or more were counted and plotted against drug treatments (Figure 29 and 30).

Colonies of fifty cells or more in both cell lines showed that A431-A6 control had 71% less colony formation than A431wt control. When 1μM gefitinib was applied, the number of colonies significantly decreased in A431wt and A431-A6 cells to 18.5 ± 1.5 and 4.5 ± 1.5, which reflects 59.3% and 90.1% inhibition, respectively ($P < 0.05$). The use of 1μM BIM-I was able to marginally decrease the number of colonies to 43 ± 13 (5.5%) and 38 ± 5 (16.5%) in A431wt and A431-A6 cells, respectively.

On the other hand, when 1μM gefitinib and 1μM BIM-I were used together as a combinatorial treatment, the number of colonies was significantly decreased to 8.5 ± 0.5 and 1.5 ± 0.5 in A431wt and A431-A6 cells which represents 81.3% and 96.7% growth inhibition, respectively ($P < 0.05$) (Figure 30A-C). Similar trends were observed when we quantified the counts from colonies with 20, 30, 40 cells or more (Figure 30).The experiment was repeated twice, and the results supported our previous findings (sections 3.13, 3.14, and 3.16) of the enhanced growth inhibition observed when a TKI is combined with a selective PKC inhibitor in AnxA6 overexpressing cells.

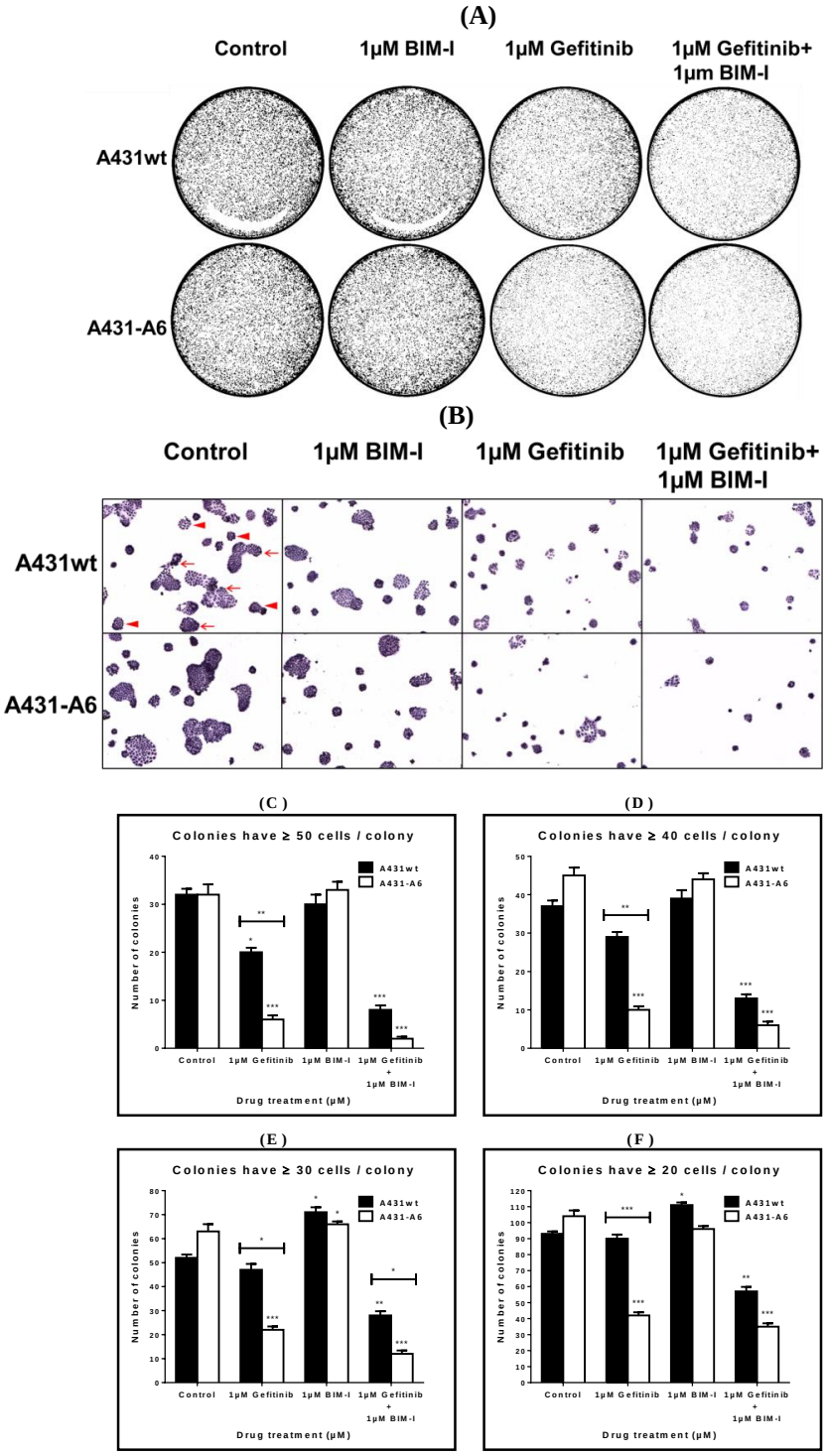

Figure 29. Clonogenic assay of A431 cells treated with 1µM gefitinib and 1µM BIM-I alone or in combination. (A) A431wt and A431-A6 cells were plated in six-well culture plates at a density of 7000 cells per well and incubated with 1µM gefitinib, 1µM BIM-I, and a combination of both drugs for five days as indicated. Then cells were fixed and stained. One photo/well was taken to document the density of colony formation in the wells. (B) 10 images/well were randomly taken using the P.A.L.M. DuoFlex Combi System (Carl Zeiss). The arrows indicate colonies composed of 50 cells or more, while arrowheads point at colonies of less than 50 cells. (C-F) Colonies of 50, 40, 30, and 20 cells or more were counted in 10 images/condition and plotted against drug treatments. The error bars represent the SD. Statistical analysis was performed using student's unpaired t-test and based on the analysis of 10 images/well that were randomly taken of the same experiment. * represents a significant decrease of colony formation compared to A431wt control; * $P < 0.05$, ** $P < 0.01$, *** $P < 0.001$.

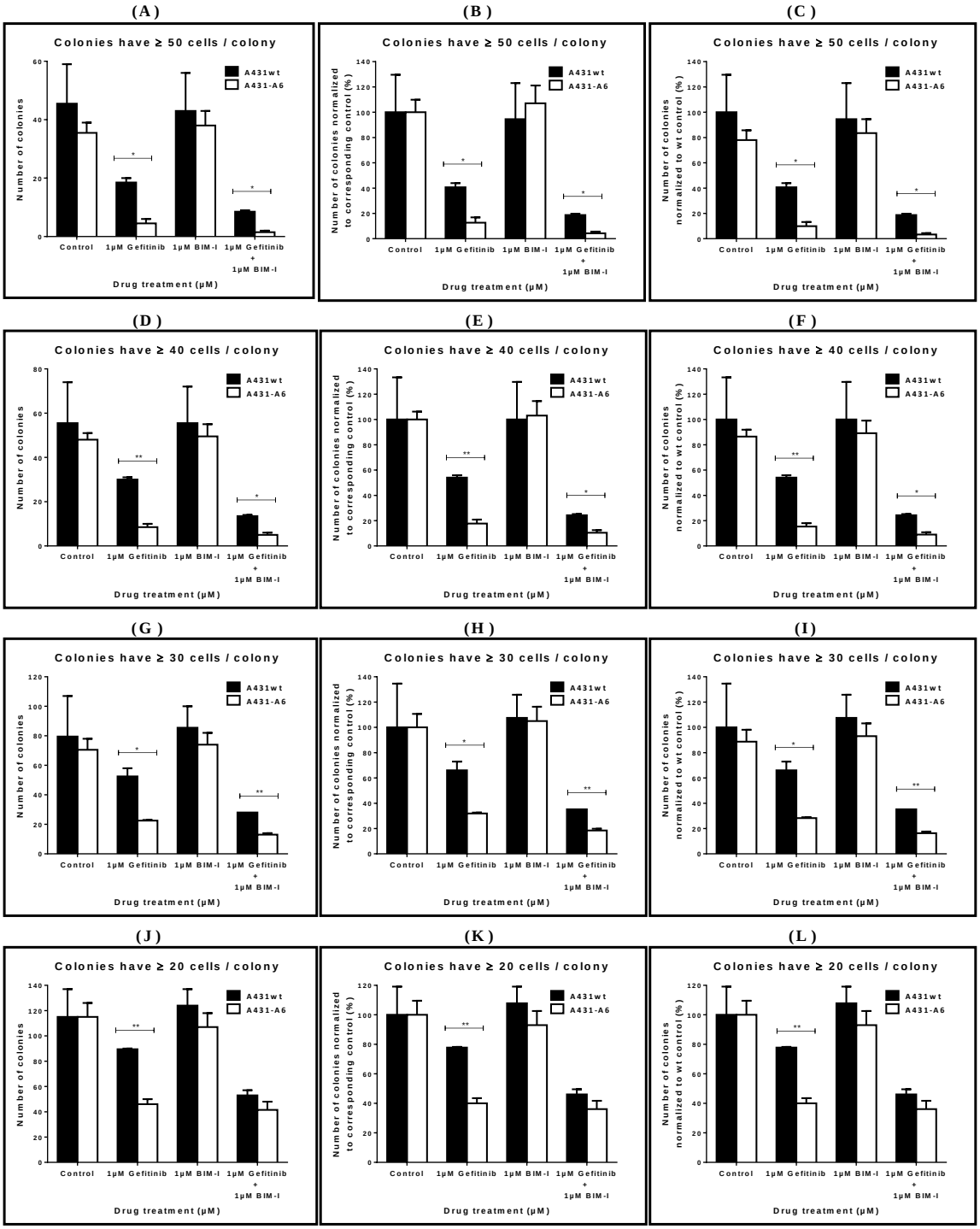

Figure 30. The inhibitory effect of gefitinib, BIM-I, and their combination on the growth of A431wt and A431-A6 cells. A431wt and A431-A6 cells were incubated with 1μM gefitinib, 1μM BIM-I, and a combination of both drugs for five days. Colonies of 20, 30, 40, and 50 cells or more were counted. Data represents the mean ± SEM of two independent experiments. (A, D, G, J) The number of colonies of A431wt and A431-A6 were plotted against drug treatments where each colony is 50, 40, 30, 20 cells or more, respectively. (B, E, H, K) The number of colonies of A431wt and A431-A6 were normalized to A431wt control and A431-A6 control, respectively, and plotted against drug treatments where each colony is 50, 40, 30, 20 cells or more, respectively. (C, F, I, L) The number of colonies of A431wt and A431-A6 were normalized to A431wt control and plotted against drug treatments where each colony is 50, 40, 30, 20 cells or more, respectively. Statistical analysis was performed using student's unpaired t-test where * represents a significant decrease of colony formation when comparing the number of colonies formed by A431wt and A431-A6 cells that were treated with the same drug treatments; * $P < 0.05$, ** $P < 0.01$.

3.18 Reduced cell growth of AnxA6 expressing cells treated with $cPLA_2$ inhibitors

Grewal and coworkers previously showed that AnxA6 overexpression inhibits caveolae formation in a $cPLA_2$-dependant manner (75). Given the inhibitory effects of AnxA6 on the EGFR pathway and the role of caveolin-1 and caveolae for EGFR signaling (3, 66, 75, 76), we wanted to investigate the oncogenic cell growth of AnxA6 overexpressing cells treated with $cPLA_2$ inhibitor. MTS assay was employed in which we treated the cells with MAFP, an irreversible inhibitor of $cPLA_2$. A431wt and A431-A6 cells were seeded at a density of 4000 and 8000 cells per well, and incubated with 5µM and 10µM MAFP for three days. Quadruple repeats were made for each treatment. Then, MTS reagent was added and the plates were incubated for 30 minutes. The absorbance was detected at 490 nm, and the percentage viability was calculated and plotted against MAFP concentrations. When 4000 cells/well were treated with 5µM and 10µM MAFP, the viability of the cells was 80.8% and 95.4% in A431wt cells, and 77.6% and 77.2% in A431-A6 cells, respectively. While when 8000 cells/well were treated with 5µM and 10µM MAFP, the viability was 81.3% and 106.4% in A431wt cells, and 57.7% and 67.3% in A431-A6 cells, respectively (Figure 31). The results showed more reduction of growth in A431-A6 cells compared to A431wt cells treated with the same doses of MAFP, and more inhibition was observed with the higher density of cells in the wells. These findings could indicate an increased involvement of $cPLA_2$-dependant pathways in cell growth in A431-A6 cells.

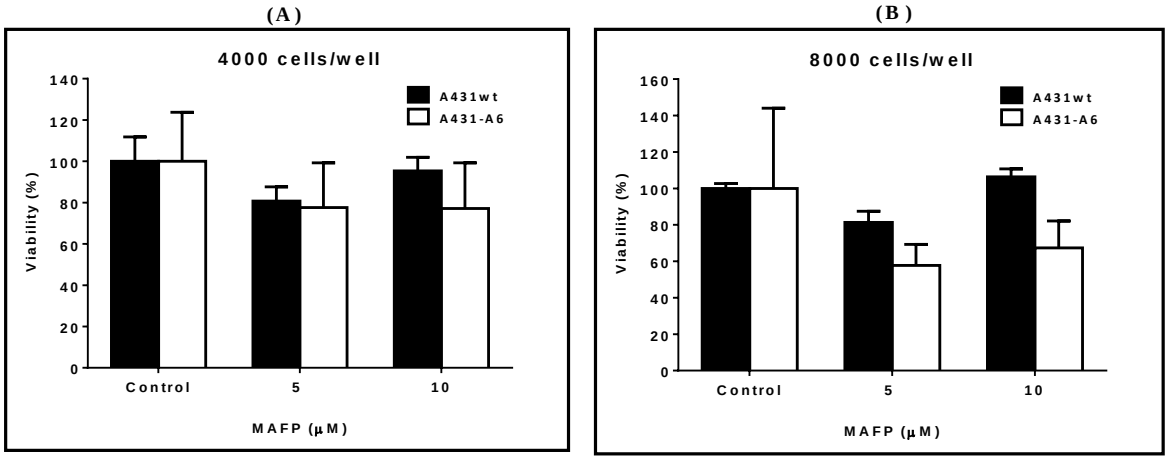

Figure 31. MTS assay showing the effect of MAFP on A431wt and A431-A6 cell growth. A431wt and A431-A6 cells were seeded at a density of (A) 4000 and (B) 8000 cells per well, and incubated with 5µM and 10µM MAFP for three days. Quadruple repeats were made for each treatment. Then, MTS reagent was added and the plates were incubated for 30 minutes. The absorbance was detected at 490 nm, and the percentage viability was calculated and plotted against MAFP concentrations. The error bars represent the SD.

Chapter 4: Discussion

4.1 Anti-cancer drugs targeting oncogenic EGFR

Cancer is a complex disease of a multigenic nature. EGFR overexpression or constitutive activation, owing to mutations, was found to correlate with the development of different types of cancers (241). Hence, blocking the sustained EGFR signaling was crucial to prevent tumor growth in these cancers, which led to the discovery of several potential anti-cancer agents such as EGFR inhibitors. TKIs and mAbs are the two major categories of EGFR inhibitors, terminating the signal via two different mechanisms. TKIs are small molecules that compete with ATP for binding to the intracellular tyrosine kinase catalytic domain of EGFR, leading to EGFR inhibition. In contrast, mAbs target the extracellular domain of the receptor preventing ligand binding, which is followed by EGFR endocytosis and signal termination (124, 125). Erlotinib, gefitinib, as examples of TKIs, and cetuximab, as an example of mAbs, are among the several FDA approved anti-EGFR drugs which achieved clinical success in treating patients with certain types of cancer (126). Despite this success, many patients are still unable to benefit from these drugs, a phenomenon that is still not fully understood, but could be attributed to inter-patient variation, mutation, and intrinsic/acquired resistance (126, 129-135, 138-140, 242). In addition, these drugs face other challenges in cancer treatment such as the high dose used and the lack of specificity of some drugs. For instance, TKIs target other kinases in addition to EGFR, that can lead to serious side effects (243). This justifies the need to identify novel biological markers that could predict the treatment outcome in those patients and help making important clinical decisions.

Some scaffold proteins were suggested as possible biomarkers, for example, the actin binding protein cortactin. The amplification of the gene CTTN, which encodes cortactin, was

identified in several cancers (244-246). Cortactin overexpression induced a sustained EGFR signaling upon attenuation of the receptor downregulation, which was reported to increase cell proliferation in HNSCC cells (141, 142). It also decreased the sensitivity towards gefitinib in HNSCC cells (141). These findings promoted cortactin as a possible marker for the prediction of patients' response towards EGFR-targeted therapies (141). However, other markers with a potential role in cancer still need to be identified.

4.2 Annexin A6 is a scaffold of the EGFR/Ras/MAPK pathway with the potential to increase the efficacy of drugs targeting EGFR

Alternative splicing is known to generate two isoforms of AnxA6 (AnxA6-1, AnxA6-2). The two isoforms only differ by 6 amino acids at position 524–529 (VAAEIL). The majority of cells and tissues only express the larger AnxA6-1 isoform. This includes skeletal muscle, liver, heart, spleen and lymph nodes as well as endothelial and endocrine cells nature, secretory epithelia, and macrophages (3). Little is known about the smaller AnxA6-2 isoform, which appears abundant in only a few transformed cell lines (94). Most cellular functions, including the tumour suppressor activity, have been linked to the larger AnxA6-1 isoform. In line with this, Fleet et al (96) reported that AnxA6-1 specifically inhibits the EGF-dependant calcium influx in A431 cells transfected with AnxA6 isoforms, and that AnxA6-2 does not have observable effect on growth rate or cellular phenotype. Several other observations suggest that the AnxA6-2 isoform has several different roles compared to AnxA6-1 in relation to Ca^{2+} homeostasis as well as membrane transport (247, 248). However, based on current knowledge, the AnxA6-2 isoform does not contribute to tumorigenic behaviour.

In addition, AnxA6 is multifunctional protein that negatively influences the activity of the EGFR/Ras/MAPK pathway. It binds to several negative regulators of the cascade such as

p120GAP and PKCα (66), and increases their ability to inhibit EGFR/Ras signaling. In fact, the elevated levels of AnxA6 decreased EGFR/Ras/MAPK activity and reduced oncogenic cell growth in several EGFR-related cell models (29). Thus, we hypothesized that high/low AnxA6 levels could be a potential biomarker that may predict the treatment outcome in EGFR-related cancers treated with drugs targeting the EGFR/Ras/MAPK pathway. Therefore, we compared cell and colony growth of cells lacking AnxA6 (A431wt) with cells overexpressing AnxA6 (A431-A6) in the presence of anti-cancer drugs targeting the EGFR/Ras/MAPK pathway.

In this study, clonogenic and MTS assays demonstrated that AnxA6 overexpression increased the sensitivity towards the TKIs erlotinib, gefitinib, and AG1478 to decrease the oncogenic cell growth in A431 cells (Figure 6-12). Importantly, we observed an increased potency of erlotinib and gefitinib at low concentrations in A431-A6 cells compared to A431wt cells (Figure 6, 7, 9, 10). Although 1μM erlotinib or gefitinib are generally considered too low for complete inhibition in cell culture studies (234, 237), it was able to induce substantial growth inhibition upon AnxA6 overexpression in A431 cells.

Despite these findings, marginal difference was observed between the control and cetuximab-treated cells, which did not fit expectations. Although we identified a trend of A431-A6 cells being more sensitive to cetuximab treatment than A431wt cells (Figure 13), we do not consider this significant, as our clonogenic assays showed no growth inhibition when we compared the suppression of growth following cetuximab monotherapy to the corresponding cell line control (Figure 13, 20, 21). Given that the literature confirms that cetuximab monotherapy markedly inhibits proliferation in A431 and other cell lines (233, 234), one could speculate that A431 cells used in this study may have developed resistance towards cetuximab. Consequently, interpretation of the data obtained from combining cetuximab with TKIs (Figure 20 and 21) is not forthcoming.

We have also explored the effect of AnxA6 on cell proliferation when MEK1/2 signaling was blocked. PD98059, a MEK1/2 inhibitor, was tested in clonogenic assays in A431 cells with and without AnxA6 overexpression. In agreement with the TKIs results, the proliferation and colony formation were more inhibited in A431-A6 cells than A431wt cells (Figure 15).

4.3 Combinatorial drug treatment is potentiated upon AnxA6 overexpression

After our findings with monotherapies, we next investigated several combinatorial treatments in AnxA6 overexpressing cells. We first identified the influence of blocking MEK1/2 signaling on the erlotinib-induced growth inhibition with elevated AnxA6 levels. The clonogenic assays revealed that the cotreatment of erlotinib with PD98059 was more effective in reducing oncogenic cell growth compared to single drug treatments (Figure 16 and 17). Moreover, the combinatorial therapy resulted in a more potent suppression of colony formation in A431-A6 cells compared to A431wt cells. Similar results were obtained when gefitinib was combined with PD98059 under the same experimental conditions (Figure 18 and 19). These data, in line with other studies, suggests that combining TKIs with MEK1/2 inhibitors could be a successful strategy in reducing oncogenic cell growth (229-231), particularly in cancer cells with elevated AnxA6 levels.

Given that AnxA6 inhibits EGFR in a PKCα-dependent manner, we followed these findings by another set of clonogenic assays in which we tested TKIs and PKCα inhibitors alone or in combination. Gö 6976, a PKCα and PKCβ1 inhibitor, moderately decreased colony formation of A431wt and A431-A6 cells; while BIM-I, a conventional PKC inhibitor, did not affect cell growth of any of the cell lines (Figure 22-25, 27-30). However, the cotreatment of erlotinib with either Gö 6976 or BIM-I effectively suppressed proliferation more than the individual drugs, and the growth inhibition was more pronounced in A431-A6 cells than A431wt cells.

Similar findings were observed with gefitinib combined with either PKCα-targeting drugs, except that the combination of gefitinib with Gö 6976 potently inhibited growth in both cell lines equally (97.7%). The increased potency of TKIs together with PKCα inhibitors in A431-A6 cells was unexpected, as PKCα knockdown restored EGFR signaling in A431-A6 cells (29). These findings need further investigation, but we believe that other PKCα activities, not related to EGFR signaling, may have contributed to these observations.

The increased potency of TKIs when administered alone or in combination with MEK1/2 or PKCα inhibitors could be owed to the tumor suppressor potential of AnxA6, which exerts its inhibitory effect on the EGFR/Ras/MAPK cascade in a p120GAP- and PKCα-dependent manner (22, 29). In 2009, Grewal and coworkers reported that elevated AnxA6 levels correlated with Ras inactivation in breast cancer cells (22). This inactivation was shown to be a consequence of AnxA6 binding to p120GAP which potentiated the targeting of p120GAP to Ras-GTP at the plasma membrane that lead to Ras downregulation (22). In addition, AnxA6 is a scaffolding protein for PKCα which potentiates PKCα membrane targeting and association with the EGFR, leading to EGFR signal termination (29). The interaction between AnxA6 and PKCα promotes EGFR downregulation via the increased ability of PKCα to phosphorylate EGFR at its threonine 654 leading to EGFR tyrosine phosphorylation inhibition (29). Both of these mechanisms would reduce the active pool of EGFR, Ras, and MAPK proteins, hence providing the basis for increased drug efficiency, even at low concentrations.

In contrast, other studies have identified opposing findings regarding the role of AnxA6 in tumor progression. AnxA6 depletion in invasive BT-549 breast cancer cells induced rapid degradation of activated EGFR, and elevated the sensitivity towards EGFR-targeted TKIs. However, the reduced AnxA6 expression in these cells enhanced tumor proliferation (249). It should be noted that in contrast to the EGFR cancer models showed here and previously by

the Grewal group (22), BT-549 cells express only moderate levels of AnxA6 and EGFR. In BT-549 cells, the author discussed the role that AnxA6 plays in lipid rafts formation and consequently, maintaining a sustained localization of EGFR on the cell surface (250, 251). The modulation of lipid rafts formation upon AnxA6 depletion was suggested to disrupt the localization of EGFR on the membranes, inducing receptor degradation which promoted the sensitivity towards TKIs targeting the receptor in invasive breast cancer cells (249). Taken together, AnxA6 might exert different effects on EGFR, depending on the cell and cancer subtypes.

Interestingly, our observations with Gö 6976 and BIM-I reflect the controversial results in various studies regarding the use of PKC inhibitors in cancer (29, 151, 232, 252-256). Gö 6976 was investigated in another study, in which the response of cells depended on the cell lines tested (253). A431wt showed no growth inhibition, while H-Ras mutant NSCLC cell lines displayed a minimal growth inhibitory response (253). However, in the same study EGFR mutant cell lines showed major growth retardation, upon Gö 6976 treatment, both *in vivo* and *in vitro* (253). This significant inhibitory effect of Gö 6976 was suggested to be PKC-independent (253), particularly as the drug previously showed effects against other kinases (255, 256). In addition, BIM-I was tested against the K-Ras mutant cell line A549 and displayed a minimal response in MTS assays (253). However, BIM-I showed 1.2 fold inhibition of serum-induced proliferation in lacto-somatotroph GH3 cells, and when combined with gefitinib further suppression of growth was observed that was more than the additive effect (232). This was referred to the possible inhibition of multiple signaling molecules by the various PKC isoforms inhibited by BIM-I (151, 232, 257).

Although PKCα was reported to transactivate EGFR and its downstream signaling (254), other studies illustrated the inhibitory role of PKCα on EGFR activity (29, 252). In SCC12 squamous carcinoma cells, multiple proteins such as caveolin-1, ganglioside GM3, and

tetraspanin CD82 are believed to modulate the binding of PKCα to EGFR in order to suppress the EGFR signaling (252). In addition, PKCα knockdown was found to minimally increase the cell growth of A431wt cells, and markedly elevate the number of colonies of AnxA6 overexpressing A431 cells, which pointed at the role that PKCα and its scaffolding proteins, including AnxA6, plays in EGFR inactivation (29). Therefore, given the multiple PKCα substrates involved in the EGFR pathway and other signaling cascades, the results for the combinatorial use of TKIs with PKCα inhibitors are difficult to interpret and require future investigations.

4.4 Potential contribution of $cPLA_2$ in EGFR signaling in annexin A6 overexpressing cells

AnxA6 was also reported to induce inhibition of $cPLA_2$ (75), an enzyme that was found elevated in various cancers (163, 258, 259). Hence, we employed the MTS assay to identify the impact of AnxA6 overexpression on the response of A431 cells to $cPLA_2$ inhibition. In line with our previous findings, we found more suppression of growth in A431-A6 cells compared to A431wt cells, which would suggest an increased involvement of $cPLA_2$ in the proliferation of A431-A6 cells. In fact, the negative influence of AnxA6 on $cPLA_2$ activity was identified to be indirect and does not involve a direct interaction between AnxA6 and $cPLA_2$ (75). $cPLA_2$ is phosphorylated by ERK1/2 at serine 505, a process that increases the enzymatic activity of $cPLA_2$. Thus, the inhibitory effect of AnxA6 on the EGFR/Ras/MAPK pathway could suppress $cPLA_2$ activity (19, 260, 261). In addition, AnxA6 sequesters cholesterol in LE leading to the reduction of cholesterol levels in the Golgi apparatus. This change of cholesterol homeostasis interferes with $cPLA_2$ translocation to the Golgi, a process that is required for the export of caveolin from Golgi to plasma membranes. Therefore, caveolae formation was inhibited, which would affect cellular signaling, lipid trafficking,

endocytosis, and the formation of membrane structures (3, 19, 66, 75, 76), all of which are relevant for EGFR activity.

4.5 Conclusion and future directions

Taken together, our data strongly support the hypothesis that elevated AnxA6 levels increase the efficacy of single or combinatorial treatments targeting EGFR-related cancer cell growth. This study supports current findings that combining different drugs targeting different members of the EGFR/Ras/MAPK signaling cascade may provide advanced therapeutic benefit. In summary, addressing Aims 1-4 delivered the following findings:

- **Aim 1:** As hypothesized, AnxA6 expression increased the efficacy of EGFR-TKIs (erlotinib, gefitinib, AG1478) in EGFR overexpressing A431 cancer cells.
- **Aim 2:** As hypothesized, AnxA6 expression increased the sensitivity of A431 cells towards monoclonal anti-EGFR antibodies (cetuximab).
- **Aim 3:** The efficacy of EGFR-TKIs (erlotinib, gefitinib) was not improved when examined in combination with anti-EGFR antibodies in EGFR overexpressing cancer cells. This is irrespective of the presence or absence of AnxA6.
- **Aim 4:** The efficacy of EGFR-TKIs (erlotinib, gefitinib) in combination with MEK1/2 or PKC inhibitors was increased upon AnxA6 expression in EGFR overexpressing A431 cells.

In particular, the treatment of A431 cells with TKIs combined with clinically proven MEK1/2 inhibitors could turn into a successful strategy, particularly in cancer cells with elevated AnxA6 levels. As such, this study places the determination of AnxA6 levels in the avenue of potential novel markers for predicting treatment responses in EGFR-related cancers.

Hence, in order to further develop AnxA6 levels as a prognostic tool in EGFR-related cancers, future studies should aim to:

1. Correlate AnxA6 levels in EGFR-related tumors of patients with treatment outcomes.

   Up to date, Grewal and coworkers identified reduced AnxA6 levels in EGFR-related breast cancers as well as glioma (22, 29). Hence, in these cancers, AnxA6 expression could become a biomarker for predicting patient response to EGFR targeting anticancer agents. In addition, AnxA6 is often downregulated in melanoma, myeloma, gastric and liver cancers (262, 263). In particular in the latter, EGFR signaling contributes to hepatocarcinogenesis (264). All of these cancer types might become suitable for AnxA6 to serve as a biomarker in the future.

2. Determining the tumor growth of EGFR overexpressing cancer cells, such as A431 with and without AnxA6 using xenografts in mice, will be an important step to establish a tumor suppressor role of AnxA6 in vivo. Moreover, the treatment of A431wt and A431-A6 xenografts with EGFR-TKIs or mAbs targeting EGFR will validate if increased drug sensitivity of AnxA6 expressing cells in cell cultures also occurs in more complex in vivo settings. Alternatively, exposing the AnxA6-KO mice to physiological stress, using well-established treatments with carcinogens, could identify increased tumour initiation, growth and progression in the absence of AnxA6.

3. Strategies to upregulate AnxA6 will remain difficult, as AnxA6 is a constitutively expressed gene that is not induced by hormones, steroids or other factors. However, with the ongoing improvements in gene therapy technologies, one could envisage AnxA6 upregulation, possible via viral-mediated gene transfer. Grewal and coworkers have already succeeded to deliver and overexpress AnxA6 in the liver of mice using adenoviral expression vectors (Grewal et al., unpublished data). Alternatively, the

development of AnxA6-like molecules (peptides) could be examined for their potential to improve the efficacy of anti-EGFR therapeutics.

Altogether, determining AnxA6 levels in EGFR-related tumors could become a useful tool in the future in order to predict patients most likely to benefit from drugs targeting oncogenic EGFR/Ras/MAPK activity.

Chapter 5: References

1. Crosetto N, Tikkanen R, Dikic I. Oncogenic breakdowns in endocytic adaptor proteins. FEBS letters. 2005;579(15):3231-8.

2. Ferguson KM. Structure-based view of epidermal growth factor receptor regulation. Annual review of biophysics. 2008;37:353-73.

3. Grewal T, Enrich C. Annexins—modulators of EGF receptor signalling and trafficking. Cellular signalling. 2009;21(6):847-58.

4. Lanzetti L, Di Fiore PP. Endocytosis and cancer: an 'insider'network with dangerous liaisons. Traffic. 2008;9(12):2011-21.

5. Roepstorff K, Grovdal L, Grandal M, Lerdrup M, van Deurs B. Endocytic downregulation of ErbB receptors: mechanisms and relevance in cancer. Histochemistry and cell biology. 2008;129(5):563-78.

6. Sorkin A, Goh LK. Endocytosis and intracellular trafficking of ErbBs. Experimental cell research. 2009;315(4):683-96.

7. von Zastrow M, Sorkin A. Signaling on the endocytic pathway. Current opinion in cell biology. 2007;19(4):436-45.

8. Warren CM, Landgraf R. Signaling through ERBB receptors: multiple layers of diversity and control. Cellular signalling. 2006;18(7):923-33.

9. Grewal T, Tebar F, Pol A, Enrich C. Involvement of targeting and scaffolding proteins in the regulation of the EGFR/Ras/MAPK pathway in oncogenesis. Current signal transduction therapy. 2006;1(2):147-67.

10. Mercer KE, Pritchard CA. Raf proteins and cancer: B-Raf is identified as a mutational target. Biochimica et biophysica acta. 2003;1653(1):25-40.

11. Knobbe CB, Reifenberger J, Reifenberger G. Mutation analysis of the Ras pathway genes NRAS, HRAS, KRAS and BRAF in glioblastomas. Acta neuropathologica. 2004;108(6):467-70.

12. Bos JL. Ras oncogenes in human cancer: a review. Cancer research. 1989;49(17):4682-9.

13. Donovan S, Shannon KM, Bollag G. GTPase activating proteins: critical regulators of intracellular signaling. Biochimica et biophysica acta. 2002;1602(1):23-45.

14. Cullen PJ, Lockyer PJ. Integration of calcium and Ras signalling. Nature reviews molecular cell biology. 2002;3(5):339-48.

15. Downward J. Targeting RAS signalling pathways in cancer therapy. Nature reviews cancer. 2003;3(1):11-22.

16. Grewal T, Enrich C. Molecular mechanisms involved in Ras inactivation: the annexin A6-p120GAP complex. Bioessays. 2006;28(12):1211-20.

17. Yarden Y. The EGFR family and its ligands in human cancer. signalling mechanisms and therapeutic opportunities. European journal of cancer. 2001;37 Suppl 4:S3-8.

18. Schlessinger J. Cell signaling by receptor tyrosine kinases. Cell. 2000;103(2):211-25.

19. Enrich C, Rentero C, de Muga SV, Reverter M, Mulay V, Wood P, et al. Annexin A6-Linking Ca(2+) signaling with cholesterol transport. Biochimica et biophysica acta. 2011;1813(5):935-47.

20. Sebolt-Leopold JS, Herrera R. Targeting the mitogen-activated protein kinase cascade to treat cancer. Nature reviews cancer. 2004;4(12):937-47.

21. Hawkins TE, Roes J, Rees D, Monkhouse J, Moss SE. Immunological development and cardiovascular function are normal in annexin VI null mutant mice. Molecular and cellular biology. 1999;19(12):8028-32.

22. Vila de Muga S, Timpson P, Cubells L, Evans R, Hayes TE, Rentero C, et al. Annexin A6 inhibits Ras signalling in breast cancer cells. Oncogene. 2009;28(3):363-77.

23. Grewal T, Evans R, Rentero C, Tebar F, Cubells L, de Diego I, et al. Annexin A6 stimulates the membrane recruitment of p120GAP to modulate Ras and Raf-1 activity. Oncogene. 2005;24(38):5809-20.

24. Theobald J, Smith PD, Jacob SM, Moss SE. Expression of annexin VI in A431 carcinoma cells suppresses proliferation: a possible role for annexin VI in cell growth regulation. Biochimica et biophysica acta -Molecular cell research. 1994;1223(3):383-90.

25. Theobald J, Hanby A, Patel K, Moss SE. Annexin VI has tumour-suppressor activity in human A431 squamous epithelial carcinoma cells. British journal of cancer. 1995;71(4):786-8.

26. Bardeesy N, Kim M, Xu J, Kim RS, Shen Q, Bosenberg MW, et al. Role of epidermal growth factor receptor signaling in RAS-driven melanoma. Molecular and cellular biology. 2005;25(10):4176-88.

27. Francia G, Mitchell SD, Moss SE, Hanby AM, Marshall JF, Hart IR. Identification by differential display of annexin-VI, a gene differentially expressed during melanoma progression. Cancer research. 1996;56(17):3855-8.

28. Ullrich A, Schlessinger J. Signal transduction by receptors with tyrosine kinase activity. Cell. 1990;61(2):203-12.

29. Koese M, Rentero C, Kota BP, Hoque M, Cairns R, Wood P, et al. Annexin A6 is a scaffold for PKCalpha to promote EGFR inactivation. Oncogene. 2013;32(23):2858-72.

30. Li S, Couvillon AD, Brasher BB, Van Etten RA. Tyrosine phosphorylation of Grb2 by Bcr/Abl and epidermal growth factor receptor: a novel regulatory mechanism for tyrosine kinase signaling. The EMBO journal. 2001;20(23):6793-804.

31. Iversen L, Tu HL, Lin WC, Christensen SM, Abel SM, Iwig J, et al. Molecular kinetics. Ras activation by SOS: allosteric regulation by altered fluctuation dynamics. Science. 2014;345(6192):50-4.

32. Malaney S, Daly RJ. The ras signaling pathway in mammary tumorigenesis and metastasis. Journal of mammary gland biology and neoplasia. 2001;6(1):101-13.

33. Cook SJ, Lockyer PJ. Recent advances in Ca 2+-dependent Ras regulation and cell proliferation. Cell calcium. 2006;39(2):101-12.

34. Sigismund S, Woelk T, Puri C, Maspero E, Tacchetti C, Transidico P, et al. Clathrin-independent endocytosis of ubiquitinated cargos. Proceedings of the national academy of sciences of the United States of America. 2005;102(8):2760-5.

35. Sigismund S, Argenzio E, Tosoni D, Cavallaro E, Polo S, Di Fiore PP. Clathrin-mediated internalization is essential for sustained EGFR signaling but dispensable for degradation. Developmental cell. 2008;15(2):209-19.

36. Raiborg C, Rusten TE, Stenmark H. Protein sorting into multivesicular endosomes. Current opinion in cell biology. 2003;15(4):446-55.

37. Tanaka N, Kyuuma M, Sugamura K. Endosomal sorting complex required for transport proteins in cancer pathogenesis, vesicular transport, and non-endosomal functions. Cancer science. 2008;99(7):1293-303.

38. Rosse C, Linch M, Kermorgant S, Cameron AJ, Boeckeler K, Parker PJ. PKC and the control of localized signal dynamics. Nature reviews molecular cell biology. 2010;11(2):103-12.

39. Corbalan-Garcia S, Gomez-Fernandez JC. The C2 domains of classical and novel PKCs as versatile decoders of membrane signals. Biofactors. 2010;36(1):1-7.

40. Griner EM, Kazanietz MG. Protein kinase C and other diacylglycerol effectors in cancer. Nature reviews cancer. 2007;7(4):281-94.

41. Mochly-Rosen D, Das K, Grimes KV. Protein kinase C, an elusive therapeutic target? Nature reviews drug discovery. 2012;11(12):937-57.

42. Kheifets V, Mochly-Rosen D. Insight into intra- and inter-molecular interactions of PKC: design of specific modulators of kinase function. Pharmacological research. 2007;55(6):467-76.

43. Steinberg SF. Structural basis of protein kinase C isoform function. Physiological reviews. 2008;88(4):1341-78.

44. Hoque M, Rentero C, Cairns R, Tebar F, Enrich C, Grewal T. Annexins - scaffolds modulating PKC localization and signaling. Cellular signalling. 2014;26(6):1213-25.

45. Babiychuk EB, Draeger A. Annexins in cell membrane dynamics. Ca(2+)-regulated association of lipid microdomains. Journal of cell biology. 2000;150(5):1113-24.

46. Orito A, Kumanogoh H, Yasaka K, Sokawa J, Hidaka H, Sokawa Y, et al. Calcium-dependent association of annexin VI, protein kinase C alpha, and neurocalcin alpha on the raft fraction derived from the synaptic plasma membrane of rat brain. Journal of neuroscience research. 2001;64(3):235-41.

47. Prevostel C, Alice V, Joubert D, Parker PJ. Protein kinase C(alpha) actively downregulates through caveolae-dependent traffic to an endosomal compartment. Journal of cell science. 2000;113 (Pt 14):2575-84.

48. Quilliam LA, Rebhun JF, Castro AF. A growing family of guanine nucleotide exchange factors is responsible for activation of Ras-family GTPases. Progress in nucleic acid research and molecular biology. 2002;71:391-444.

49. Cooper JA, Kashishian A. In vivo binding properties of SH2 domains from GTPase-activating protein and phosphatidylinositol 3-kinase. Molecular and cellular biology. 1993;13(3):1737-45.

50. Wang Z, Tung PS, Moran MF. Association of p120 ras GAP with endocytic components and colocalization with epidermal growth factor (EGF) receptor in response to EGF stimulation. Cell growth and differentiation. 1996;7(1):123-33.

51. Jones RB, Gordus A, Krall JA, MacBeath G. A quantitative protein interaction network for the ErbB receptors using protein microarrays. Nature. 2006;439(7073):168-74.

52. Agell N, Bachs O, Rocamora N, Villalonga P. Modulation of the Ras/Raf/MEK/ERK pathway by Ca(2+), and calmodulin. Cellular signalling. 2002;14(8):649-54.

53. Fivaz M, Meyer T. Reversible intracellular translocation of KRas but not HRas in hippocampal neurons regulated by Ca2+/calmodulin. Journal of cell biology. 2005;170(3):429-41.

54. Villalonga P, Lopez-Alcala C, Chiloeches A, Gil J, Marais R, Bachs O, et al. Calmodulin prevents activation of Ras by PKC in 3T3 fibroblasts. Journal of biological chemistry. 2002;277(40):37929-35.

55. San Jose E, Benguria A, Geller P, Villalobo A. Calmodulin inhibits the epidermal growth factor receptor tyrosine kinase. Journal of biological chemistry. 1992;267(21):15237-45.

56. Aifa S, Johansen K, Nilsson UK, Liedberg B, Lundstrom I, Svensson SP. Interactions between the juxtamembrane domain of the EGFR and calmodulin measured by surface plasmon resonance. Cellular signalling. 2002;14(12):1005-13.

57. Aifa S, Frikha F, Miled N, Johansen K, Lundstrom I, Svensson SP. Phosphorylation of Thr654 but not Thr669 within the juxtamembrane domain of the EGF receptor inhibits calmodulin binding. Biochemical and biophysical research communications. 2006;347(2):381-7.

58. McLaughlin S, Smith SO, Hayman MJ, Murray D. An electrostatic engine model for autoinhibition and activation of the epidermal growth factor receptor (EGFR/ErbB) family. Journal of general physiology. 2005;126(1):41-53.

59. Llado A, Tebar F, Calvo M, Moreto J, Sorkin A, Enrich C. Protein kinaseCdelta-calmodulin crosstalk regulates epidermal growth factor receptor exit from early endosomes. Molecular biology of the cell. 2004;15(11):4877-91.

60. Llado A, Timpson P, Vila de Muga S, Moreto J, Pol A, Grewal T, et al. Protein kinase Cdelta and calmodulin regulate epidermal growth factor receptor recycling from early endosomes through Arp2/3 complex and cortactin. Molecular biology of the cell. 2008;19(1):17-29.

61. Tebar F, Villalonga P, Sorkina T, Agell N, Sorkin A, Enrich C. Calmodulin regulates intracellular trafficking of epidermal growth factor receptor and the MAPK signaling pathway. Molecular biology of the cell. 2002;13(6):2057-68.

62. Reutelingsperger CP, van Heerde W, Hauptmann R, Maassen C, van Gool RG, de Leeuw P, et al. Differential tissue expression of Annexin VIII in human. FEBS letters. 1994;349(1):120-4.

63. Pepinsky RB, Hauptmann R. Detection of VAC-beta (annexin-8) in human placenta. FEBS letters. 1992;306(1):85-9.

64. Moss SE, Morgan RO. The annexins. Genome biology. 2004;5(4):219.

65. Gerke V, Creutz CE, Moss SE. Annexins: linking Ca2+ signalling to membrane dynamics. Nature reviews molecular cell biology. 2005;6(6):449-61.

66. Grewal T, Koese M, Rentero C, Enrich C. Annexin A6-regulator of the EGFR/Ras signalling pathway and cholesterol homeostasis. The international journal of biochemistry and cell biology. 2010;42(5):580-4.

67. Benz J, Bergner A, Hofmann A, Demange P, Gottig P, Liemann S, et al. The structure of recombinant human annexin VI in crystals and membrane-bound. Journal of molecular biology. 1996;260(5):638-43.

68. Avila-Sakar AJ, Creutz CE, Kretsinger RH. Crystal structure of bovine annexin VI in a calcium-bound state. Biochimica et biophysica acta. 1998;1387(1-2):103-16.

69. Avila-Sakar AJ, Kretsinger RH, Creutz CE. Membrane-bound 3D structures reveal the intrinsic flexibility of annexin VI. Journal of structural biology. 2000;130(1):54-62.

70. Buzhynskyy N, Golczak M, Lai-Kee-Him J, Lambert O, Tessier B, Gounou C, et al. Annexin-A6 presents two modes of association with phospholipid membranes. A combined QCM-D, AFM and cryo-TEM study. Journal of structural biology. 2009;168(1):107-16.

71. Edwards HC, Crumpton MJ. Ca(2+)-dependent phospholipid and arachidonic acid binding by the placental annexins VI and IV. European journal of biochemistry. 1991;198(1):121-9.

72. Grewal T, Heeren J, Mewawala D, Schnitgerhans T, Wendt D, Salomon G, et al. Annexin VI stimulates endocytosis and is involved in the trafficking of low density lipoprotein to the prelysosomal compartment. Journal of biological chemistry. 2000;275(43):33806-13.

73. Kamal A, Ying Y, Anderson RG. Annexin VI-mediated loss of spectrin during coated pit budding is coupled to delivery of LDL to lysosomes. Journal of cell biology. 1998;142(4):937-47.

74. Pons M, Grewal T, Rius E, Schnitgerhans T, Jackle S, Enrich C. Evidence for the involvement of annexin 6 in the trafficking between the endocytic compartment and lysosomes. Experimental cell research. 2001;269(1):13-22.

75. Cubells L, Vila de Muga S, Tebar F, Bonventre JV, Balsinde J, Pol A, et al. Annexin A6-induced inhibition of cytoplasmic phospholipase A2 is linked to caveolin-1 export from the Golgi. Journal of biological chemistry. 2008;283(15):10174-83.

76. Cubells L, Vila de Muga S, Tebar F, Wood P, Evans R, Ingelmo-Torres M, et al. Annexin A6-induced alterations in cholesterol transport and caveolin export from the Golgi complex. Traffic. 2007;8(11):1568-89.

77. Hayes MJ, Rescher U, Gerke V, Moss SE. Annexin-actin interactions. Traffic. 2004;5(8):571-6.

78. Rescher U, Gerke V. Annexins--unique membrane binding proteins with diverse functions. Journal of cell science. 2004;117(Pt 13):2631-9.

79. Futter CE, White IJ. Annexins and endocytosis. Traffic. 2007;8(8):951-8.

80. Gerke V, Moss SE. Annexins: from structure to function. Physiological reviews. 2002;82(2):331-71.

81. Monastyrskaya K, Babiychuk EB, Hostettler A, Rescher U, Draeger A. Annexins as intracellular calcium sensors. Cell calcium. 2007;41(3):207-19.

82. Skrahina T, Piljic A, Schultz C. Heterogeneity and timing of translocation and membrane-mediated assembly of different annexins. Experimental cell research. 2008;314(5):1039-47.

83. Ortega D, Pol A, Biermer M, Jackle S, Enrich C. Annexin VI defines an apical endocytic compartment in rat liver hepatocytes. Journal of cell science. 1998;111 (Pt 2):261-9.

84. Pons M, Ihrke G, Koch S, Biermer M, Pol A, Grewal T, et al. Late endocytic compartments are major sites of annexin VI localization in NRK fibroblasts and polarized WIF-B hepatoma cells. Experimental cell research. 2000;257(1):33-47.

85. de Diego I, Schwartz F, Siegfried H, Dauterstedt P, Heeren J, Beisiegel U, et al. Cholesterol modulates the membrane binding and intracellular distribution of annexin 6. Journal of biological chemistry. 2002;277(35):32187-94.

86. Chlystun M, Campanella M, Law AL, Duchen MR, Fatimathas L, Levine TP, et al. Regulation of mitochondrial morphogenesis by annexin A6. PLoS one. 2013;8(1):e53774.

87. Turro S, Ingelmo-Torres M, Estanyol JM, Tebar F, Fernandez MA, Albor CV, et al. Identification and characterization of associated with lipid droplet protein 1: A novel membrane-associated protein that resides on hepatic lipid droplets. Traffic. 2006;7(9):1254-69.

88. Summers TA, Creutz CE. Phosphorylation of a chromaffin granule-binding protein by protein kinase C. Journal of biological chemistry. 1985;260(4):2437-43.

89. Kenton P, Johnson PM, Webb PD. The phosphorylation of p68, a calcium-binding protein associated with the human syncytiotrophoblast submembranous cytoskeleton, is modulated by growth factors, activators of protein kinase C and cyclic AMP. Biochimica et biophysica acta. 1989;1014(3):271-81.

90. Freye-Minks C, Kretsinger RH, Creutz CE. Structural and dynamic changes in human annexin VI induced by a phosphorylation-mimicking mutation, T356D. Biochemistry. 2003;42(3):620-30.

91. Golczak M, Kirilenko A, Bandorowicz-Pikula J, Pikula S. Conformational states of annexin VI in solution induced by acidic pH. FEBS letters. 2001;496(1):49-54.

92. Golczak M, Kirilenko A, Bandorowicz-Pikula J, Pikula S. N- and C-terminal halves of human annexin VI differ in ability to form low pH-induced ion channels. Biochemical and biophysical research communications. 2001;284(3):785-91.

93. Monastyrskaya K, Tschumi F, Babiychuk EB, Stroka D, Draeger A. Annexins sense changes in intracellular pH during hypoxia. The biochemical journal. 2008;409(1):65-75.

94. Edwards HC, Moss SE. Functional and genetic analysis of annexin VI. Molecular and cellular biochemistry. 1995;149-150:293-9.

95. Strzelecka-Kiliszek A, Buszewska ME, Podszywalow-Bartnicka P, Pikula S, Otulak K, Buchet R, et al. Calcium- and pH-dependent localization of annexin A6 isoforms in Balb/3T3 fibroblasts reflecting their potential participation in vesicular transport. Journal of cellular biochemistry. 2008;104(2):418-34.

96. Fleet A, Ashworth R, Kubista H, Edwards H, Bolsover S, Mobbs P, et al. Inhibition of EGF-dependent calcium influx by annexin VI is splice form-specific. Biochemical and biophysical research communications. 1999;260(2):540-6.

97. Goebeler V, Poeter M, Zeuschner D, Gerke V, Rescher U. Annexin A8 regulates late endosome organization and function. Molecular biology of the cell. 2008;19(12):5267-78.

98. Goebeler V, Ruhe D, Gerke V, Rescher U. Annexin A8 displays unique phospholipid and F-actin binding properties. FEBS letters. 2006;580(10):2430-4.

99. Pons M, Tebar F, Kirchhoff M, Peiro S, de Diego I, Grewal T, et al. Activation of Raf-1 is defective in annexin 6 overexpressing Chinese hamster ovary cells. FEBS letters. 2001;501(1):69-73.

100. Davis AJ, Butt JT, Walker JH, Moss SE, Gawler DJ. The Ca2+-dependent lipid binding domain of P120GAP mediates protein-protein interactions with Ca2+-dependent membrane-binding proteins. Evidence for a direct interaction between annexin VI and P120GAP. Journal of biological chemistry. 1996;271(40):24333-6.

101. Fauvel J, Vicendo P, Roques V, Ragab-Thomas J, Granier C, Vilgrain I, et al. Isolation of two 67 kDa calcium-binding proteins from pig lung differing in affinity for phospholipids and in anti-phospholipase A2 activity. FEBS letters. 1987;221(2):397-402.

102. Rentero C, Evans R, Wood P, Tebar F, Vila de Muga S, Cubells L, et al. Inhibition of H-Ras and MAPK is compensated by PKC-dependent pathways in annexin A6 expressing cells. Cellular signalling. 2006;18(7):1006-16.

103. Schmitz-Peiffer C, Browne CL, Walker JH, Biden TJ. Activated protein kinase C alpha associates with annexin VI from skeletal muscle. The biochemical journal. 1998;330 (Pt 2):675-81.

104. Chow A, Gawler D. Mapping the site of interaction between annexin VI and the p120GAP C2 domain. FEBS letters. 1999;460(1):166-72.

105. Chow A, Davis AJ, Gawler DJ. Investigating the role played by protein-lipid and protein-protein interactions in the membrane association of the p120GAP CaLB domain. Cellular signalling. 1999;11(6):443-51.

106. Chow A, Davis AJ, Gawler DJ. Identification of a novel protein complex containing annexin VI, Fyn, Pyk2, and the p120(GAP) C2 domain. FEBS letters. 2000;469(1):88-92.

107. Smythe E, Ayscough KR. Actin regulation in endocytosis. Journal of cell science. 2006;119(Pt 22):4589-98.

108. Kaksonen M, Toret CP, Drubin DG. Harnessing actin dynamics for clathrin-mediated endocytosis. Nature reviews molecular cell biology. 2006;7(6):404-14.

109. Schafer DA. Coupling actin dynamics and membrane dynamics during endocytosis. Current opinion in cell biology. 2002;14(1):76-81.

110. da Costa SR, Okamoto CT, Hamm-Alvarez SF. Actin microfilaments et al.--the many components, effectors and regulators of epithelial cell endocytosis. Advanced drug delivery reviews. 2003;55(11):1359-83.

111. Kobayashi R, Tashima Y. Purification, biological properties and partial sequence analysis of 67-kDa calcimedin and its 34-kDa fragment from chicken gizzard. European journal of biochemistry 1990;188(2):447-53.

112. Hosoya H, Kobayashi R, Tsukita S, Matsumura F. Ca(2+)-regulated actin and phospholipid binding protein (68 kD-protein) from bovine liver: identification as a homologue for annexin VI and intracellular localization. Cell motility and the cytoskeleton. 1992;22(3):200-10.

113. Goldberg M, Feinberg J, Lecolle S, Kaetzel MA, Rainteau D, Lessard JL, et al. Co-distribution of annexin VI and actin in secretory ameloblasts and odontoblasts of rat incisor. Cell and tissue research. 1991;263(1):81-9.

114. Monastyrskaya K, Babiychuk EB, Hostettler A, Wood P, Grewal T, Draeger A. Plasma membrane-associated annexin A6 reduces Ca2+ entry by stabilizing the cortical actin cytoskeleton. Journal of biological chemistry. 2009;284(25):17227-42.

115. Watanabe T, Inui M, Chen BY, Iga M, Sobue K. Annexin VI-binding proteins in brain. Interaction of annexin VI with a membrane skeletal protein, calspectin (brain spectrin or fodrin). Journal of biological chemistry. 1994;269(26):17656-62.

116. Patterson RL, van Rossum DB, Gill DL. Store-operated Ca2+ entry: evidence for a secretion-like coupling model. Cell. 1999;98(4):487-99.

117. Rosado JA, Sage SO. The actin cytoskeleton in store-mediated calcium entry. Journal of physiology. 2000;526 Pt 2:221-9.

118. Jardin I, Lopez JJ, Salido GM, Rosado JA. Orai1 mediates the interaction between STIM1 and hTRPC1 and regulates the mode of activation of hTRPC1-forming Ca2+ channels. Journal of biological chemistry. 2008;283(37):25296-304.

119. Lodish H, Berk A, Zipursky S. Molecular cell biology 4th edition. 2000;Section 17.9, Receptor-mediated endocytosis and the sorting of internalized proteins.

120. Roberts PJ, Der CJ. Targeting the Raf-MEK-ERK mitogen-activated protein kinase cascade for the treatment of cancer. Oncogene. 2007;26(22):3291-310.

121. Hoshino R, Chatani Y, Yamori T, Tsuruo T, Oka H, Yoshida O, et al. Constitutive activation of the 41-/43-kDa mitogen-activated protein kinase signaling pathway in human tumors. Oncogene. 1999;18(3):813-22.

122. Alessi DR, Cuenda A, Cohen P, Dudley DT, Saltiel AR. PD 098059 is a specific inhibitor of the activation of mitogen-activated protein kinase kinase in vitro and in vivo. Journal of biological chemistry. 1995;270(46):27489-94.

123. Cox AD, Der CJ. Ras family signaling: therapeutic targeting. Cancer biology and therapy. 2002;1(6):599-606.

124. Harari PM. Epidermal growth factor receptor inhibition strategies in oncology. Endocrine-related cancer. 2004;11(4):689-708.

125. Ciardiello F. Epidermal growth factor receptor tyrosine kinase inhibitors as anticancer agents. Drugs. 2000;60 Suppl 1:25-32; discussion 41-2.

126. Yewale C, Baradia D, Vhora I, Patil S, Misra A. Epidermal growth factor receptor targeting in cancer: a review of trends and strategies. Biomaterials. 2013;34(34):8690-707.

127. Nowell PC. The clonal evolution of tumor cell populations. Science. 1976;194(4260):23-8.

128. Lengauer C, Kinzler KW, Vogelstein B. Genetic instabilities in human cancers. Nature. 1998;396(6712):643-9.

129. Kim WY, Prudkin L, Feng L, Kim ES, Hennessy B, Lee JS, et al. Epidermal growth factor receptor and K-Ras mutations and resistance of lung cancer to insulin-like growth factor 1 receptor tyrosine kinase inhibitors. Cancer. 2012;118(16):3993-4003.

130. Pao W, Wang TY, Riely GJ, Miller VA, Pan Q, Ladanyi M, et al. KRAS mutations and primary resistance of lung adenocarcinomas to gefitinib or erlotinib. PLoS medicine. 2005;2(1):e17.

131. Perrone F, Lampis A, Orsenigo M, Di Bartolomeo M, Gevorgyan A, Losa M, et al. PI3KCA/PTEN deregulation contributes to impaired responses to cetuximab in metastatic colorectal cancer patients. Annals of oncology. 2009;20(1):84-90.

132. Frattini M, Saletti P, Romagnani E, Martin V, Molinari F, Ghisletta M, et al. PTEN loss of expression predicts cetuximab efficacy in metastatic colorectal cancer patients. British journal of cancer. 2007;97(8):1139-45.

133. Learn CA, Hartzell TL, Wikstrand CJ, Archer GE, Rich JN, Friedman AH, et al. Resistance to tyrosine kinase inhibition by mutant epidermal growth factor receptor variant III contributes to the neoplastic phenotype of glioblastoma multiforme. Clinical cancer research. 2004;10(9):3216-24.

134. Pao W, Miller VA, Politi KA, Riely GJ, Somwar R, Zakowski MF, et al. Acquired resistance of lung adenocarcinomas to gefitinib or erlotinib is associated with a second mutation in the EGFR kinase domain. PLoS medicine. 2005;2(3):e73.

135. Shih JY, Gow CH, Yang PC. EGFR mutation conferring primary resistance to gefitinib in non-small-cell lung cancer. The New England journal of medicine. 2005;353(2):207-8.

136. Wheeler DL, Huang S, Kruser TJ, Nechrebecki MM, Armstrong EA, Benavente S, et al. Mechanisms of acquired resistance to cetuximab: role of HER (ErbB) family members. Oncogene. 2008;27(28):3944-56.

137. Krumbach R, Schuler J, Hofmann M, Giesemann T, Fiebig HH, Beckers T. Primary resistance to cetuximab in a panel of patient-derived tumour xenograft models: activation of MET as one mechanism for drug resistance. European journal of cancer. 2011;47(8):1231-43.

138. Kalish LH, Kwong RA, Cole IE, Gallagher RM, Sutherland RL, Musgrove EA. Deregulated cyclin D1 expression is associated with decreased efficacy of the selective epidermal growth factor receptor tyrosine kinase inhibitor gefitinib in head and neck squamous cell carcinoma cell lines. Clinical cancer research 2004;10(22):7764-74.

139. Bianco R, Troiani T, Tortora G, Ciardiello F. Intrinsic and acquired resistance to EGFR inhibitors in human cancer therapy. Endocrine-related cancer. 2005;12 Suppl 1:S159-71.

140. Gong Y, Yao E, Shen R, Goel A, Arcila M, Teruya-Feldstein J, et al. High expression levels of total IGF-1R and sensitivity of NSCLC cells in vitro to an anti-IGF-1R antibody (R1507). PLoS one. 2009;4(10):e7273.

141. Timpson P, Wilson AS, Lehrbach GM, Sutherland RL, Musgrove EA, Daly RJ. Aberrant expression of cortactin in head and neck squamous cell carcinoma cells is associated with enhanced cell proliferation and resistance to the epidermal growth factor receptor inhibitor gefitinib. Cancer research. 2007;67(19):9304-14.

142. Timpson P, Lynch DK, Schramek D, Walker F, Daly RJ. Cortactin overexpression inhibits ligand-induced down-regulation of the epidermal growth factor receptor. Cancer research. 2005;65(8):3273-80.

143. Claperon A, Therrien M. KSR and CNK: two scaffolds regulating RAS-mediated RAF activation. Oncogene. 2007;26(22):3143-58.

144. McNulty DE, Li Z, White CD, Sacks DB, Annan RS. MAPK scaffold IQGAP1 binds the EGF receptor and modulates its activation. Journal of biological chemistry. 2011;286(17):15010-21.

145. Agelaki S, Spiliotaki M, Markomanolaki H, Kallergi G, Mavroudis D, Georgoulias V, et al. Caveolin-1 regulates EGFR signaling in MCF-7 breast cancer cells and

enhances gefitinib-induced tumor cell inhibition. Cancer biology and therapy. 2009;8(15):1470-7.

146. Shi F, Lemmon MA. Biochemistry. KSR plays CRAF-ty. Science. 2011;332(6033):1043-4.

147. Good MC, Zalatan JG, Lim WA. Scaffold proteins: hubs for controlling the flow of cellular information. Science. 2011;332(6030):680-6.

148. Petrelli F, Cabiddu M, Ghilardi M, Barni S. Current data of targeted therapies for the treatment of triple-negative advanced breast cancer: empiricism or evidence-based? Expert opinion on investigational drugs. 2009;18(10):1467-77.

149. Newton AC. Protein kinase C: structure, function, and regulation. Journal of biological chemistry. 1995;270(48):28495-8.

150. Kennelly PJ, Krebs EG. Consensus sequences as substrate specificity determinants for protein kinases and protein phosphatases. Journal of biological chemistry. 1991;266(15):555-15.

151. Michie AM, Nakagawa R. The link between PKCalpha regulation and cellular transformation. Immunology letters. 2005;96(2):155-62.

152. Sledge GW, Jr., Gokmen-Polar Y. Protein kinase C-beta as a therapeutic target in breast cancer. Seminars in oncology. 2006;33(3 Suppl 9):S15-8.

153. Kim KM, Kang DW, Moon WS, Park JB, Park CK, Sohn JH, et al. PKCtheta expression in gastrointestinal stromal tumor. Modern pathology. 2006;19(11):1480-6.

154. Krasnitsky E, Baumfeld Y, Freedman J, Sion-Vardy N, Ariad S, Novack V, et al. PKCeta is a novel prognostic marker in non-small cell lung cancer. Anticancer research. 2012;32(4):1507-13.

155. Toton E, Ignatowicz E, Skrzeczkowska K, Rybczynska M. Protein kinase Cepsilon as a cancer marker and target for anticancer therapy. Pharmacological reports 2011;63(1):19-29.

156. Bacher N, Zisman Y, Berent E, Livneh E. Isolation and characterization of PKC-L, a new member of the protein kinase C-related gene family specifically expressed in lung, skin, and heart. Molecular and cellular biology. 1991;11(1):126-33.

157. Kim J, Koyanagi T, Mochly-Rosen D. PKCdelta activation mediates angiogenesis via NADPH oxidase activity in PC-3 prostate cancer cells. The prostate. 2011;71(9):946-54.

158. Pajak B, Orzechowska S, Gajkowska B, Orzechowski A. Bisindolylmaleimides in anti-cancer therapy - more than PKC inhibitors. Advances in medical sciences. 2008;53(1):21-31.

159. Alessi DR. The protein kinase C inhibitors Ro 318220 and GF 109203X are equally potent inhibitors of MAPKAP kinase-1beta (Rsk-2) and p70 S6 kinase. FEBS letters. 1997;402(2-3):121-3.

160. Toullec D, Pianetti P, Coste H, Bellevergue P, Grand-Perret T, Ajakane M, et al. The bisindolylmaleimide GF 109203X is a potent and selective inhibitor of protein kinase C. Journal of biological chemistry. 1991;266(24):15771-81.

161. Martiny-Baron G, Kazanietz MG, Mischak H, Blumberg PM, Kochs G, Hug H, et al. Selective inhibition of protein kinase C isozymes by the indolocarbazole Go 6976. Journal of biological chemistry. 1993;268(13):9194-7.

162. Hooks SB, Cummings BS. Role of Ca 2+-independent phospholipase A 2 in cell growth and signaling. Biochemical pharmacology. 2008;76(9):1059-67.

163. Cummings BS. Phospholipase A 2 as targets for anti-cancer drugs. Biochemical pharmacology. 2007;74(7):949-59.

164. Cummings BS, McHowat J, Schnellmann RG. Phospholipase A2s in cell injury and death. Journal of pharmacology and experimental therapeutics. 2000;294(3):793-9.

165. Balsinde J, Winstead MV, Dennis EA. Phospholipase A 2 regulation of arachidonic acid mobilization. FEBS letters. 2002;531(1):2-6.

166. Schaloske RH, Dennis EA. The phospholipase A 2 superfamily and its group numbering system. Biochimica et biophysica acta - molecular and cell biology of lipids. 2006;1761(11):1246-59.

167. Bao S, Bohrer A, Ramanadham S, Jin W, Zhang S, Turk J. Effects of stable suppression of Group VIA phospholipase A2 expression on phospholipid content and composition, insulin secretion, and proliferation of INS-1 insulinoma cells. Journal of biological chemistry. 2006;281(1):187-98.

168. Saavedra G, Zhang W, Peterson B, Cummings B. Differential roles for cytosolic and microsomal Ca2+-independent phospholipase A2 in cell growth and maintenance of phospholipids. Journal of pharmacology and experimental therapeutics. 2006;318(3):1211-9.

169. Longo WE, Grossmann EM, Erickson B, Panesar N, Mazuski JE, Kaminski DL. The effect of phospholipase A 2 inhibitors on proliferation and apoptosis of murine intestinal cells. Journal of surgical research. 1999;84(1):51-6.

170. Hassan S, Carraway RE. Involvement of arachidonic acid metabolism and EGF receptor in neurotensin-induced prostate cancer PC3 cell growth. Regulatory peptides. 2006;133(1):105-14.

171. Teslenko V, Rogers M, Lefkowith JB. Macrophage arachidonate release via both the cytosolic Ca 2+-dependent and-independent phospholipases is necessary for cell spreading. Biochimica et biophysica acta - lipids and lipid metabolism. 1997;1344(2):189-99.

172. Bonventre JV. Phospholipase A2 and signal transduction. Journal of the American society of nephrology. 1992;3(2):128-50.

173. Xu J, Weng YI, Simoni A, Krugh BW, Liao Z, Weisman GA, et al. Role of PKC and MAPK in cytosolic PLA2 phosphorylation and arachadonic acid release in primary murine astrocytes. Journal of neurochemistry. 2002;83(2):259-70.

174. Balsinde J, Balboa MA, Li W-H, Llopis J, Dennis EA. Cellular regulation of cytosolic group IV phospholipase A2 by phosphatidylinositol bisphosphate levels. Journal of immunology. 2000;164(10):5398-402.

175. Ramanadham S, Wolf MJ, Li B, Bohrer A, Turk J. Glucose-responsitivity and expression of an ATP-stimulatable, Ca 2+-independent phospholipase A 2 enzyme in clonal insulinoma cell lines. Biochimica et biophysica acta - lipids and lipid metabolism. 1997;1344(2):153-64.

176. Farooqui AA, Horrocks LA. Phospholipase A2-generated lipid mediators in the brain: the good, the bad, and the ugly. The neuroscientist. 2006;12(3):245-60.

177. Atsumi G, Tajima M, Hadano A, Nakatani Y, Murakami M, Kudo I. Fas-induced arachidonic acid release is mediated by Ca2+-independent phospholipase A2 but not cytosolic phospholipase A2, which undergoes proteolytic inactivation. Journal of biological chemistry. 1998;273(22):13870-7.

178. Farooqui AA, Litsky ML, Farooqui T, Horrocks LA. Inhibitors of intracellular phospholipase A 2 activity: their neurochemical effects and therapeutical importance for neurological disorders. Brain research bulletin. 1999;49(3):139-53.

179. Bonventre JV. Roles of phospholipases A 2 in brain cell and tissue injury associated with ischemia and excitotoxicity. Journal of lipid mediators and cell signalling. 1996;14(1):15-23.

180. Balsinde J, Balboa MaA, Dennis EA. Antisense inhibition of group VI Ca2+-independent phospholipase A2 blocks phospholipid fatty acid remodeling in murine P388D1 macrophages. Journal of biological chemistry. 1997;272(46):29317-21.

181. Balsinde J, Dennis EA. Function and inhibition of intracellular calcium-independent phospholipase A2. Journal of biological chemistry. 1997;272(26):16069-72.

182. Balsinde J, Dennis EA. Bromoenol lactone inhibits magnesium-dependent phosphatidate phosphohydrolase and blocks triacylglycerol biosynthesis in mouse P388D1 macrophages. Journal of biological chemistry. 1996;271(50):31937-41.

183. Denizot Y, Chianéa T, Labrousse F, Truffinet V, Delage M, Mathonnet M. Platelet-activating factor and human thyroid cancer. European journal of endocrinology. 2005;153(1):31-40.

184. Dong Q, Patel M, Scott KF, Graham GG, Russell PJ, Sved P. Oncogenic action of phospholipase A 2 in prostate cancer. Cancer letters. 2006;240(1):9-16.

185. Laye JP, Gill JH. Phospholipase A 2 expression in tumours: a target for therapeutic intervention? Drug discovery today. 2003;8(15):710-6.

186. Yamashita S, Yamashita J, Ogawa M. Overexpression of group II phospholipase A2 in human breast cancer tissues is closely associated with their malignant potency. British journal of cancer. 1994;69(6):1166.

187. Graff JR, Konicek BW, Deddens JA, Chedid M, Hurst BM, Colligan B, et al. Expression of group IIa secretory phospholipase A2 increases with prostate tumor grade. Clinical cancer research. 2001;7(12):3857-61.

188. Jiang J, Neubauer BL, Graff JR, Chedid M, Thomas JE, Roehm NW, et al. Expression of group IIA secretory phospholipase A2 is elevated in prostatic intraepithelial neoplasia and adenocarcinoma. The American journal of pathology. 2002;160(2):667-71.

189. Yamashita J, Ogawa M, Sakai K. Prognostic significance of three novel biologic factors in a clinical trial of adjuvant therapy for node-negative breast cancer. Surgery. 1995;117(6):601-8.

190. Yamashita S, Yamashita J, Sakamoto K, Inada K, Nakashima Y, Murata K, et al. Increased expression of membrane-associated phospholipase A2 shows malignant potential of human breast cancer cells. Cancer. 1993;71(10):3058-64.

191. Yamashita S, Ogawa M, Sakamoto K, Abe T, Arakawa H, Yamashita J. Elevation of serum group II phospholipase A2 levels in patients with advanced cancer. Clinica chimica acta. 1994;228(2):91-9.

192. Kudo I, Murakami M. Phospholipase A 2 enzymes. Prostaglandins and other lipid mediators. 2002;68:3-58.

193. Seeds MC, Bass DA. Regulation and metabolism of arachidonic acid. Clinical reviews in allergy and immunology. 1999;17(1-2):5-26.

194. Umezu-Goto M, Tanyi J, Lahad J, Liu S, Yu S, Lapushin R, et al. Lysophosphatidic acid production and action: validated targets in cancer? Journal of cellular biochemistry. 2004;92(6):1115-40.

195. Sun B, Zhang X, Talathi S, Cummings BS. Inhibition of Ca2+-independent phospholipase A2 decreases prostate cancer cell growth by p53-dependent and independent mechanisms. Journal of pharmacology and experimental therapeutics. 2008;326(1):59-68.

196. Song Y, Wilkins P, Hu W, Murthy K, Chen J, Lee Z, et al. Inhibition of calcium-independent phospholipase A2 suppresses proliferation and tumorigenicity of ovarian carcinoma cells. Biochemical journal. 2007;406:427-36.

197. Beckett CS, Pennington K, McHowat J. Activation of MAPKs in thrombin-stimulated ventricular myocytes is dependent on Ca2+-independent PLA2. American journal of physiology - cell physiology. 2006;290(5):C1350-C4.

198. Lupo G, Nicotra A, Giurdanella G, Anfuso CD, Romeo L, Biondi G, et al. Activation of phospholipase A 2 and MAP kinases by oxidized low-density lipoproteins in immortalized GP8. 39 endothelial cells. Biochimica et biophysica acta - molecular and cell biology of lipids. 2005;1735(2):135-50.

199. Yang CM, Chiu CT, Wang CC, Chien CS, Hsiao LD, Lin CC, et al. Activation of mitogen-activated protein kinase by oxidized low-density lipoprotein in canine cultured vascular smooth muscle cells. Cellular signalling. 2000;12(4):205-14.

200. Huang Z, Liu S, Street I, Laliberte F, Abdullah K, Desmarais S, et al. Methyl arachidonyl fluorophosphonate, a potent irreversible cPLA2 inhibitor, blocks the mobilization of arachidonic acid in human platelets and neutrophils. Mediators of inflammation. 1994;3:307-8.

201. Lio YC, Reynolds LJ, Balsinde J, Dennis EA. Irreversible inhibition of Ca(2+)-independent phospholipase A2 by methyl arachidonyl fluorophosphonate. Biochimica et biophysica acta. 1996;1302(1):55-60.

202. Al-Lazikani B, Banerji U, Workman P. Combinatorial drug therapy for cancer in the post-genomic era. Nature biotechnology. 2012;30(7):679-92.

203. Zimmermann GR, Lehar J, Keith CT. Multi-target therapeutics: when the whole is greater than the sum of the parts. Drug discovery today. 2007;12(1):34-42.

204. Vanneman M, Dranoff G. Combining immunotherapy and targeted therapies in cancer treatment. Nature reviews cancer. 2012;12(4):237-51.

205. Slamon DJ, Leyland-Jones B, Shak S, Fuchs H, Paton V, Bajamonde A, et al. Use of chemotherapy plus a monoclonal antibody against HER2 for metastatic breast cancer that overexpresses HER2. New England journal of medicine. 2001;344(11):783-92.

206. Marty M, Cognetti F, Maraninchi D, Snyder R, Mauriac L, Tubiana-Hulin M, et al. Randomized phase II trial of the efficacy and safety of trastuzumab combined with docetaxel in patients with human epidermal growth factor receptor 2–positive metastatic breast cancer administered as first-line treatment: the M77001 study group. Journal of clinical oncology. 2005;23(19):4265-74.

207. Nahta R, Esteva F. Trastuzumab: triumphs and tribulations. Oncogene. 2007;26(25):3637-43.

208. Swain SM, Kim S-B, Cortés J, Ro J, Semiglazov V, Campone M, et al. Pertuzumab, trastuzumab, and docetaxel for HER2-positive metastatic breast cancer (CLEOPATRA study): overall survival results from a randomised, double-blind, placebo-controlled, phase 3 study. The lancet oncology. 2013;14(6):461-71.

209. Blumenthal GM, Scher NS, Cortazar P, Chattopadhyay S, Tang S, Song P, et al. First FDA approval of dual anti-HER2 regimen: pertuzumab in combination with trastuzumab and docetaxel for HER2-positive metastatic breast cancer. Clinical cancer research. 2013;19(18):4911-6.

210. Baselga J, Cortes J, Kim SB, Im SA, Hegg R, Im YH, et al. Pertuzumab plus trastuzumab plus docetaxel for metastatic breast cancer. The New England journal of medicine. 2012;366(2):109-19.

211. Geyer CE, Forster J, Lindquist D, Chan S, Romieu CG, Pienkowski T, et al. Lapatinib plus capecitabine for HER2-positive advanced breast cancer. New England journal of medicine. 2006;355(26):2733-43.

212. Ryan Q, Ibrahim A, Cohen MH, Johnson J, Ko C-w, Sridhara R, et al. FDA drug approval summary: lapatinib in combination with capecitabine for previously treated metastatic breast cancer that overexpresses HER-2. The oncologist. 2008;13(10):1114-9.

213. Cunningham D, Humblet Y, Siena S, Khayat D, Bleiberg H, Santoro A, et al. Cetuximab monotherapy and cetuximab plus irinotecan in irinotecan-refractory metastatic colorectal cancer. New England journal of medicine. 2004;351(4):337-45.

214. Sobrero AF, Maurel J, Fehrenbacher L, Scheithauer W, Abubakr YA, Lutz MP, et al. EPIC: phase III trial of cetuximab plus irinotecan after fluoropyrimidine and oxaliplatin failure in patients with metastatic colorectal cancer. Journal of clinical oncology. 2008;26(14):2311-9.

215. Ribeiro Gomes J, Cruz MR. Combination of afatinib with cetuximab in patients with EGFR-mutant non-small-cell lung cancer resistant to EGFR inhibitors. OncoTargets and therapy. 2015;8:1137-42.

216. Pircher A, Manzl C, Fiegl M, Popper H, Pirker R, Hilbe W. Overcoming resistance to first generation EGFR TKIs with cetuximab in combination with chemotherapy in an EGFR mutated advanced stage NSCLC patient. Lung Cancer. 2014;83(3):408-10.

217. Abdel-Rahman O. Targeting BRAF aberrations in advanced colorectal carcinoma: from bench to bedside. Future oncology 2016;12(1):25-30.

218. Yalcin S, Trad D, Kader YA, Halawani H, Demir OG, Mall R, et al. Personalized treatment is better than one treatment fits all in the management of patients with mCRC: a consensus statement. Future Oncology. 2014;10(16):2643-57.

219. Er TK, Chen CC, Bujanda L, Herreros-Villanueva M. Current approaches for predicting a lack of response to anti-EGFR therapy in KRAS wild-type patients. BioMed research international. 2014;2014:591867.

220. Wiedmann MW, Caca K. Molecularly targeted therapy for gastrointestinal cancer. Current cancer drug targets. 2005;5(3):171-93.

221. Abera MB, Kazanietz MG. Protein kinase Calpha mediates erlotinib resistance in lung cancer cells. Molecular pharmacology. 2015;87(5):832-41.

222. Gill GN, Lazar CS. Increased phosphotyrosine content and inhibition of proliferation in EGF-treated A431 cells. Nature. 1981;293(5830):305-7.

223. Kaetzel MA, Pula G, Campos B, Uhrin P, Horseman N, Dedman JR. Annexin VI isoforms are differentially expressed in mammalian tissues. Biochimica et biophysica acta - molecular cell research. 1994;1223(3):368-74.

224. Stögbauer F, Weigert J, Neumeier M, Wanninger J, Sporrer D, Weber M, et al. Annexin A6 is highly abundant in monocytes of obese and type 2 diabetic individuals and is downregulated by adiponectin in vitro. Experimental and molecular medicine. 2009;41(7):501-7.

225. Osherov N, Levitzki A. Epidermal-growth-factor-dependent activation of the src-family kinases. European journal of biochemistry. 1994;225(3):1047-53.

226. Levitzki A, Gazit A. Tyrosine kinase inhibition: an approach to drug development. Science. 1995;267(5205):1782-8.

227. Moyer JD, Barbacci EG, Iwata KK, Arnold L, Boman B, Cunningham A, et al. Induction of apoptosis and cell cycle arrest by CP-358,774, an inhibitor of epidermal growth factor receptor tyrosine kinase. Cancer research. 1997;57(21):4838-48.

228. Wakeling AE, Guy SP, Woodburn JR, Ashton SE, Curry BJ, Barker AJ, et al. ZD1839 (Iressa): an orally active inhibitor of epidermal growth factor signaling with potential for cancer therapy. Cancer research. 2002;62(20):5749-54.

229. Janmaat ML, Rodriguez JA, Gallegos-Ruiz M, Kruyt FA, Giaccone G. Enhanced cytotoxicity induced by gefitinib and specific inhibitors of the Ras or phosphatidyl inositol-3 kinase pathways in non-small cell lung cancer cells. International journal of cancer 2006;118(1):209-14.

230. Normanno N, De Luca A, Maiello MR, Campiglio M, Napolitano M, Mancino M, et al. The MEK/MAPK pathway is involved in the resistance of breast cancer cells to the EGFR tyrosine kinase inhibitor gefitinib. Journal of cellular physiology. 2006;207(2):420-7.

231. Normanno N, Campiglio M, Maiello MR, De Luca A, Mancino M, Gallo M, et al. Breast cancer cells with acquired resistance to the EGFR tyrosine kinase inhibitor gefitinib show persistent activation of MAPK signaling. Breast cancer research and treatment. 2008;112(1):25-33.

232. Vlotides G, Siegel E, Donangelo I, Gutman S, Ren SG, Melmed S. Rat prolactinoma cell growth regulation by epidermal growth factor receptor ligands. Cancer research. 2008;68(15):6377-86.

233. Huang S, Armstrong EA, Benavente S, Chinnaiyan P, Harari PM. Dual-agent molecular targeting of the epidermal growth factor receptor (EGFR): combining anti-EGFR antibody with tyrosine kinase inhibitor. Cancer research. 2004;64(15):5355-62.

234. Matar P, Rojo F, Cassia R, Moreno-Bueno G, Di Cosimo S, Tabernero J, et al. Combined epidermal growth factor receptor targeting with the tyrosine kinase inhibitor gefitinib (ZD1839) and the monoclonal antibody cetuximab (IMC-C225): superiority over single-agent receptor targeting. Clinical cancer research 2004;10(19):6487-501.

235. Rafehi H, Orlowski C, Georgiadis GT, Ververis K, El-Osta A, Karagiannis TC. Clonogenic assay: adherent cells. Journal of visualized experiments. 2011(49):e2573-e.

236. Franken NA, Rodermond HM, Stap J, Haveman J, van Bree C. Clonogenic assay of cells in vitro. Nature protocols. 2006;1(5):2315-9.

237. Huether A, Höpfner M, Baradari V, Schuppan D, Scherübl H. EGFR blockade by cetuximab alone or as combination therapy for growth control of hepatocellular cancer. Biochemical pharmacology. 2005;70(11):1568-78.

238. Qiao L, Yacoub A, McKinstry R, Park JS, Caron R, Fisher PB, et al. Pharmocologic inhibitors of the mitogen activated protein kinase cascade have the potential to interact with ionizing radiation exposure to induce cell death in carcinoma cells by multiple mechanisms. Cancer biology and therapy. 2002;1(2):168-76.

239. Ciardiello F, Tortora G. Epidermal growth factor receptor (EGFR) as a target in cancer therapy: understanding the role of receptor expression and other molecular determinants that could influence the response to anti-EGFR drugs. European journal of cancer. 2003;39(10):1348-54.

240. Viloria-Petit A, Crombet T, Jothy S, Hicklin D, Bohlen P, Schlaeppi JM, et al. Acquired resistance to the antitumor effect of epidermal growth factor receptor-blocking antibodies in vivo: a role for altered tumor angiogenesis. Cancer research. 2001;61(13):5090-101.

241. Kim Y, Apetri M, Luo B, Settleman JE, Anderson KS. Differential effects of tyrosine kinase inhibitors on normal and oncogenic EGFR signaling and downstream effectors. Molecular cancer research. 2015;13(4):765-74.

242. Fukino K, Shen L, Matsumoto S, Morrison CD, Mutter GL, Eng C. Combined total genome loss of heterozygosity scan of breast cancer stroma and epithelium reveals multiplicity of stromal targets. Cancer research. 2004;64(20):7231-6.

243. Dancey J, Sausville EA. Issues and progress with protein kinase inhibitors for cancer treatment. Nature reviews drug discovery. 2003;2(4):296-313.

244. Hui R, Campbell DH, Lee CS, McCaul K, Horsfall DJ, Musgrove EA, et al. EMS1 amplification can occur independently of CCND1 or INT-2 amplification at 11q13

and may identify different phenotypes in primary breast cancer. Oncogene. 1997;15(13):1617-23.

245. Rodrigo JP, Garcia LA, Ramos S, Lazo PS, Suarez C. EMS1 gene amplification correlates with poor prognosis in squamous cell carcinomas of the head and neck. Clinical cancer research. 2000;6(8):3177-82.

246. Luo ML, Shen XM, Zhang Y, Wei F, Xu X, Cai Y, et al. Amplification and overexpression of CTTN (EMS1) contribute to the metastasis of esophageal squamous cell carcinoma by promoting cell migration and anoikis resistance. Cancer research. 2006;66(24):11690-9.

247. Domon MM, Nasir MN, Pikula S, Besson F. Influence of the 524-VAAEIL-529 sequence of annexins A6 in their interfacial behavior and interaction with lipid monolayers. Journal of colloid and interface science. 2013;403:99-104.

248. Podszywalow-Bartnicka P, Kosiorek M, Piwocka K, Sikora E, Zablocki K, Pikula S. Role of annexin A6 isoforms in catecholamine secretion by PC12 cells: distinct influence on calcium response. Journal of cellular biochemistry. 2010;111(1):168-78.

249. Koumangoye RB, Nangami GN, Thompson PD, Agboto VK, Ochieng J, Sakwe AM. Reduced annexin A6 expression promotes the degradation of activated epidermal growth factor receptor and sensitizes invasive breast cancer cells to EGFR-targeted tyrosine kinase inhibitors. Molecular cancer. 2013;12(1):167.

250. Irwin ME, Mueller KL, Bohin N, Ge Y, Boerner JL. Lipid raft localization of EGFR alters the response of cancer cells to the EGFR tyrosine kinase inhibitor gefitinib. Journal of cellular physiology. 2011;226(9):2316-28.

251. Lu YC, Chen HC. Involvement of lipid rafts in adhesion-induced activation of Met and EGFR. Journal of biomedical science. 2011;18:78.

252. Wang XQ, Yan Q, Sun P, Liu JW, Go L, McDaniel SM, et al. Suppression of epidermal growth factor receptor signaling by protein kinase C-alpha activation requires CD82, caveolin-1, and ganglioside. Cancer research. 2007;67(20):9986-95.

253. Taube E, Jokinen E, Koivunen P, Koivunen JP. A novel treatment strategy for EGFR mutant NSCLC with T790M-mediated acquired resistance. International journal of cancer. 2012;131(4):970-9.

254. Stewart JR, O'Brian CA. Protein kinase C-{alpha} mediates epidermal growth factor receptor transactivation in human prostate cancer cells. Molecular cancer therapeutics. 2005;4(5):726-32.

255. Grandage VL, Everington T, Linch DC, Khwaja A. Go6976 is a potent inhibitor of the JAK 2 and FLT3 tyrosine kinases with significant activity in primary acute myeloid leukaemia cells. British journal of haematology. 2006;135(3):303-16.

256. Kohn EA, Yoo CJ, Eastman A. The protein kinase C inhibitor Go6976 is a potent inhibitor of DNA damage-induced S and G2 cell cycle checkpoints. Cancer research. 2003;63(1):31-5.

257. Serova M, Ghoul A, Benhadji KA, Cvitkovic E, Faivre S, Calvo F, et al. Preclinical and clinical development of novel agents that target the protein kinase C family. Seminars in oncology. 2006;33(4):466-78.

258. Wendum D, Svrcek M, Rigau V, Boëlle P-Y, Sebbagh N, Parc R, et al. COX-2, inflammatory secreted PLA2, and cytoplasmic PLA2 protein expression in small bowel adenocarcinomas compared with colorectal adenocarcinomas. Modern pathology. 2003;16(2):130-6.

259. Kawamoto S, Shoji M, Setoguchi Y, Kato M, Hashizume S, Ichikawa A, et al. Molecular cloning of the 31 kDa cytosolic phospholipase A2, as an antigen recognized by the lung cancer-specific human monoclonal antibody, AE6F4. Cytotechnology. 1995;17(2):103-8.

260. Gijon MA, Spencer DM, Siddiqi AR, Bonventre JV, Leslie CC. Cytosolic phospholipase A2 is required for macrophage arachidonic acid release by agonists that Do and Do not mobilize calcium. Novel role of mitogen-activated protein kinase pathways in cytosolic phospholipase A2 regulation. Journal of biological chemistry. 2000;275(26):20146-56.

261. Lin LL, Wartmann M, Lin AY, Knopf JL, Seth A, Davis RJ. cPLA2 is phosphorylated and activated by MAP kinase. Cell. 1993;72(2):269-78.

262. Qi H, Liu S, Guo C, Wang J, Greenaway FT, Sun MZ. Role of annexin A6 in cancer. Oncology letters. 2015;10(4):1947-52.

263. Meier EM, Rein-Fischboeck L, Pohl R, Wanninger J, Hoy AJ, Grewal T, et al. Annexin A6 protein is downregulated in human hepatocellular carcinoma. Molecular and cellular biochemistry. 2016.

264. Berasain C, Avila MA. The EGFR signalling system in the liver: from hepatoprotection to hepatocarcinogenesis. Journal of gastroenterology. 2014;49(1):9-23.